# GLOBAL PHASE PORTRAITS OF THE QUADRATIC SYSTEMS HAVING A SINGULAR AND IRREDUCIBLE INVARIANT CURVE OF DEGREE 3

JAUME LLIBRE[1] AND CHARA PANTAZI[2]

Abstract. Any singular irreducible cubic after an affine transformation can be written as either $y^2 = x^3$, or $y^2 = x^2(x+1)$, or $y^2 = x^2(x-1)$. We classify the phase portraits of all quadratic polynomial differential systems having the invariant cubic $y^2 = x^2(x+1)$. We prove that there are 65 different topological phase portraits for such quadratic polynomial differential systems.

## 1. Introduction and statement of the main result

Quadratic polynomial differential systems (or simply *quadratic systems*) are systems that can be written into the form

$$\dot{x} = P(x,y) = P_0 + P_1 + P_2, \qquad \dot{y} = Q(x,y) = Q_0 + Q_1 + Q_2, \tag{1}$$

where $P_i$ and $Q_i$ are real polynomials of degree $i$ in the variables $(x,y)$ and $P_2^2 + Q_2^2 \neq 0$.

An extensive literature is dedicated to the study of the quadratic systems these last years. For a good survey see the book of Reyn [37] or the book of Artes et.al [4], and references therein. For example, the following families of quadratic systems have been studied: homogeneous [16], semi-homogeneous [12], bounded [18], reversible [24, 17], Hamiltonian [2, 15], Lienard [19], integrable using Carleman and Painlevé tools [25], rational integrable [5, 6, 7], the ones having a star nodal point [10], a center [42, 31, 17, 42], one focus and one antisaddle [3], with a semi–elementary triple node [8], chordal [21, 22], with four infinite singular points and one invariant straight line [38], with invariant lines [41], and so on. There is also an extensively literature about Hilbert's sixteen problem and quadratic systems, see for example [13, 23, 29, 30, 31, 44], and the notion of ciclicity [45, 26, 15], and so on. For the study of some geometric properties of quadratic systems see [39, 40], and others. In particular we pay attention on reference [28] where the authors present a classification of all quadratic systems having one real reducible invariant algebraic curve of degree 3.

In [11] it is proved that a cubic algebraic curve (or simply a cubic) is singular and irreducible if and only if it can be written after affine transformations into one of the forms

$$y^2 = x^3, \qquad y^2 = x^2(x+1), \qquad y^2 = x^2(x-1).$$

See Figure 1.

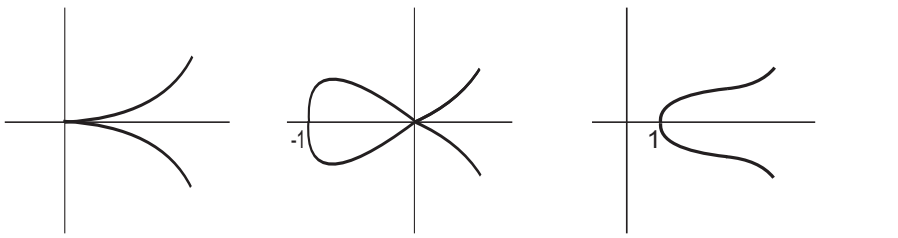


$f_1 = y^2 - x^3$ $\qquad$ $f_2 = y^2 - x^2(x+1)$ $\qquad$ $f_3 = y^2 - x^2(x-1)$

Figure 1. Singular and irreducible algebraic curves of degree 3.

The goal of this paper is to continue the classification of the phase portraits in the Poincaré disc of the quadratic systems having some invariant cubic. Thus our main result is to provide all distinct topological phase portraits of the quadratic systems having the invariant cubic $y^2 = x^2(x+1)$.

Let $f = f(x, y) = 0$ be a real polynomial. We say that $f = 0$ *is an invariant algebraic curve* of system (1) if it satisfies

$$P\frac{\partial f}{\partial x} + Q\frac{\partial f}{\partial y} = Kf,$$

for some polynomial $K$ called the *cofactor* of the curve $f = 0$. Note that an invariant algebraic curve is formed by orbits of system (1).

It is easy to check that the quadratic systems (1) having $f = y^2 - x^2(x+1) = 0$ as invariant algebraic curve are

$$\begin{aligned} \dot{x} &= ax + by + ax^2 + (3b - 2c)xy, \\ \dot{y} &= bx + ay + cx^2 + \frac{3}{2}axy + \left(\frac{9}{2}b - 3c\right)y^2, \end{aligned} \tag{2}$$

See the appendix for a summary of about the *Poincaré compactification* of a polynomial differential system and the definition of the *Poincaré disc* $\mathbb{D}$, which roughly speaking is to identify the interior of the unit closed disc $\mathbb{D}$ centered at the origin with the plane $\mathbb{R}^2$ and its boundary $\mathbb{S}^1$ with the infinity of $\mathbb{R}^2$, in the plane we can go to infinity in as many as directions as points has the circle $\mathbb{S}^1$. Then the Poincaré compactification consists in extend the quadratic differential system from the interior of $\mathbb{D}$ to its boundary $\mathbb{S}^1$, i.e. to the infinity of $\mathbb{R}^2$. In this way we can control the orbits of a polynomial differential in a neighborhood of the infinity, and in particular of a quadratic system.

Our main result is the following.

**Theorem 1.** *For the quadratic systems* (2) *there are* 65 *non topological equivalent phase portraits in the Poincaré disc.*

The rest of the paper is dedicated to proof Theorem 1.

## 2. Quadratic systems with the invariant algebraic curve $y^2 - x^2(x+1) = 0$

All quadratic systems admitting $y^2 - x^2(x+1) = 0$ as the invariant cubic $y^2 - x^2(x+1) = 0$ can be written as systems (2). We distinguish the following cases.

2.1. **Case $a = 0$ and $c = 0$.** Then $b \neq 0$ otherwise the system is not quadratic, and without loss of generality we can consider $b = 1$. Then system (2) becomes

$$\dot{x} = y(1 + 3x), \quad \dot{y} = \frac{1}{2}\left(2x + 9y^2\right), \tag{3}$$

and has the rational first integral

$$H(x, y) = \frac{27\,y^2 + 9\,x + 1}{(3\,x + 1)^3}.$$

System (3) has the three invariant algebraic curves: $f_2 = 0$, $g_1 = 3x + 1 = 0$ and $g_3 = 27\,y^2 + 9\,x + 1$. Additionally, has the three finite singular points $P_0(0,\ 0)$, $P_-\left(-1/3,\ -\sqrt{6}/9\right)$ and $P_+\left(-1/3,\ \sqrt{6}/9\right)$. $P_0$ is a saddle, $P_-$ is an unstable node and $P_+$ is a stable node.

In what follows we use the notation introduced in the Appendix for studying the infinite singular points using the Poincaré compactification. The origin of the chart $(U_1, F_1)$ is a nilpotent singular point and using Theorem 3.5 of [20] is a saddle, and doing blows ups we get its local phase portrait as it shows in Figure 2. Moreover, the origin of the local chart $U_2$ is a hyperbolic stable node. The local and the global phase portraits of system (3) are given in Figure 2.

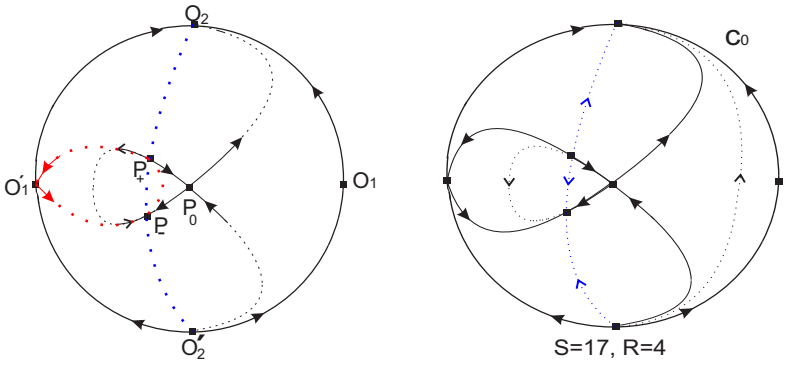


FIGURE 2. The local and the global phase portraits of system (3). Here $a = c = 0$, $b = 1$ in system (2).

2.2. **Case $a = 0$ and $c \neq 0$.** Without loss of generality we can consider $c = 1$, and system (2) can be written as

$$\begin{aligned} \dot{x} &= by + (3b-2)xy, \\ \dot{y} &= bx + x^2 + \left(\frac{9}{2}b - 3\right) y^2, \end{aligned} \tag{4}$$

where this $b$ is the old $b/c$. For $b = 2/3$ system (4) is a Hamiltonian system with the first integral $H = x^3 + x^2 - y^2$. System (4) for $b \neq 2/3$ has the rational first integral

$$H(x,y) = \frac{b^3 + 3\,b^2\,(3\,b-2)\,x + 2\,\left(9\,b^2 - 12\,b + 4\right)x^2 + \left(27\,b^3 - 54\,b^2 + 36\,b - 8\right)y^2}{(3\,bx + b - 2\,x)^3}.$$

The curve $g_2 = b^3 + 3\,b^2\,(3\,b-2)\,x + 2\,\left(9\,b^2 - 12\,b + 4\right)x^2 + \left(27\,b^3 - 54\,b^2 + 36\,b - 8\right)y^2 = 0$ is a conic for $b \neq 2/3$ and it is classified as follows: For $b \in (-\infty, 0) \cup (0, 2/3)$ is a hyperbola, for $b \in (2/3, 8/9)$ an imaginary ellipse, and for $b > 8/9$ is a real ellipse. For $b = 0$ we obtain two real invariant straight lines that intersect into a point. For $b = 8/9$ the conic is formed by two parallel imaginary straight lines.

System (4) has the finite singular points (whenever they exist)

$$P_0(0,0),\ P_1(-b,0),\ P_-\left(\frac{b}{2-3\,b}, -\frac{b\sqrt{2\,b-2}}{(3\,b-2)^{3/2}}\right),\ P_+\left(\frac{b}{2-3\,b}, \frac{b\sqrt{2\,b-2}}{(3\,b-2)^{3/2}}\right).$$

Note that the points $P_-$ and $P_+$ are the intersection points of the three curves $f_2 = 0$, $g_2 = 0$ and $g_1 = (3\,b-2)x + b = 0$.

For $b \in (0, 2/3) \cup (1,\ \infty)$ the point $P_1$ is on the left hand side of the straight line passing through the points $P_-$ and $P_+$. For $b \in (-\infty, 0) \cup (0, 2/3) \cup (1, +\infty)$ the points $P_\pm$ exist. For $b = 0$ the four points collide into $P_0$. For $b = 1$ the three points $P_+, P_-$ and $P_1$ collide between them. For $2/3 \leq b < 1$ only exist the finite singular points $P_0$ and $P_1$.

The point $P_0$ has the Jacobian matrix

$$\begin{pmatrix} 0 & b \\ b & 0 \end{pmatrix},$$

and its eigenvalues are $\pm b$. For $b = 0$ the point $P_0$ is linearly zero and doing blow–ups we obtain that its local phase portrait is the union of two elliptic and two parabolic sectors, see Figure 4.

The point $P_1$ has the Jacobian matrix

$$\begin{pmatrix} 0 & -3\,b^2 + 3\,b \\ -b & 0 \end{pmatrix},$$

| $b$ | $-\infty$ | | 0 | | $2/3$ | | $8/9$ | | 1 | $\infty$ |
|---|---|---|---|---|---|---|---|---|---|---|
| $P_0$ | | $S$ | *pepep* | $S$ | $S$ | $S$ | $S$ | $S$ | $S$ | $S$ |
| $P_1$ | | $C$ | – | $C$ | $C$ | $C$ | $C$ | $C$ | *peph* | $S$ |
| $P_+$ | | $N^s$ | – | $N^s$ | – | – | – | – | – | $N^u$ |
| $P_-$ | | $N^u$ | – | $N^u$ | – | – | – | – | – | $N^s$ |
| $Q_-$ | | $S$ | $S$ | $S$ | – | – | – | – | – | – |
| $Q_+$ | | $S$ | $S$ | $S$ | – | – | – | – | – | – |
| $O_2$ | | $N^u$ | $N^u$ | $N^u$ | $N^s$ | $N^s$ | $N^s$ | $N^s$ | $N^s$ | $N^s$ |

TABLE 1. The finite singular points of system (4)

and its eigenvalues are $\pm b\sqrt{3b-3}$. For $b=0$ the point $P_1$ coincides with $P_0$. For $b=1$ the point $P_1$ is a nilpotent point and by Theorem 3.5 of [20] we have that $P_1$ is the union of one elliptic and one hyperbolic sectors separated by two parabolic sectors, see Figure 9.

The eigenvalues of the point $P_+$ are

$$\lambda_1 = \frac{\left(6\sqrt{2\,b-2}b+\sqrt{2}\sqrt{(b-1)\,(3\,b-2)^2}-4\sqrt{2\,b-2}\right)b}{(3\,b-2)^{3/2}},$$
$$\lambda_2 = -\frac{b\left((-6\,b+4)\sqrt{2\,b-2}+\sqrt{2}\sqrt{(b-1)\,(3\,b-2)^2}\right)}{(3\,b-2)^{3/2}}.$$

The eigenvalues of the point $P_-$ are

$$\lambda_1 = \frac{\left(-6\sqrt{2\,b-2}b+\sqrt{2}\sqrt{(b-1)\,(3\,b-2)^2}+4\sqrt{2\,b-2}\right)b}{(3\,b-2)^{3/2}},$$
$$\lambda_2 = -\frac{\left(6\sqrt{2\,b-2}b+\sqrt{2}\sqrt{(b-1)\,(3\,b-2)^2}-4\sqrt{2\,b-2}\right)b}{(3\,b-2)^{3/2}}.$$

For both points $P_\pm$ the product of its eigenvalues is $6\,b^2\,(b-1)/(3\,b-2)$.

In the chart $(U_1, F_1)$ for $b<2/3$ we obtain the infinite singular points

$$Q_+\left(\sqrt{\frac{2}{2-3b}},\ 0\right), \quad Q_-\left(-\sqrt{\frac{2}{2-3b}},\ 0\right).$$

The eigenvalues of the points $Q_\pm$ are $\pm\sqrt{4-6b}$.

The singular point at the origin of the chart $(U_2, F_2)$ has the Jacobian matrix

$$\begin{pmatrix} 1-3b/2 & b \\ 0 & 3-9b/2 \end{pmatrix},$$

and its eigenvalues are

$$\lambda_1 = 1-3/2\,b, \quad \lambda_2 = 3-9/2\,b.$$

Thus, for $b\neq 2/3$ it is a node, whereas for $b=2/3$ it is a nilpotent singular point, and by Theorem 3.5 of [20] it is a stable node.

We note that the family (2) is invariant under the symmetry

$$(x, y, a, t) \to (x, -y, -a, -t). \tag{5}$$

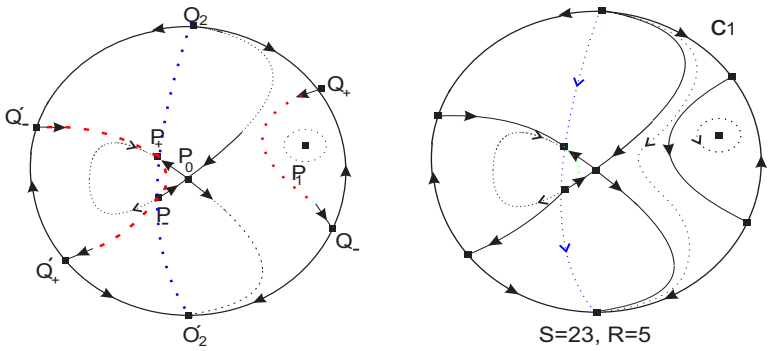


FIGURE 3. The local and the global phase portraits of system (4). Here $a = 0$, $b < 0$ and $c = 1$. The curve $g_2 = 0$ is a hyperbola.

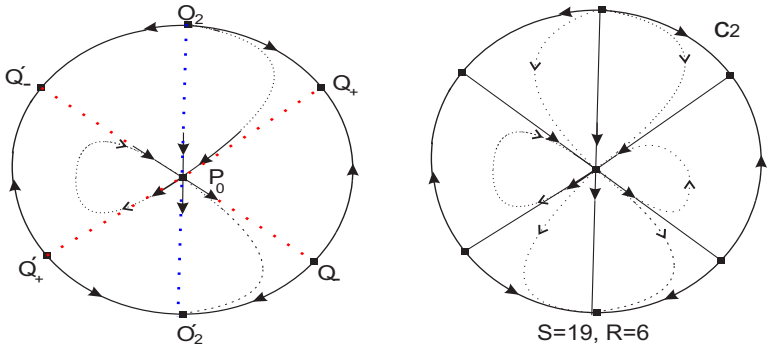


FIGURE 4. The local and the global phase portraits of system (4). Here $a = b = 0$ and $c = 1$. The curve $g_2 = 0$ are two intersecting real lines

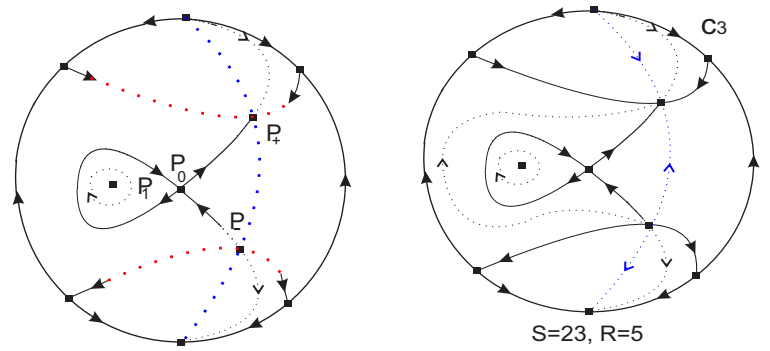


FIGURE 5. The local and the global phase portraits of system (4). Here $a = 0$, $b \in (0, 2/3)$ and $c = 1$. The curve $g_2 = 0$ is a hyperbola.

2.3. **Case $a \neq 0$.** Due to the symmetry (5) without loss of generality we can restrict our study to $a > 0$. We distinguish the following cases.

**Case 1:** $c = 0$. Then system (2) becomes

$$\dot{x} = ax + by + ax^2 + 3\,bxy, \qquad \dot{y} = bx + ay + \frac{3}{2}\,axy + \frac{9}{2}\,by^2. \tag{6}$$

In order to study this family we distinguish the following two subcases according to the parameter $b$.

**Subcase** $c = b = 0$. Then system (2) becomes

$$\dot{x} = ax(x + 1), \qquad \dot{y} = \frac{1}{2}ay(2 + 3x), \tag{7}$$

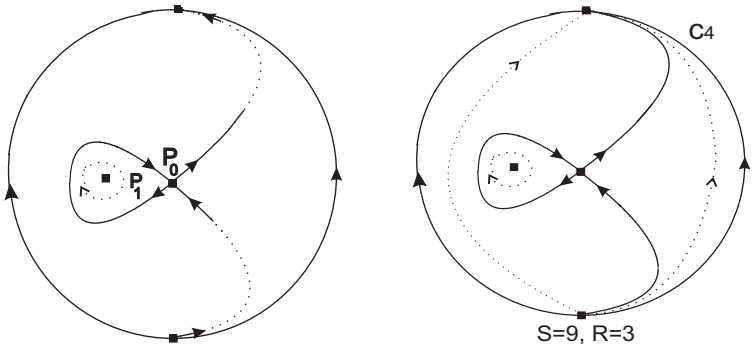


FIGURE 6. The local and the global phase portraits of system (4). Here $a = 0$, $b = 2/3$ and $c = 1$. The system is Hamiltonian with $H(x, y) = -x^3 - x^2 + y^2$. $F = e^x$ is an exponential factor.

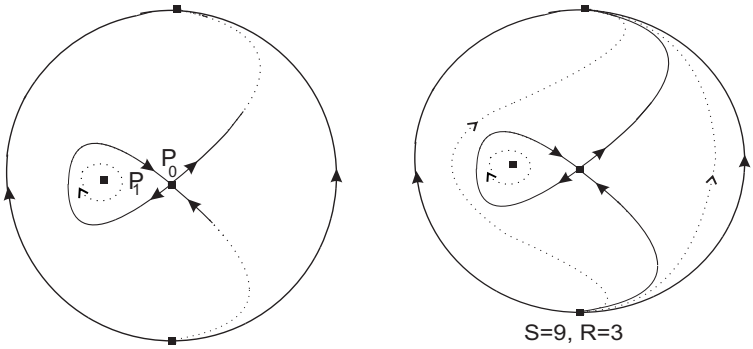


FIGURE 7. The local and the global phase portraits of system (4). Here $a = 0$, $b \in (2/3, 8/9]$ and $c = 1$. For $b \in (2/3, 8/9)$ the curve $g_2 = 0$ is an imaginary ellipse whereas for $b = 8/9$ are two parallel imaginary straight lines.

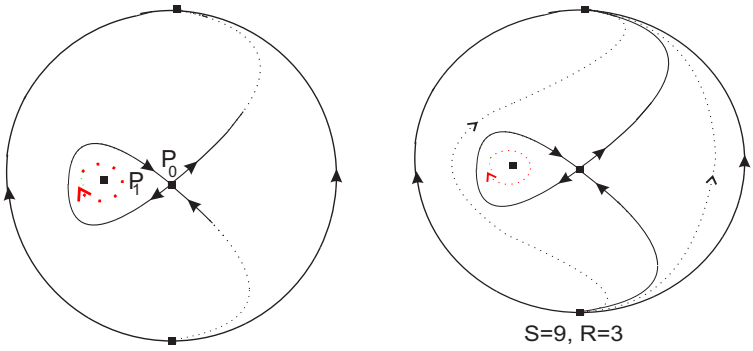


FIGURE 8. The local and the global phase portraits of system (4). Here $a = 0$, $b \in (8/9, 1)$ and $c = 1$. The curve $g_2 = 0$ is a real ellipse.

and it has the rational first integral $H = x^2(x+1)/y^2$. Without loss of generality we can consider that $a = 1$. The unique finite singular points are $P_0 = (0, 0)$ and $P = (-1, 0)$. The point $P_0$ is an unstable node. The point $P \in \{f_2 = 0\}$ is a stable node. The origin $O_2$ of the chart $(U_2, F_2)$ has a Jacobian matrix identically zero. Doing blow ups $O_2$ is the union of one parabolic and one hyperbolic sector. The local and the global phase portrait of system (7) is given in Figure 11.

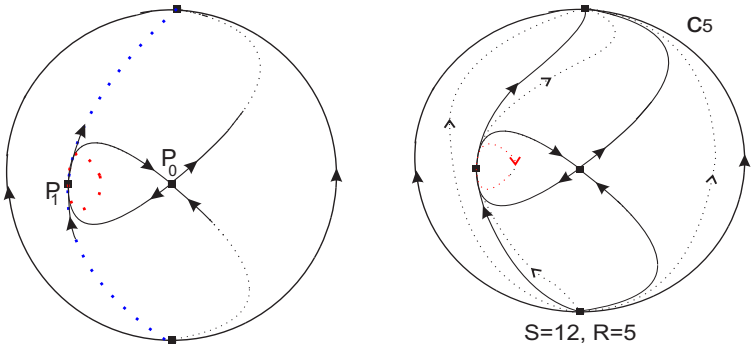


FIGURE 9. The local and the global phase portraits of system (4). Here $a = 0$, $b = c = 1$. The curve $g_2 = 0$ is a real ellipse.

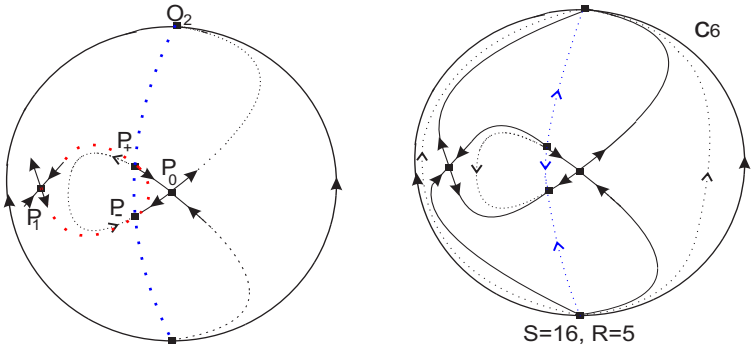


FIGURE 10. The local and the global phase portraits of system (4). Here $a = 0$, $b > 1$ and $c = 1$. The curve $g_2 = 0$ is a real ellipse.

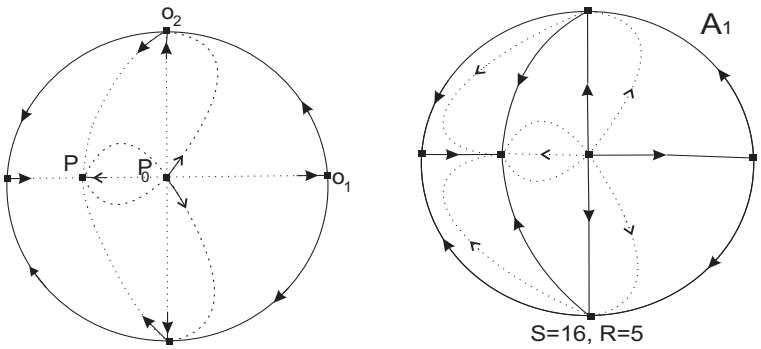


FIGURE 11. The local and the global phase portraits of system (7). Here $a = 1$ and $b = c = 0$.

**Subcase** $c = 0, b \neq 0$. Since $b \neq 0$ without loss of generality we can assume that $b = 1$. System (6) can be written as

$$\dot{x} = ax + y + ax^2 + 3\,xy, \qquad \dot{y} = x + ay + \frac{3}{2}\,axy + \frac{9}{2}\,y^2, \tag{8}$$

where now $a$ is the previous $a/b$.

System (8) has three finite singular points:

$$P_0 = (0,0), \qquad P_\pm = \left(-\frac{1}{3} + \frac{1}{18}\,a^2 \pm \frac{1}{18}\,A, \quad \frac{1}{54}\,\frac{-9\,a^2 \pm 3\,A - a^4 \mp a^2 A}{a}\right),$$

with $A = a\sqrt{24 + a^2}$. Note that $P_0, P_\pm$ are points of the curve $f_2 = 0$. For $a = 1$ the point $P_+$ collides with $P_0$. The point $P_-$ is always on the left hand side of the point $P_+$. For $a > \sqrt{3}$ the

point $P_-$ is upper the point $P_+$, here left hand side or upper are with respect to the $x$ and $y$ axes.

The linear part at the origin $P_0$ has eigenvalues $a+1$ and $a-1$. So, for $a \in (0,1)$ the origin $P_0$ is a saddle. For $a>1$ it is an unstable node. For $a=1$ we have that $P_0$ is semi–hyperbolic and using Theorem 2.19 of [20] we obtain that is a saddle–node.

Now we set

$$B_- = \; a^2\left(a^6 - a^4A + 30\,a^4 - 18\,a^2A + 378\,a^2 + 1728 - 72\,A\right),$$

and note that for $a>0$ we have that $B_->0$. At the point $P_-$ the eigenvalues are

$$\lambda_{1,2} = \frac{1}{72}\,\frac{-24\,A - 42\,a^2 - a^4 + a^2A \pm \sqrt{2B_-}}{a} < 0,$$

and consequently that $P_-$ is a stable node.

We additionally set

$$B_+ = a^2\left(a^6 + 30\,a^4 + a^4A + 378\,a^2 + 18\,a^2A + 1728 + 72\,A\right),$$

and for $a>0$ we have that $B_+>0$. The eigenvalues associated to the point $P_+$ are

$$\lambda_{1,2} = -\frac{1}{72}\,\frac{42\,a^2 + a^4 + a^2A - 24\,A \pm \sqrt{2B_+}}{a}.$$

We have that $\lambda_1>0$ and $\lambda_2>0$ if $a\in(0,1)$, and $\lambda_1\lambda_2<0$ if $a>1$. So for $a\in(0,1)$ the point $P_+$ is an unstable node and for $a>1$ is a saddle.

In the chart $(U_1,F_1)$ we obtain the two infinite singular points $O_1(0,0)$ and $Q(-1/3,0)$. The origin $O_1$ is a saddle, and the point $Q_+$ has eigenvalues 0 and $-a/2$, so it is semi-hyperbolic. By Theorem 2.19 of [20] we obtain that the point $Q$ is a saddle–node. The origin of the chart $(U_2,F_2)$ is a stable node.

The local and the global phase portraits of system (7) are given in Figures 12, 13, 14, 15 and 16.

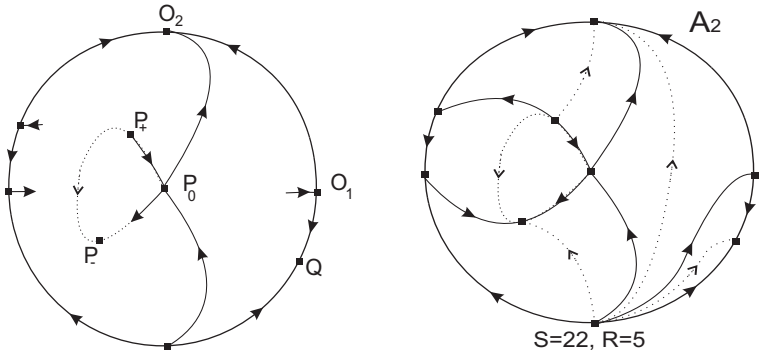


FIGURE 12. The local and the global phase portraits of system (7). Here $c=0$, $b=1$ and $a\in(0,1)$.

For $a=1$ system (8) has only two singular points. The origin has eigenvalues $0, 2$ and using Theorem 2.19 of [20] it is a saddle–node. The singular point $(-5/9,\ -10/27)$ is a stable node and is on the curve $f_2=0$, see Figure 13.

**Case 2:** $c\neq 0$. Without loss of generality we can consider $c=1$. System (2) becomes

$$\begin{aligned} \dot{x} &= ax + by + ax^2 + (3b-2)xy, \\ \dot{y} &= bx + ay + x^2 + \frac{3}{2}axy + \left(\frac{9}{2}b - 3\right)y^2. \end{aligned} \tag{9}$$

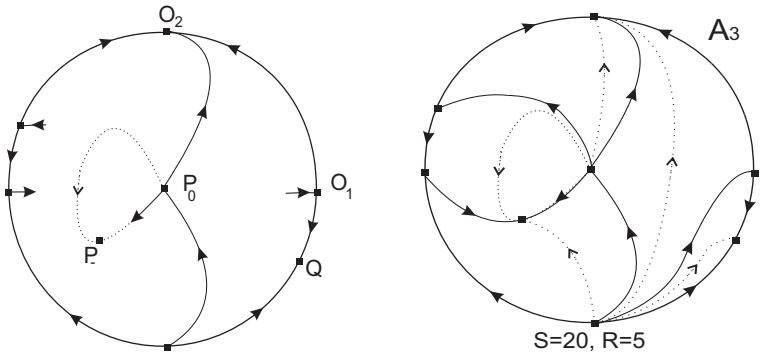


FIGURE 13. The local and the global phase portraits of system (7). Here $c = 0$, $a = b = 1$.

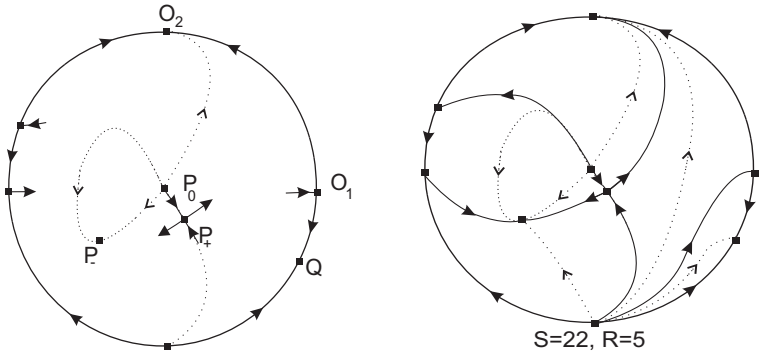


FIGURE 14. The local and the global phase portraits of system (7). Here $c = 0$, $b = 1$ and $a \in (1, \sqrt{3})$.

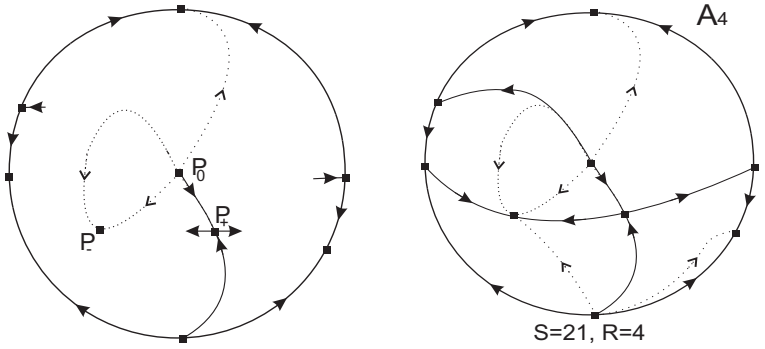


FIGURE 15. The local and the global phase portraits of system (7). Here $c = 0$, $b = 1$ and $a = \sqrt{3}$.

System (9) has the following finite singular points (whenever are defined):

$$P_0 = (0, 0), \qquad P_1 = \left(-b, \frac{a}{3}\right), \qquad P_\pm = (x_0, y_0),$$

with

$$x_0 = \frac{a^2 - 6\,b^2 + 4\,b \pm a\sqrt{24\,b^2 - 40\,b + a^2 + 16}}{2\,(3\,b - 2)^2},$$
$$y_0 = \frac{-9\,ab^2 + 18\,ab - a^3 - 8\,a \pm (3\,b^2 - a^2 - 2\,b)\sqrt{24\,b^2 - 40\,b + a^2 + 16}}{2\,(3\,b - 2)^3}.$$

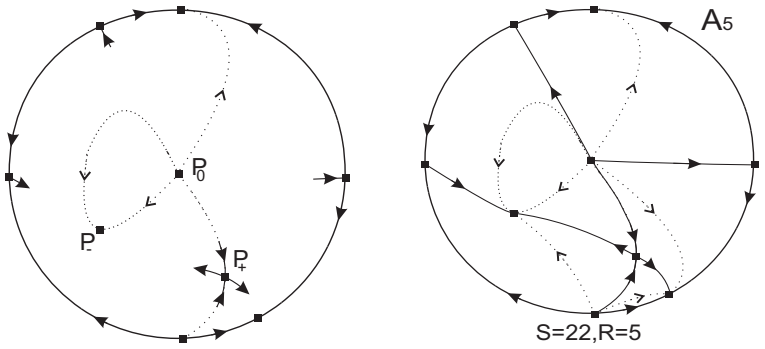


FIGURE 16. The local and the global phase portraits of system (7). Here $c = 0$, $b = 1$ and $a > \sqrt{3}$.

In the chart $(U_1, F_1)$ system (9) has the infinite singular points (whenever they exist)

$$Q_{\mp} = \left( \frac{-a \pm \sqrt{a^2 - 24\,b + 16}}{2(3\,b - 2)}, \quad 0 \right).$$

The origin of the chart $(U_2, F_2)$ is an infinite singular point of system (9).

We define the following bifurcations curves

$$\begin{array}{ll} g_1 = a^2 + 16 - 24b, & g_5 = a + b = 0, \\ g_2 = 3b - 2 = 0, & g_6 = 9a^2b^2 - 24a^2b + 64a^2 - 432b^2 + 432b^3 = 0, \\ g_3 = 24\,b^2 - 40\,b + a^2 + 16 = 0, & g_7 = a^2 + 9b^3 - 9b^2. \\ g_4 = a - b = 0, & \end{array}$$

We also consider the curves

$$h = a^2 + \sqrt{g_1}\,a - 6\,b^2 + 4\,b, \qquad j_1 = b - \frac{1}{3}a. \tag{10}$$

2.4. **Finite Singular Points.**

**Lemma 2.** *The number of finite singular points of system* (9) *is given in Figure* 18.

*Proof.* Note that the points $P_{\pm}$ are not defined whenever $g_2 = 0$ and also when $g_3 < 0$. Addicionally, on $g_3 = 0$ the two points $P_{\pm}$ collide between them. Moreover, on the curve $g_7 = 0$ for $b \in (-\infty, 0)$ the point $P_1$ collide with the point $P_+$ and for $b \in (0, 1)$ the point $P_1$ collide with $P_-$. For $a = b = 8/9$ the point $P_+$ collide with $P_0$ whereas the point $P_-$ collide with $P_1$. On the straight line $g_5 = 0$ the point $P_+$ colapse with $P_0$. On $g_4 = 0$ for $a = b > 4/5$ the point $P_+$ colapse with $P_0$, whereas for $0 < a = b < 4/5$ the point $P_-$ colapse with $P_0$. Finally for $a = b = 4/5$ the points $P_{\pm}$ collide with the point $P_0$. □

**Lemma 3.** *The local phase portrait at the point* $P_0$ *is given in Figure* 19.

*Proof.* The point $P_0$ has eigenvalues $a \pm b$. Hence for $b > a$ or $b < -a$ we have that $P_0$ is a hyperbolic saddle. For $b > a$ or $b > -a$ the point $P_0$ is a hyperbolic unstable node. Over the straight lines $g_4 = 0$ and $g_5 = 0$ the point $P_0$ is a semi–hyperbolic singular point, and from Theorem 2.19 of [20] we have that for $a \neq 4/5$ it is a saddle–node whereas for $a = 4/5$ it is a saddle. □

**Remark 4.** *The finite singular points* $P_{\pm}$ *are always points of the invariant curve* $f_2 = 0$. *So cannot be foci or centers.*

**Lemma 5.** *The local phase portrait at the point* $P_1$ *is given in Figure* 20.

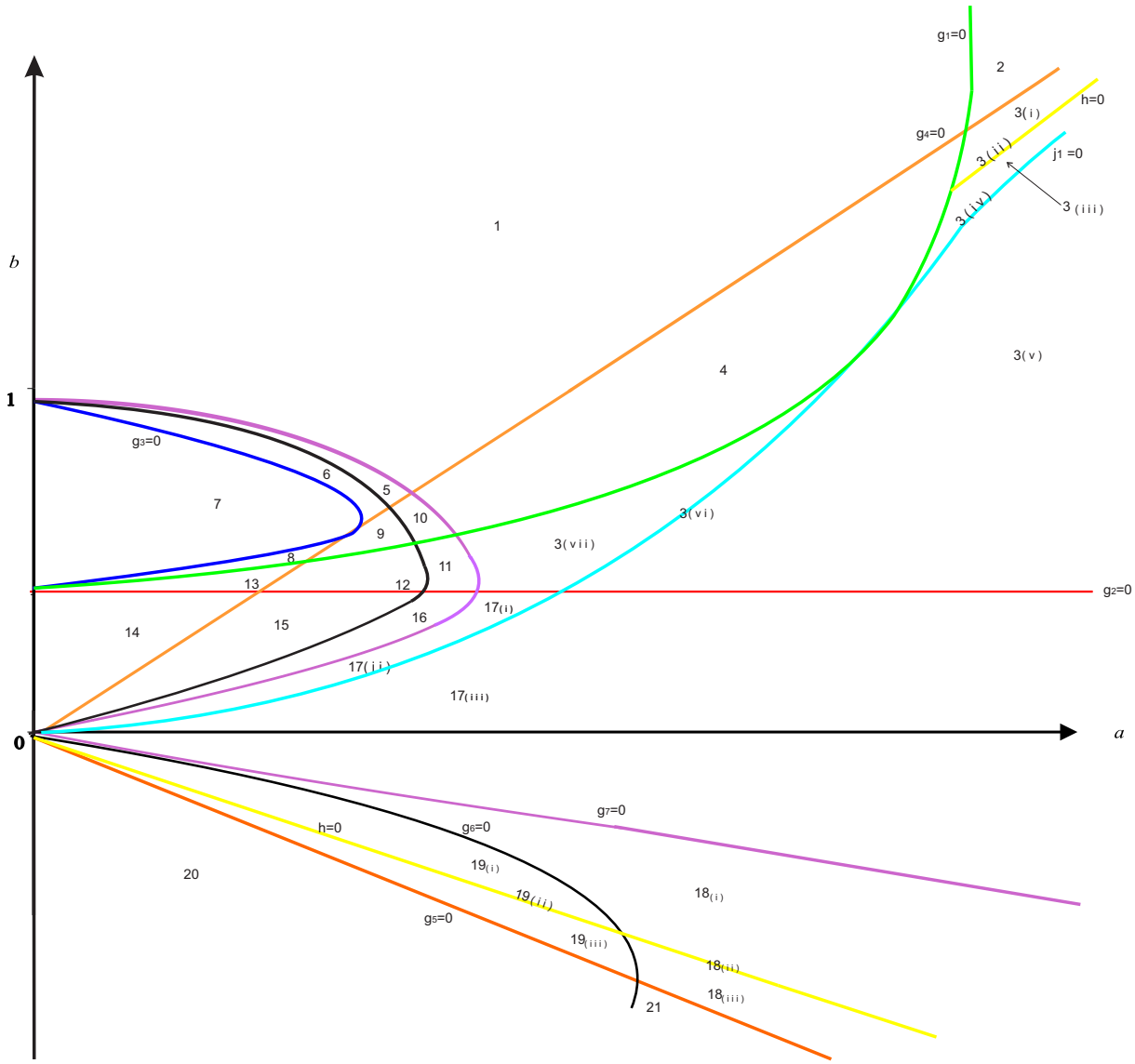


FIGURE 17. $c = 1, a > 0$. The bifurcation curves define 21 regions. It is a qualitative picture.

*Proof.* The point $P_1$ has eigenvalues $e_\pm = ab/4 - a/3 \pm \sqrt{g_6}/12$. For $g_6 < 0$ the eigenvalues become comblex with non–zero real part. On $g_6 = 0$ we have that $e_+ = e_-$ and $P_1$ is a node and for $g_6 > 0$ we have two different real eigenvalues. Note that $e_- e_+ = -g_7/3$. Hence, for $g_7 > 0$ we have that $P_1$ is a hyperbolic saddle, whereas for $g_7 < 0$ and $g_6 > 0$ the point $P_1$ is a hyperbolic stable node. On $g_7 = 0$one of the eigenvalues of $P_1$ becomes zero and $P_1$ is semi–hyperbolic, and from Theorem 2.19 of [20] we have that $P_1$ is a saddle–node. □

**Lemma 6.** *The local phase portrait at the singular point $P_+$ is given in Figure* 21.

*Proof.* We recall that the point $P_+$ is defined for $g_2 \neq 0$ and $g_3 \geq 0$. On the curve $g_3 = 0$ the point $P_+$ coincides with $P_-$. For $a = b = 4/5 \in \{g_3 = 0\} \cap \{g_4 = 0\}$ the points $P_+$ and $P_-$ collide with $P_0$. Additionally, the point $P_+$ has the eigenvalues

$$\frac{a(-a^2 - 42\,b^2 + 76\,b - 32\,) + \left(-a^2 + 24\,b^2 - 16\,b\right)\sqrt{g_3} \pm \sqrt{2A_+}}{8\,(3\,b - 2)^2},$$

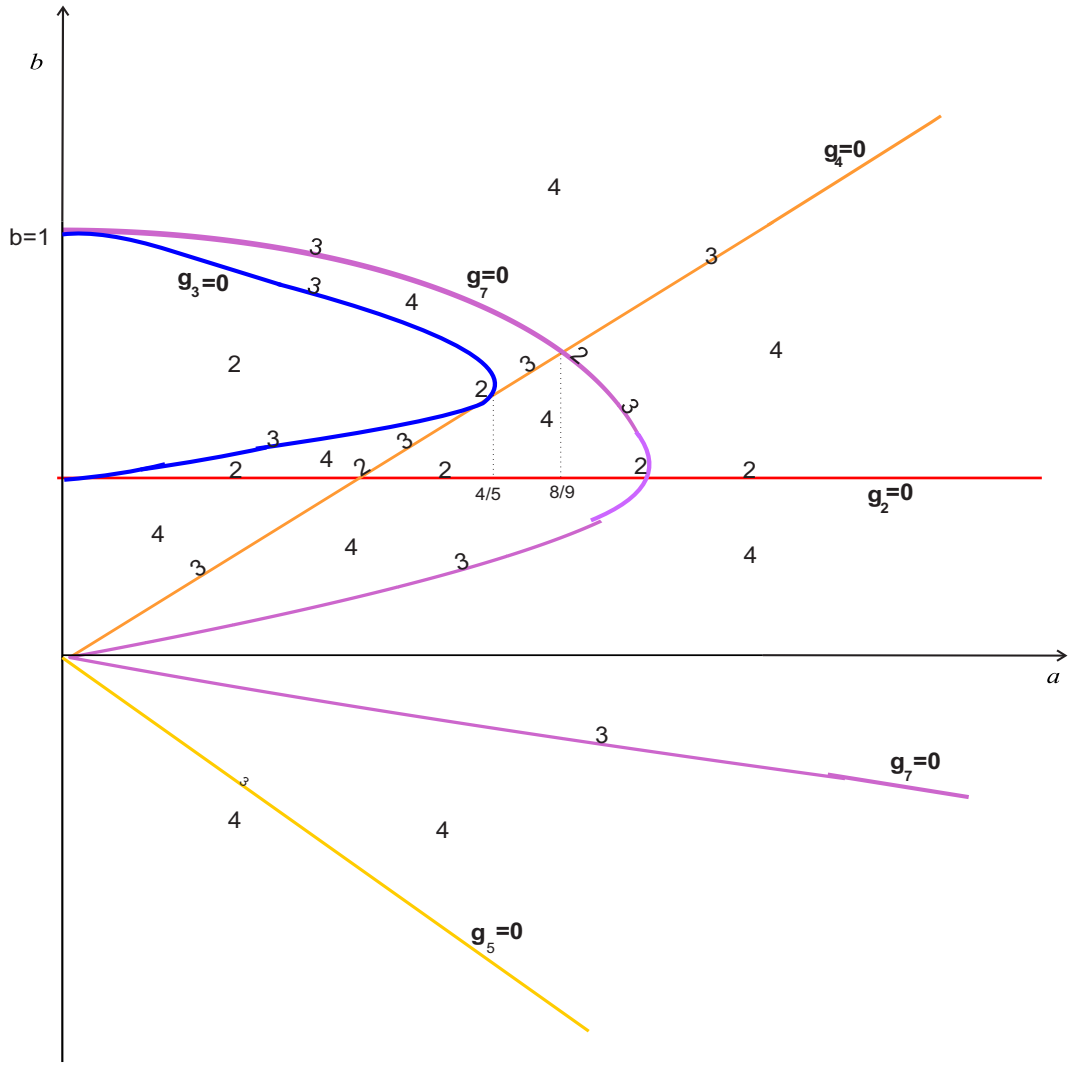


FIGURE 18. The number of finite singular points of system (9) in the different regions, lines and points.

where

$$\begin{aligned} A_{\pm} &= \left(\pm a^5 \pm 18a^3b^2 \pm 72ab^4 \mp 12a^3b \mp 96ab^3 \pm 32a\,b^2\right)\sqrt{g_3} \\ &+a^6 + 30\,a^4b^2 + 378\,a^2b^4 + 1728\,b^6 - 32\,a^4b - 792\,a^2b^3 - 5184\,b^5 + 8\,a^4 \\ &+552\,a^2b^2 + 5760\,b^4 - 128\,a^2b - 2816\,b^3 + 512\,b^2. \end{aligned}$$

We observe that both eigenvalues cannot be zero simultaneously. Note that $A_+ \geq 0$ due to Remark 4. The product of the eigenvalues $det_+$ is

$$det_+ = -\frac{a\left(45\,b^3 + 2\,a^2 - 78\,b^2 + 32\,b\right)\sqrt{g_3}}{4\left(3\,b-2\right)^3} - \frac{g_3\left(-9\,b^3 + 2\,a^2 + 6\,b^2\right)}{4\left(3\,b-2\right)^3}.$$

If $det_+ < 0$ then $P_+$ is a saddle, see Figure 21. Note that $det_+ = 0$ on $g_3 = 0$, $g_5 = 0$ and for $a = b > 4/5$ on $g_4 = 0$. For $b < 0$ on the points of the curve $g_7 = 0$ we have that $det_+ = 0$. In these cases we have that $P_+$ is a semi–hyperbolic singular point and so we apply Theorem 2.19 of [20], see also Figure 21. If $det_+ > 0$ the point $P_+$ is a node, see Figure 21. □

**Lemma 7.** *The local phase portrait at the point $P_-$ is given in Figure 22.*

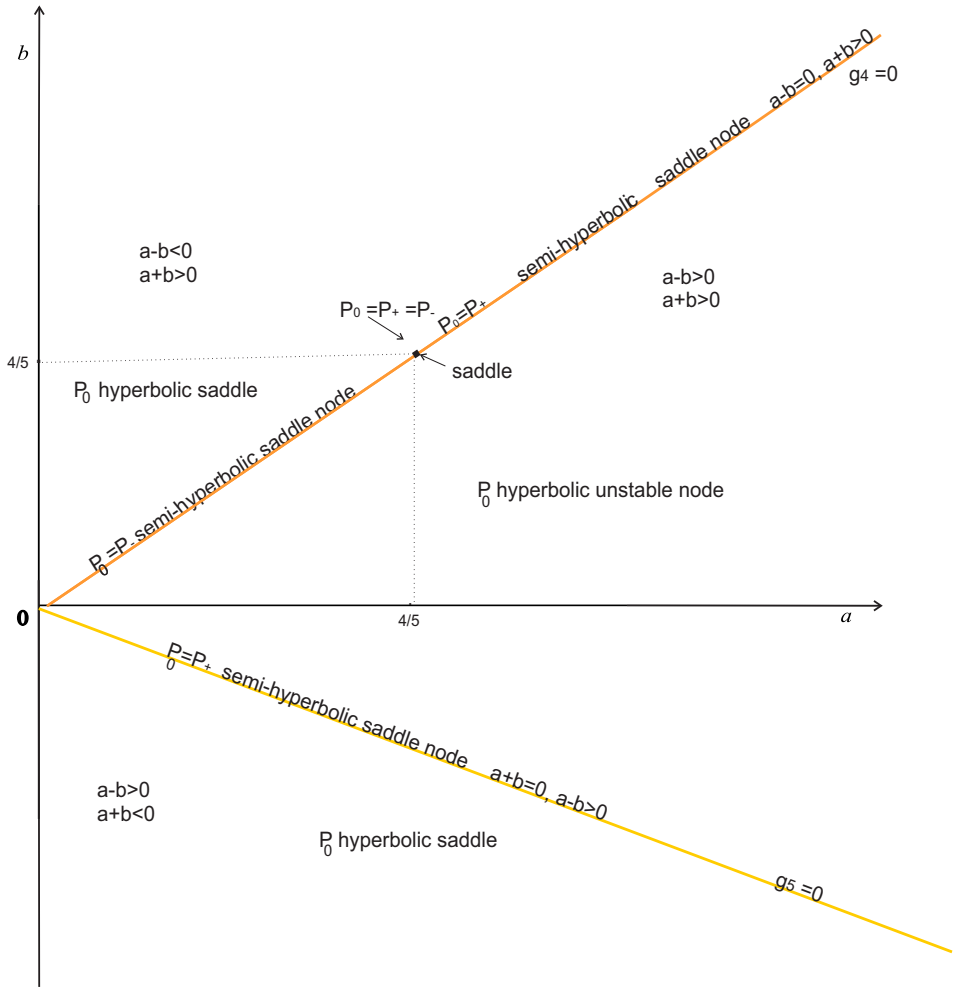


FIGURE 19. The local phase portrait at the origin $P_0 = (0, 0)$.

*Proof.* The point $P_-$ is defined for $g_3 \geq 0$ and $g_2 \neq 0$, and has eigenvalues

$$\frac{a(-a^2 - 42\,b^2 + 76\,b - 32) + \left(a^2 - 24\,b^2 + 16\,b\right)\sqrt{g_3} \pm \sqrt{2A_-}}{8\,(3\,b-2)^2},$$

where $A_-$ is defined in Lemma 6.

Note that for all the values of the parameters we have that $A_- \geq 0$, see also Remark 4. The product of the eigenvalues $det_-$ is

$$det_- = \frac{a\left(45\,b^3 + 2\,a^2 - 78\,b^2 + 32\,b\right)\sqrt{g_3}}{4\,(3\,b-2)^3} - \frac{g_3\,\left(-9\,b^3 + 2\,a^2 + 6\,b^2\right)}{4\,(3\,b-2)^3}.$$

If $det_- < 0$ the point $P_-$ is a saddle, see Figure 22. For $g_3 = 0$ we have that $det_- = 0$. Additionally, for $b > 0$ on the points of $g_7 = 0$ we have that $det_- = 0$. For $b > 4/5$ and additionally $g_4 = 0$ we also have $det_- = 0$. In these cases the point $P_-$ is semi–hyperbolic and so we apply Theorem 2.19 of [20], see Figure 22. If $det_- > 0$ the point $P_-$ is a node, see Figure 22. □

## 2.5. **Infinite singular points.**

**Lemma 8.** *The number of infinite singular points of system* (9) *is given in Figure* 23.

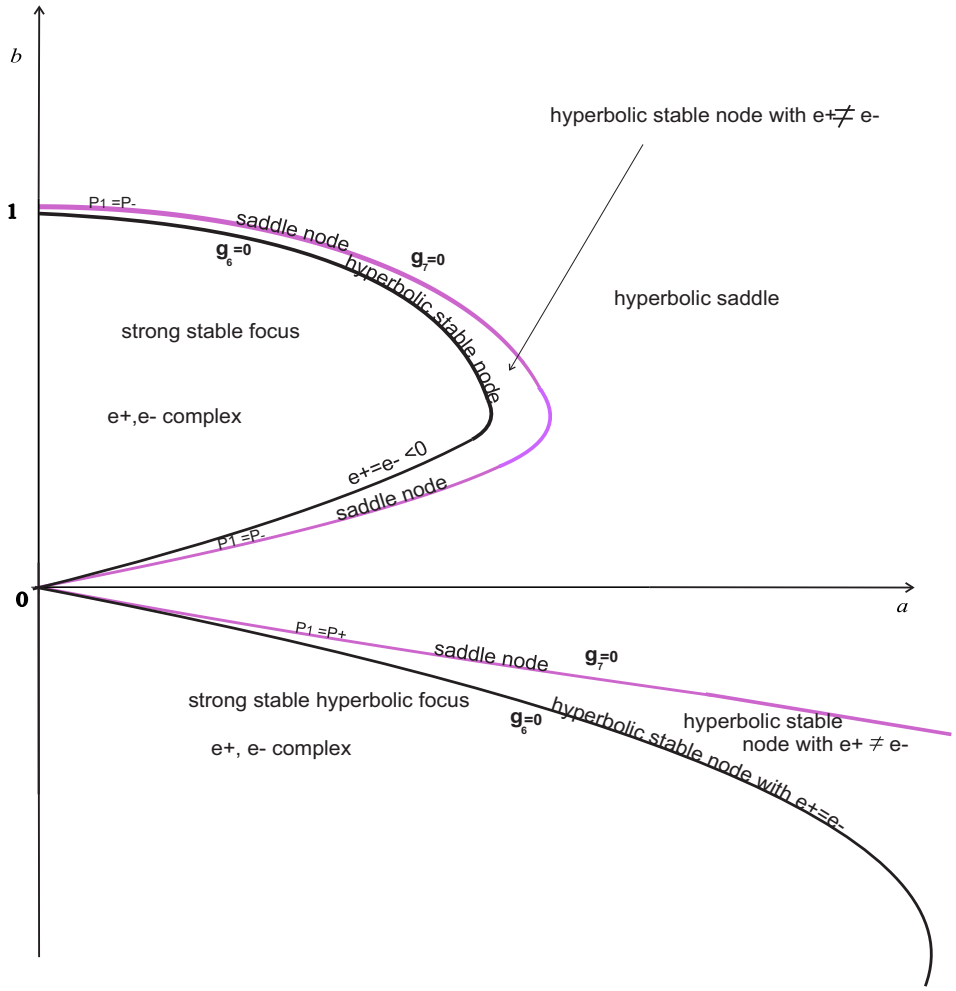


FIGURE 20. The local phase portrait at the singular point $P_1 = (-b, a/3)$.

*Proof.* In the local chart $(U_1, F_1)$ system (9) becomes

$$\begin{aligned}\dot{z}_1 &= 1 + bz_2 + \frac{1}{2}\,az_1 + \left(\frac{3}{2}\,b - 1\right) {z_1}^2 - b{z_1}^2 z_2,\\ \dot{z}_2 &= -z_2\,\left(az_2 + bz_1\,z_2 + a + 3\,bz_1 - 2\,z_1\,c\right),\end{aligned}$$

and for $g_1 \geq 0$ and $g_2 \neq 0$ it has the infinite singular points

$$Q_\pm = \left(\frac{-a \pm \sqrt{g_1}}{2g_2},\quad 0\right).$$

Note that neither $Q_-$ nor $Q_+$ coincide with the origin of the chart $(U_1, F_1)$. The two points $Q_\pm$ collided between them over the curve $g_1 = 0$.

In the local chart $(U_2, F_2)$ system (9) becomes

$$\begin{aligned}\dot{z}_1 &= bz_2 + \left(-\frac{3}{2}\,b + 1\right) z_1 - \frac{1}{2}\,a{z_1}^2 - b{z_1}^2 z_2 - {z_1}^3,\\ \dot{z}_2 &= -\frac{1}{2}\,z_2\,\left(2\,bz_1\,z_2 + 2\,az_2 + 2\,{z_1}^2 + 3\,az_1 + 9\,b - 6\right),\end{aligned}$$

and the origin of the local chart $(U_2, F_2)$ is an infinite singular point. □

**Lemma 9.** *The stability of the infinite singular points of system* (9) *in the local chart* $(U_1, F_1)$ *is given in Figure* 24.

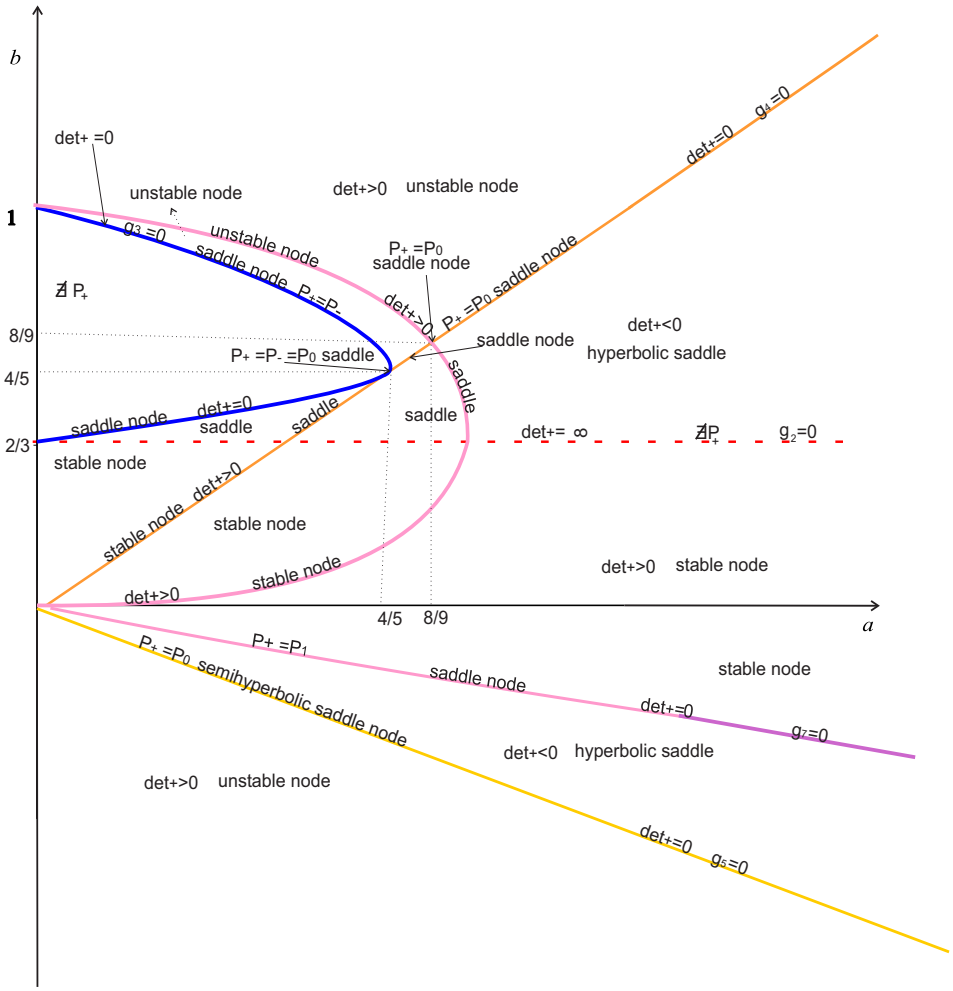


FIGURE 21. The local phase portrait at the singular point $P_+$.

*Proof.* We recall that the points $Q_\pm$ are not defined on $g_2 = 0$. For $g_1 < 0$ are not real points, so we will consider them only when $g_1 \geq 0$. The point $Q_+$ has eigenvalues

$$\frac{-a \pm \sqrt{5\,a^2 + 4\,a\sqrt{g_1} - 96\,b + 64}}{4}.$$

Note that on $g_1 = 0$ the point $Q_+$ collide with $Q_-$ and is a semi–hyperbolic saddle–node. Also note that both eigenvalues at the point $Q_+$ cannot be zero. The product of the eigenvalues is

$$Det_+ = -1/4\,a^2 - 1/4\,a\sqrt{g_1} + 6\,b - 4,$$

and for $g_1 > 0$ we have that $Det_+ < 0$, and so the point $Q_+$ is a saddle. The point $Q_-$ has eigenvalues

$$\frac{-a \pm \sqrt{5\,a^2 - 4\,a\sqrt{g_1} - 96\,b + 64}}{4},$$

and on $g_1 = 0$ is a semi–hyperbolic saddle–node. The product of the eigenvalues at the point $Q_-$ is

$$Det_- = -1/4\,a^2 + 1/4\,a\sqrt{g_1} + 6\,b - 4.$$

The point $Q_-$ changes from a saddle to a node when the values of the parameters of the system cross the line $g_2 = 0$, see Figure 24. □

**Lemma 10.** *For $b < 2/3$ the origin of the local chart $(U_2, F_2)$ is an unstable node. If $b > 2/3$ is a stable node. If $b = 2/3$ the origin is the union of an elliptic and a hyperbolic sector separated by two parabolic sectors.*

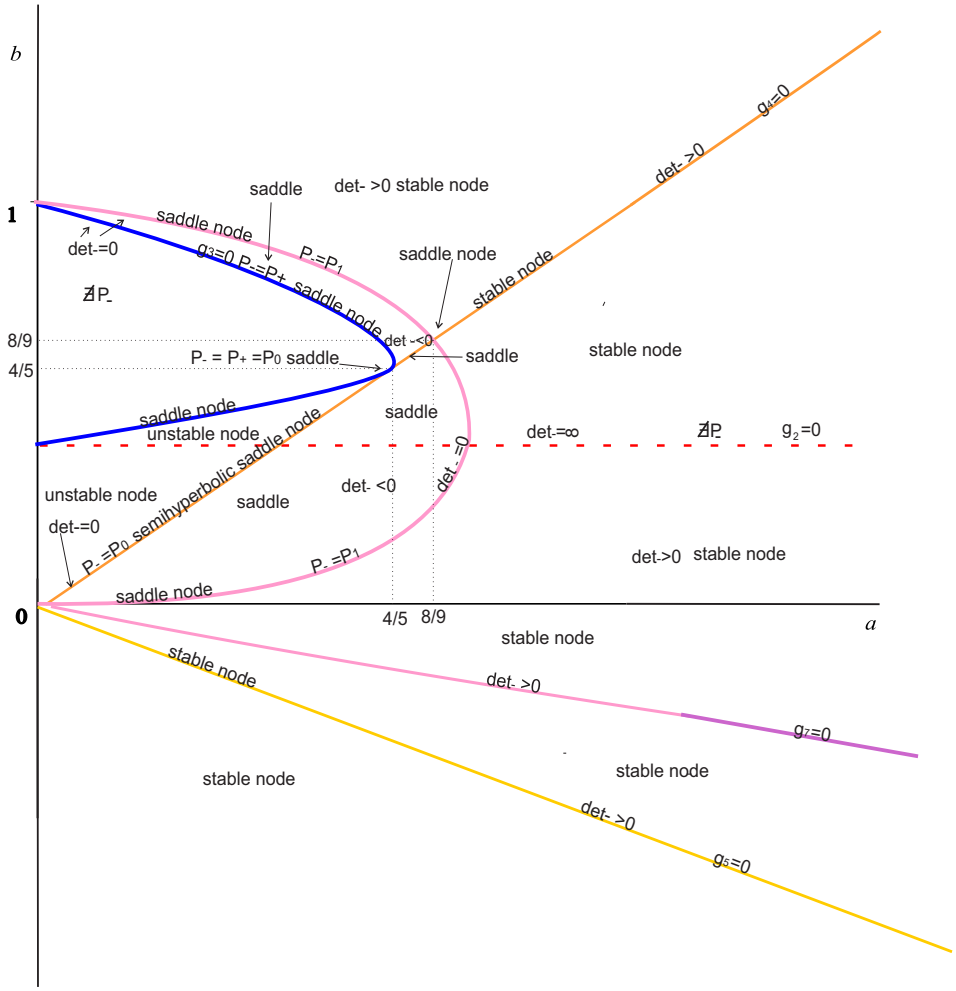


FIGURE 22. The local phase portrait at the singular point $P_-$.

*Proof.* The origin $O_2 = (0, 0)$ of the chart $(U_2, F_2)$ has the Jacobian matrix

$$\begin{pmatrix} -3/2\,b + 1 & b \\ 0 & 3 - 9/2\,b \end{pmatrix},$$

with eigenvalues $-3b/2 + 1$ and $3 - 9b/2$. For $b > 2/3$ the point $O_2$ is a stable hyperbolic node whereas for $b < 2/3$ becomes an unstable hyperbolic node. For $b = 2/3$ both eigenvalues become zero, (the Jacobian is not identically zero) so $O_2$ is a nilpotent singular point. Using Theorem 3.5 of [20] and the blow up technique we obtain that the point $O_2$ is the union of an elliptic and a hyperbolic sector separated by two parabolic sectors. Note that the straight line of the infinity locally is contained in the two parabolic sectors. □

**Proposition 11.** *For $g_1 > 0$ we obtain two distinct infinite singular points $Q_-$ and $Q_+$. On the curve $g_1 = 0$ the two points collided: $Q_- = Q_+$ and one eigenvalue of them becomes zero. For $g_1 < 0$ the two infinite singular points $Q_-$ and $Q_+$ do not exist.*

*On the curve $g_2 = 0$ the singular points $P_\pm$ and $Q_\pm$ do not exist. The point $P_+$ changes from a saddle to a node when the parameters of the system cross the line $g_2 = 0$. $Q_-$ changes from a node to a saddle when the parameters of the system cross this line and at this line the origin of $(U_2, F_2)$ is a nilpotent singular point, see Figure 24.*

*On the bifurcation curve $g_3 = 0$ the two finite singular points $P_\pm$ collided between them. On $g_3 = 0$ for $a = b = 4/5$ the points $P_\pm$ collide to $P_0$. For $g_3 < 0$ the points $P_\pm$ do not exist. For $g_3 > 0$ see Figures 21 and 22.*

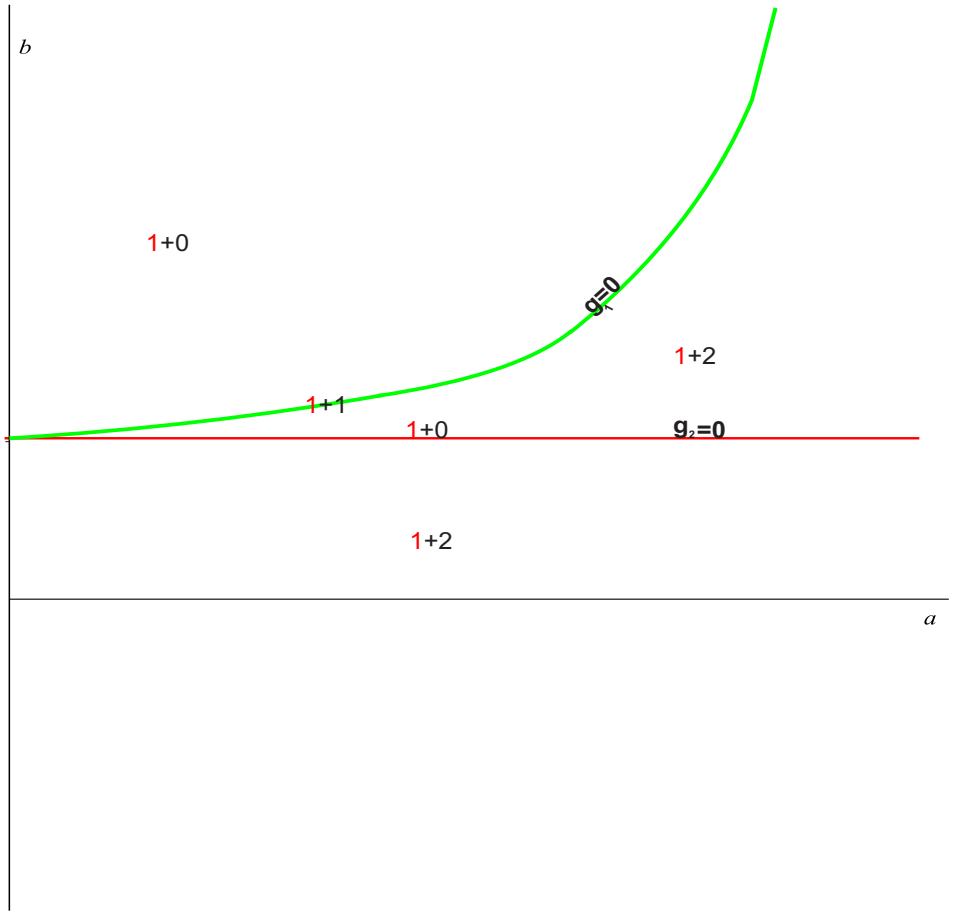


FIGURE 23. The number of the infinite singular points of system (9).

*On the line* $g_4 = 0$ *the point* $P_0$ *for* $a \neq 4/5$ *is a semi–hyperbolic saddle–node, whereas for* $a = 4/5$ *is a saddle. For* $a = b > 4/5$ *the point* $P_+$ *colapse with* $P_0$ *whereas for* $0 < a = b < 4/5$ *the point* $P_-$ *colapse with* $P_0$*. For* $a = b = 4/5$ *both points* $P_\pm$ *collide to* $P_0$ *and is a saddle. For* $a = b \in (4/5, 8/9)$ *the point* $P_-$ *is a saddle whereas for* $a = b > 8/9$ *is a stable node. For* $a = b > 4/5$ *the point* $P_+$ *changes from a saddle to a node. For* $b < 4/5$ *the point* $P_-$ *changes from a saddle to a node when the parameters of the system cross the line* $g_4 = 0$*, see Figures* 18, 19, 21 *and* 22.

*On the line* $g_5 = 0$ *the* $P_0$ *is a semi–hyperbolic saddle–node. The point* $P_+$ *colapse to* $P_0$*. The point* $P_+$ *changes from a saddle to a node when the parameters of the system cross this line, see Figures* 19 *and* 21.

*On the curve* $g_6 = 0$ *the point* $P_1$ *is a hyperbolic stable node. For* $g_6 < 0$ *we have that* $P_1$ *has complex eigenvalues and consequently is a strong stable focus. For* $g_6 > 0$ *we have that* $P_1$ *has real eigenvalues, see Figure* 20.

*On the curve* $g_7 = 0$ *the point* $P_-$ *collided with* $P_1$ *when* $b > 0$ *whereas for* $b < 0$ *the point* $P_+$ *collide with* $P_1$*. Note that the product of the eigenvalues of* $P_1$ *is* $g_7/(-3)$*. On* $g_7 = 0$ *the point* $P_1$ *is a semi–hyperbolic saddle–node.* $P_1$ *changes from a saddle to a node when the parameters of the system cross this line. The point* $P_1$ *changes from a saddle to a node when the parameters of the system cross the line* $g_7 = 0$*, see Figure* 20.

*Proof.* The proof of Proposition 11 follows directly from Lemmas 2, 3, 5, 6, 7, 8, 9 and 10. □

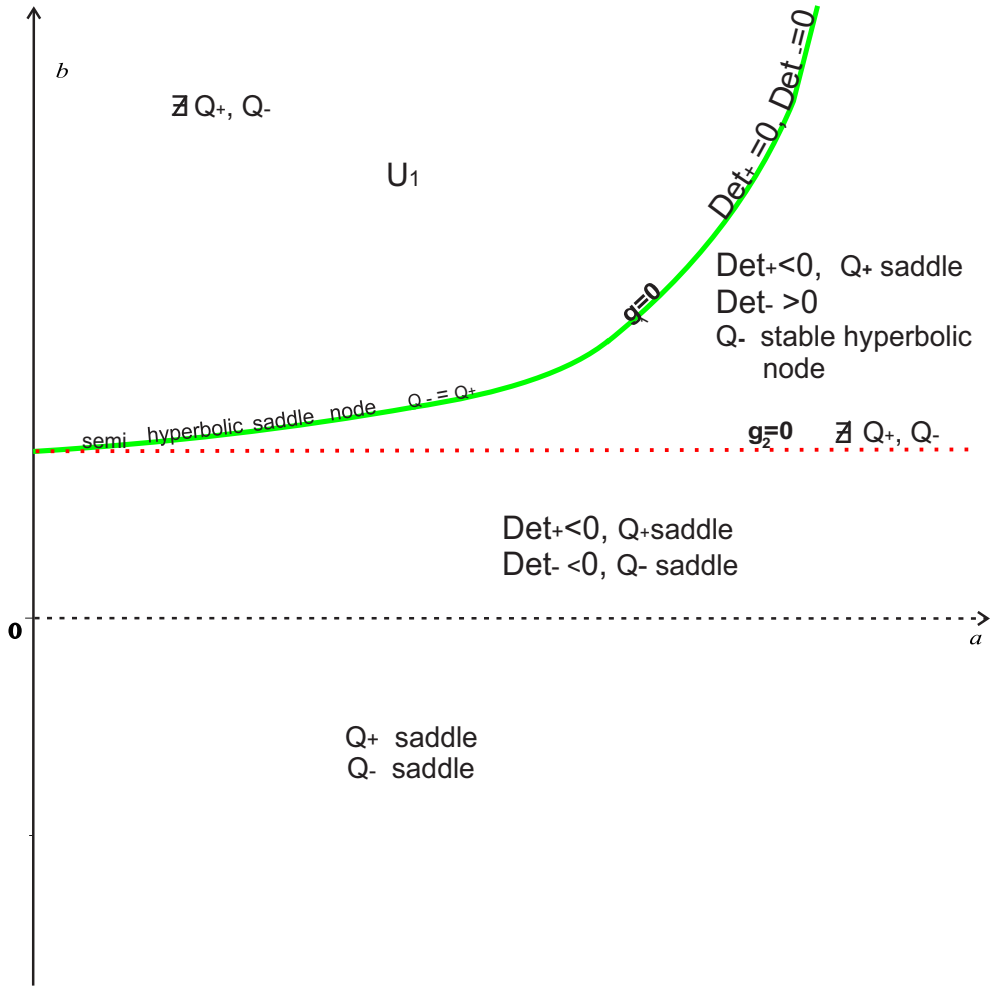


FIGURE 24. The infinite singular points of the local chart $(U_1, F_1)$.

## 3. Phase portraits

In this section we study the global phase portraits of system (9): We draw the local phase portrait of the finite and infinite singular points in the Poincaré disc, see for details on the Poincaré compactification the Appendix 5. Additionally we plot in the Poincaré disc the invariant algebraic curve $f_2 = 0$. Finally, we should present all the global phase portraits.

Let $L$ be a straight line and let $q$ be a point of $L$. We say that $q$ is a *contact point* of the straight line $L$ with a vector field $X$, if the vector $X(q)$ is parallel to $L$.

For quadratic systems the following two results are well known.

**Lemma 12.** *On any straight line which is not invariant the total number of singular points and contact points is two. If there are two such points, $P_1$ and $P_2$, then the orbits intersecting the line $\infty P_1$ cross in the same sense as the orbits intersecting the line $P_2\infty$, and in the opposite sense the orbits $P_1P_2$.*

For a proof of Lemma 12 see the lemma in page 296 of Coppel [14].

**Lemma 13.** *On any non invariant straight line through a finite singular point $P$ reaching the infinity in a pair of infinite singular points the orbits crossing the segment $\infty P$ have opposite sense to the orbits crossing the segment $P\infty$.*

Lemma 13 is equivalent to Lemma 12 when one of the contacts points mentioned in Lemma 12 goes to infinity. For a proof of Lemma 13 see [1].

**Remark 14.** *In what follows when we apply Lemmas 12 or 13 we must check that the straight lines mentioned in these lemmas are not invariant. In case that there are invariant we shall state this fact explicitly.*

The following theorem also appears in Coppel's paper [14].

**Theorem 15.** *A singular point in the interior of a closed path of a quadratic system must be either a focus or a center.*

Here a *closed path* is an invariant curve of the quadratic system contained in $\mathbb{R}^2$ homeomorphic to a circle such that in its neighborhood contained in the bounded region limited by it the Poincaré return map is defined.

**Remark 16.** *In fact the proof which appears in Coppel's paper* [14] *also works when the closed path of the quadratic system has some piece at infinity. So Theorem 15 also holds for closed paths having some orbit at infinity.*

**Theorem 17.** *Let $X$ be a vector field of class $\mathcal{C}^1$ on an open set $\Delta \subseteq \mathbb{R}^2$. Consider $\gamma$ a closed path of $X$ such that the bounded region $\mathcal{R}$ limited by $\gamma$ is contained in $\Delta$. Then there exist a singular point of $X$ in $\mathcal{R}$, inside the region limited by $\gamma$.*

The proof of Theorem 17 is the same as the proof of Theorem 1.31 of [20].

The next result is due to Berlinskiĭ [9].

**Theorem 18.** *Suppose that a quadratic system has four singular points. If the quadrilateral with vertices at these points is convex then two opposite singular points are saddles and the other two are antisaddles (nodes, foci, or centers). But if the quadrilateral is not convex then, either the three exterior vertices are saddles and the interior vertex is an antisaddle, or the exterior vertices are antissaddles and the interior vertex is a saddle.*

Next we prove that system (9) has no limit cycles.

**Lemma 19.** *System* (9) *has no limit cycles.*

*Proof.* Consider system (9) and $X = (P, Q)$ the corresponding vector field. According to Theorem 15 a possible limit cycle can appears only surrounding a focus. Note that for system (9) we only have a focus in the interior of the loop of the curve $f_2 = 0$ for the values of the parameters in the regions $r_6, r_7, r_8, r_9, r_{12}, r_{13}, r_{14}, r_{15}$, and on the lines $L_4, L_5, L_6, L_7, L_{13}, L_{14}, L_{26}, L_{27}, L_{28}, L_{29}$. Also we have a focus on the right side of this curve for the values of the parameters in the regions $r_{19}$ and $r_{20}$ and on the line $L_8$. The divergence of the system $(P f_2^{-4/3},\ Q f_2^{-4/3})$ is

$$D = \frac{\partial(P\, f_2^{-4/3})}{\partial x} + \frac{\partial(Q\, f_2^{-4/3})}{\partial y} = -\frac{a\,(3\,x+4)}{6\,(-x^3-x^2+y^2)^{4/3}} = -\frac{a\,(3\,x+4)}{6 f_2^{4/3}}.$$

Note that the vertical straight line $3x + 4 = 0$ does not intersect the invariant curve $f_2 = 0$. Hence $D$ does not change sign in the regions containing the focus. Hence, by the Bendixon–Dulac criterium (see Theorem 7.12 of [20]) there are no periodic orbits in the mentioned regions and lines in the $(a, b)$ parameter plane, and so there are no limit cycles. □

In what follows a *heteroclinic loop* is formed by two saddles $P_1$ and $P_2$ and two different separatrices connecting these saddles and forming a loop in such a way that at least in one of the two sides of the loop a Poincaré return map is defined. Let $\mu_i < 0 < \lambda_i$ be the eigenvalues of the saddles $P_i$ for $i = 1, 2$. Set

$$k = \frac{\mu_1}{\lambda_1}\frac{\mu_2}{\lambda_2}.$$

If $k < 1$ then the loop in the region limited by it is unstable, and if $k > 1$ then the loop is stable, see Poincaré [36] (see Theorem XVII).

For regions $r_{19}$, $r_{20}$ and the line $L_8$ we have the following result.

**Lemma 20.** *For the values of the parameters in the regions $r_{19}$, $r_{20}$, and on the line $L_8$ system (9) has no connection between the separatrices of the saddles $Q_\pm$.*

*Proof.* We assume that there is a connection between the separatrices of the saddles $Q_\pm$ of system (9) for the values of the parameters in the regions $r_{19}$ and $r_{20}$. Then there is a heteroclinic loop containing a focus. Note that for the points $Q\pm$ (see also Lemma 9)

$$k = \left(\frac{-a - \sqrt{5\,a^2 + 4\,a\sqrt{g_1} - 96\,b + 64}}{-a + \sqrt{5\,a^2 + 4\,a\sqrt{g_1} - 96\,b + 64}}\right)\left(\frac{-a - \sqrt{5\,a^2 - 4\,a\sqrt{g_1} - 96\,b + 64}}{-a + \sqrt{5\,a^2 - 4\,a\sqrt{g_1} - 96\,b + 64}}\right) > 1.$$

Thus the heteroclinic loop is stable. Since the focus in the interior of the heteroclinic loop is also stable it must exist a cicle limit by the Poincaré–Bendixson Theorem (see for instance Corollary 1.30 of [20]). But this is in contradiction with Lemma 19.

Now we consider the values of the parameters on the line $L_8$. If there is a connection between the separatrices of the points $Q_1$ and $Q_2$, then they form a heteroclinic loop that must contain the focus. Working in a similar way as in Lemma 20 for the saddles $Q_1$ and $Q_2$ we obtain

$$k = \frac{\left(-a + \sqrt{5\,a^2 - 4\,a\sqrt{d} + 96\,a + 64}\right)\left(-a + \sqrt{5\,a^2 + 4\,a\sqrt{d} + 96\,a + 64}\right)}{\left(-a - \sqrt{5\,a^2 - 4\,a\sqrt{d} + 96\,a + 64}\right)\left(-a - \sqrt{5\,a^2 + 4\,a\sqrt{d} + 96\,a + 64}\right)} > 1,$$

with $d = a^2 + 24\,a + 16$. Thus this heteroclinic loop is stable. Since the focus in the interior of the heteroclinic loop is also stable by the Poincaré–Bendixon Theorem it must exist a limit cycle. But this is in contradiction with Lemma 19. □

3.1. **Phase portraits in the regions.** The bifurcation curves define 21 regions, see Figure 17. Here we are going to present all the phase portraits of system (9) in the Poincaré disc for the values of the parameters in each one of the 21 regions.

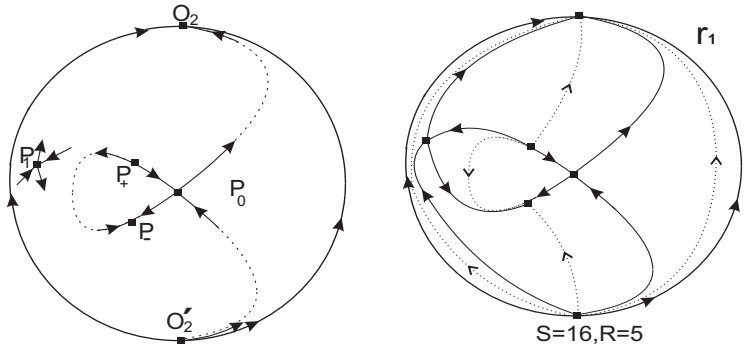


FIGURE 25. The local and the global phase portraits of system (9) corresponding to the region $r_1$.

For the region $r_1$ we realize the following steps, see also Figure 25.

(i) According to Theorem 22 of the Appendix first we draw the separatrices in the Poincaré disc and then we should draw an orbit in each canonical region. This determines completely the global phase portraits in the Poincaré disc.
(ii) We first draw the local phase portrait of the finite and infinite singular points in the Poincaré disc, see Figure 25.
(iii) Next we study the $\alpha --$ and the $\omega --$limits of the separatrices.

(iv) Since in the region $r_1$ does not exist any focus we have that no limit cycle exist for the quadratic system (9), see Theorem 15.

(v) We should only study the separatrices of the point $P_1$ (saddle). The two unstable separatrices can only reach the infinite stable node $O_2$ or the finite stable node $P_-$. Additionally the $\omega--$limit of thess two unstable separatrices cannot be the same stable node, otherwise they should define a closed region and it should contain a stable separatrix without its $\alpha--$limit.

(vi) Finally, we obtain the unique global phase portrait in Figure 25.

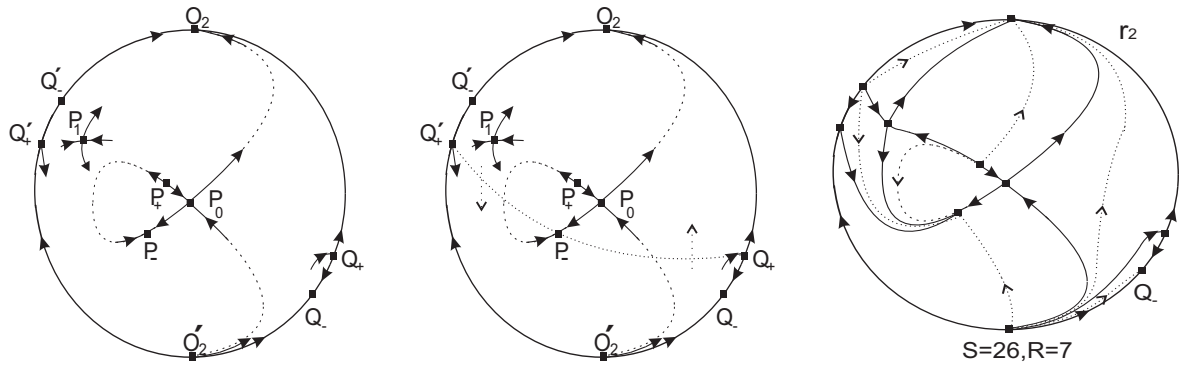


(a) (b) (c)

FIGURE 26. The local and the global phase portraits of systems (9) corresponding to the region $r_2$.

Next we describe the phase portrait of system (9) corresponding to the values of the parameters in the region $r_2$, see Figure 26.

(i) In the finite region the stable separatrix of $Q_+$ can only have as $\alpha--$limit the unstable node $O_2'$.

(ii) By similar arguments as in the region $r_1$ we have that the two unstable separatrices of the point $P_1$ can only have as $\omega--$limit the points $O_2$ and $P_-$.

(iii) The unstable separatrix $\gamma$ of the infinite point $Q_+'$ in the finite region could have as $\omega--$limit the points $P_-$, $P_1$ or $O_2$. Consider the straight line passing on the points $Q_+'$, $P_-$ and $Q_+$. In the region $r_2$ the point $P_1$ is always upper this straight line. According to Lemma 13 the vector field have opposite direction in the two half–lines $Q_+'P_-$ and $P_-Q_+$. Additionally note that $P_1$ is always at the same side of the straight line in the region $r_2$. Therefore the $\omega--$limit of $\gamma$ must be the point $P_-$, see Figure 26(b).

(iv) The two stable separatrices of $P_1$ have the $\alpha--$limits at the points $P_+$ and $Q_-'$.

(v) Finally we obtain the unique global phase portrait in Figure 26(c).

In what follows we describe the phase portrait of system (9) corresponding to the region $r_3$, see Figure 27.

(i) Consider the straight line passing through the points $Q_+, P_+$ and $Q_+'$. We distinguish the following cases.

(i.1) The point $P_-$ is below this straight line, see Figure 27(a). Then the direction of the loop on the curve $f_2 = 0$ determines the direction of the vector field on this line, see also Lemma 13. The separatrices of the points $P_+$, $Q_+$ and $Q_+'$ are as in Figure 27(a).

(i.2) For $a$ and $b$ satisfying the equation $h = 0$ (see (10)) the point $P_-$ belong to this straight line and now the line is invariant for the vector field (9), see Figure 27(b).

(i.3) The point $P_-$ is above this straight line. Then the direction of the vector field in the segment $Q_+'P_+$ is determined by the unstable node $O_2'$ see Figures 27(c),(d),($e_1$),

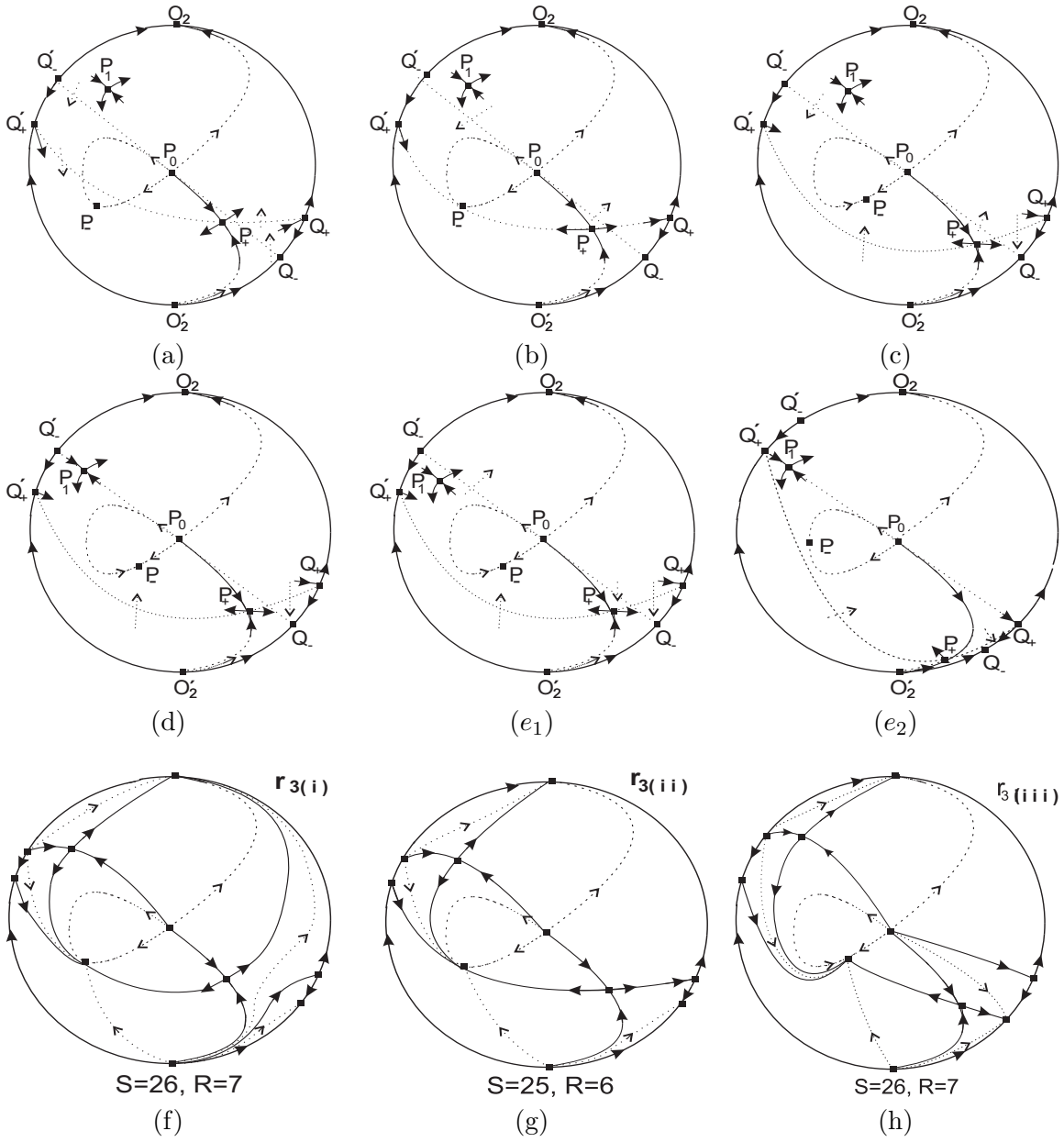


FIGURE 27. The local and the global phase portraits corresponding to the region $r_3$.

$(e_2)$. Also note that the unstable separatrix of the saddle $Q_+$ must be upper this straight line, see also Lemma 13 (and also check the stable separatrix of the saddle $Q'_+$). For the same reason the unstable separatrices of the point $P_+$ must be as they are shown in Figures 27(c),(d),$(e_1)$,$(e_2)$.

Now consider the straight line $L$ passing through the points $Q_-, P_0$ and $Q'_-$.

- ($j_1$) The point $P_1$ can be upper this straight line $L$. Then, the unstable separatrices of $P_1$ can only have $\omega$–limit the points $O_2$ and $P_-$. This determines the direction of the vector field over the straight line $L$, see Figures 27(a),(b),(c).
- ($j_2$) For the values of the parameters $a$ and $b$ in the line $3(iv)$ (so $a, b$ satisfying the equation $j_1 = 0$, see (10)) the point $P_1$ belong to the straight line $L$ and so the line becomes invariant for the vector field (9), see Figure 27(d).
- ($j_3$) The point $P_1$ can be below the straight line $L$. The unstable separatrices determine the direction of the vector field on this line, see Figure 27$(e_1)$.

(ii) In all the cases the unstable separatrices of the point $P_1$ can have as $\omega --$ limit only the points $O_2$ and $P_-$.

(iii) In all the cases the stable separatrices of the point $P_1$ can only have as $\alpha --$ limit the points $P_0$ and $Q'_-$.

(iv) Now consider the straight line $L'$ passing through the points $Q_+, P_0$ and $Q'_+$. In general, the point $P_1$ is above this straight line $L'$. So in general, in the finite region the unstable separatrix of the point $Q'_+$ must be bellow this straight line and therefore its $\omega$-limit must be the point $P_-$. However, for the values of the parameters $a$ and $b$ in the line $3(vii)$ (so $a, b$ satisfying the equation $j_1 = 0$, see (10)) the point $P_1$ belongs to this straight line $L'$ and so becomes invariant, see Figure 27($e_2$).

(v) The local phase portrait (a) yields to the global phase portrait (f). The local phase portrait (b) yields to the global phase portrait (g). The local phase portraits (c),(d),($e_1$) and ($e_2$) yields to the same global phase portrait (h). We summarize: For the values of the parameters in the regions $3(iii), 3(iv), 3(v), 3(vi)$ and $(3vii)$ we obtain the global phase portrait (h), see Figure 27.

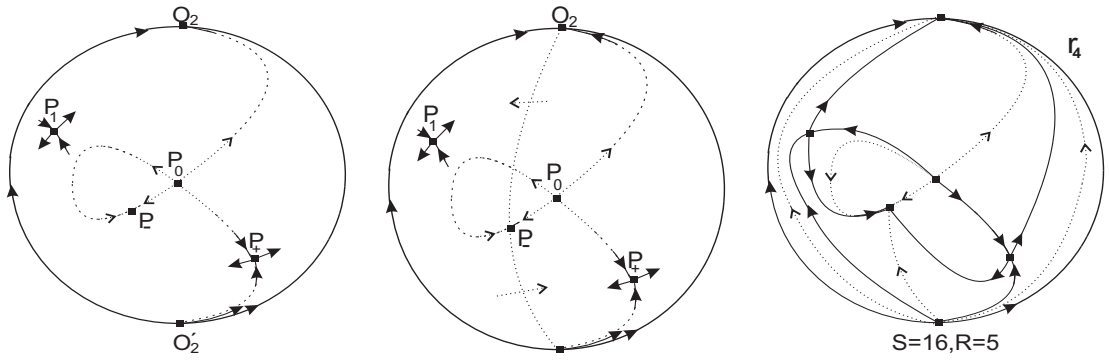


FIGURE 28. The local and the global phase portraits corresponding to the region $r_4$.

Next we describe the phase portrait of system (9) corresponding to the the region $r_4$, see Figure 28.

(i) The unstable separatrices of the point $P_1$ can only have as $\omega --$ limit the points $O_2$ and $P_-$.

(ii) Consider the straight line passing through the points $O_2, P_-$ and $O'_2$. Then the direction of the loop on the curve $f_2 = 0$ determines the direction of the vector field on this line, see also Lemma 13. Then the stable separatrices of $P_1$ can only have as $\alpha --$ limit the points $P_0$ and $O'_2$.

(iii) The unstable separatrices of $P_+$ have as $\omega --$ limit the points $O_2$ and $P_-$.

(iv) Finally we obtain the unique global phase portrait in the region $r_4$, see Figure 28.

Since by Lemma 19 system (9) have no limit cycles the phase portraits corresponding to the regions $r_i$ for $i = 5, 6, 7, 8, 9, 10$ follow immediately from their local phase portraits, see Figures 29, 30, 31, 32, 33 and 34.

In what follows we study the phase portrait of system (9) corresponding to the region $r_{11}$, see Figure 35.

(i) We consider the straight line passing through the points $P_-$ and $P_0$. Note that the points $Q_+, Q_-$ are under this straight line, and that the points $Q'_+, Q'_-$ are upper.

(ii) The unstable separatrices of the points $Q'_+$ and $P_-$ can only have as $\omega --$ limit the point $O_2$.

(iii) Then the unstable separatrix $A$ of the point $P_+$ can only have as $\omega --$ limit the point $O_2$, see also Figure 35(b).

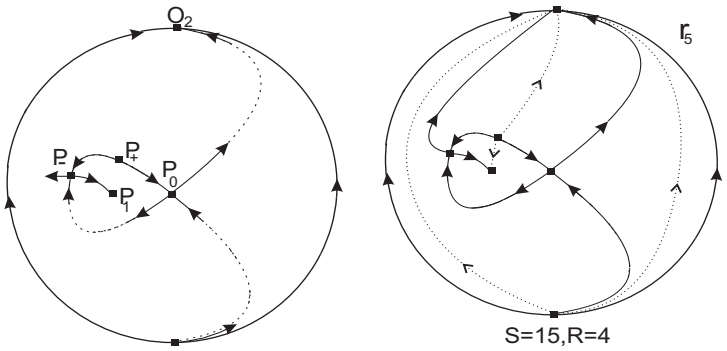


FIGURE 29. The local and the global phase portraits corresponding to the region $r_5$.

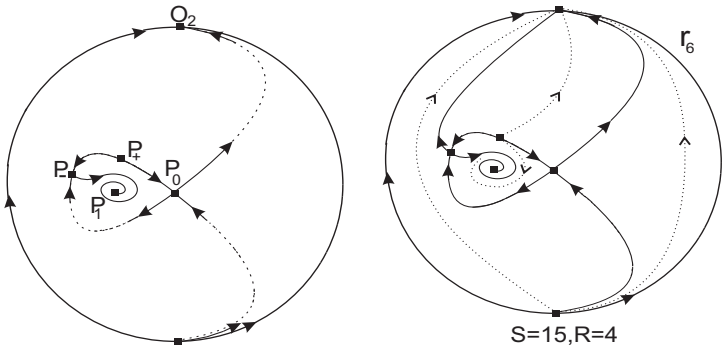


FIGURE 30. The local and the global phase portraits corresponding to the region $r_6$.

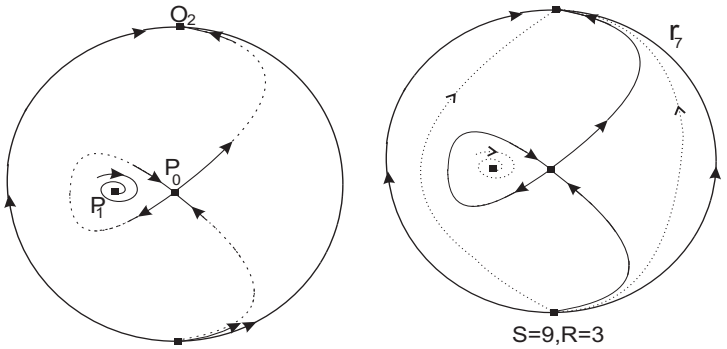


FIGURE 31. The local and the global phase portraits corresponding to the region $r_7$.

(iv) Consider the straight line passing through the points $Q_+$ and $P_+$. Then the unstable separatrix $B$ of the point $P_+$ can only have as $\omega --$ limit the stable node $Q_-$, see also Figure 35(c).
(v) The stable separatrix of the point $Q_+$ can only have as $\alpha --$ limit the point $P_0$.
(vi) Finally we obtain the global phase portrait in the region $r_{11}$, see Figure 35(d).

The phase portraits corresponding to regions $r_{12}$ and $r_{13}$ follow using the same arguments as the ones corresponding to the region $r_{11}$ and are given in Figures 36 and 37 respectively.

Next we describe the phase portrait of system (9) corresponding to the region $r_{14}$, see Figure 38.

(i) Consider the straight line passing through the points $P_0$ and $P_1$. Note that $Q_+$ and $Q_-$ are situated in the opposite sides of this straight line.

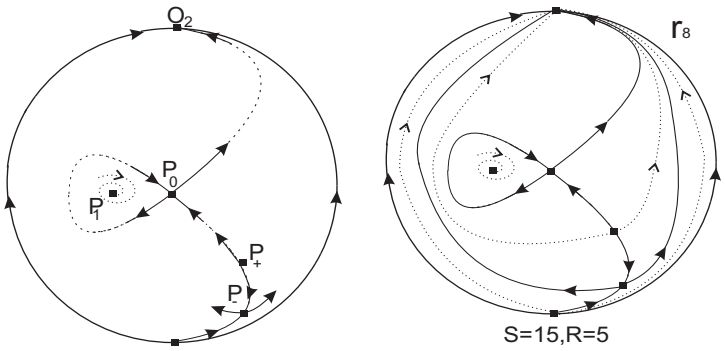


FIGURE 32. The local and the global phase portrait corresponding to the region $r_8$.

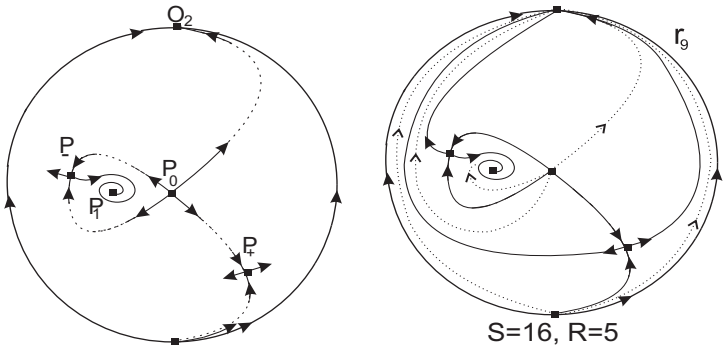


FIGURE 33. The local and the global phase portraits corresponding to the region $r_9$.

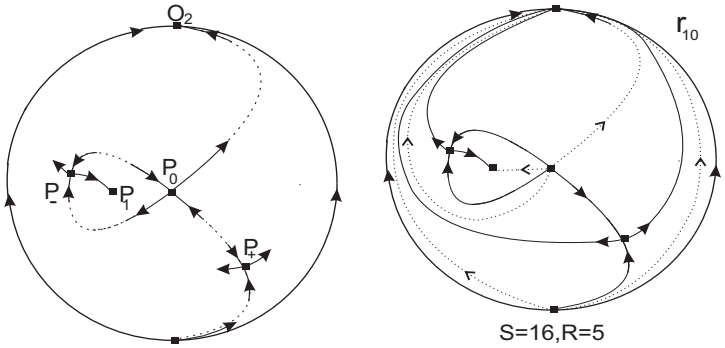


FIGURE 34. The local and the global phase portraits corresponding to the region $r_{10}$.

(ii) The unstable separatrices of the points $Q_+$ and $Q'_-$ can only have as $\omega --$ limit the point $P_+$.
(iii) The stable separatrices of the points $Q_-$ and $Q'_+$ can only have as $\alpha --$ limit the point $P_-$.
(iv) Finally we obtain the global phase portrait in the region $r_{14}$, see Figure 38.

The global phase portraits of system (9) in the regions $r_{15}$ and $r_{16}$ follow by similar arguments as in the region $r_{14}$ and are given in Figures 39 and 40.

Next we describe the phase portrait of system (9) corresponding to the region $r_{17}$, see Figure 41.

(i) Consider the straight line passing through the points $Q_+, P_0$ and $Q'_+$. In the finite region the unstable separatrix $\gamma$ of the point $Q_+$ must be over the straight line, otherwise it must have as $\omega --$limit one of the points $O'_2$ or $Q_-$. If the point $Q_-$ is the $\omega --$limit

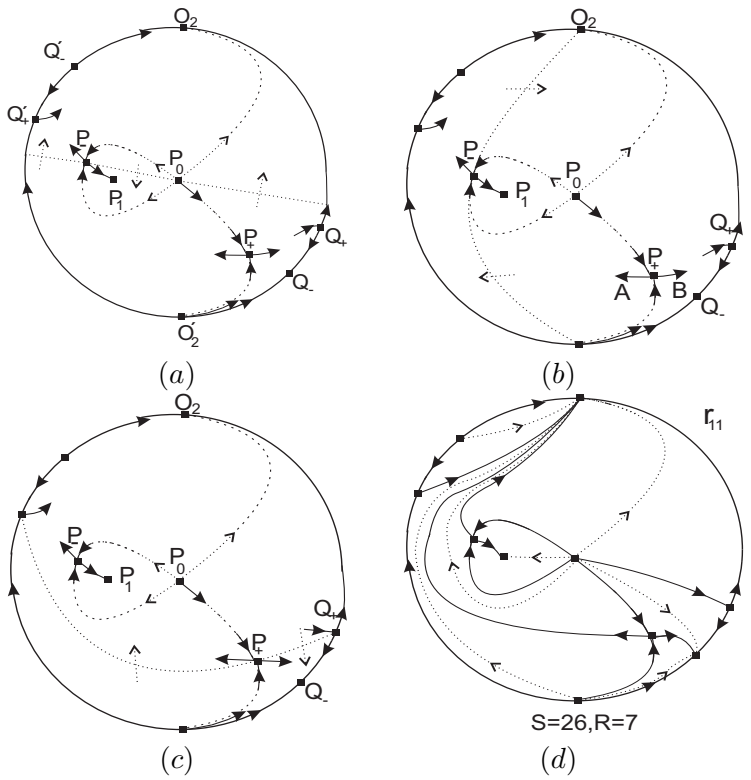


FIGURE 35. The local and the global phase portraits corresponding to the region $r_{11}$.

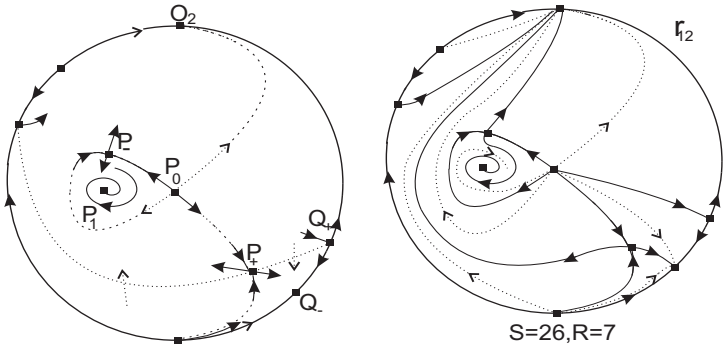


FIGURE 36. The local and the global phase portraits in the region $r_{12}$.

of $\gamma$ then there is a closed path without a singular point in its interior, a contradiction. If the $\omega--$limit of $\gamma$ is the point $O_2'$ then the stable separatrix of the point $Q_-$ cannot have an $\alpha--$limit, a contradiction. So the direction of the vector field on the straight line is determined, see Figure 41(a)). Additionally the $\omega--$limit of $\gamma$ is the point $P_+$. Moreover the stable separatrix of the point $Q_+'$ must be on the upper side of the straight line.

(ii) Consider the straight line passing through the points $Q_-', P_0$ and $Q_-$. We distinguish the following cases for the position of the point $P_1$ with respect to this line:

(ii.1) The point $P_1$ is below this straight line. The direction of the vector field on this straight line is as in Figure 41(b), otherwise one of the unstable separatrices of the point $P_1$ should have as $\omega--$ limit the point $O_2'$. This is a contradiction because then the stable separatrix of the point $Q_+'$ should not have an $\alpha$ limit. Hence in this case the global phase portrait is given in Figure 41(c).

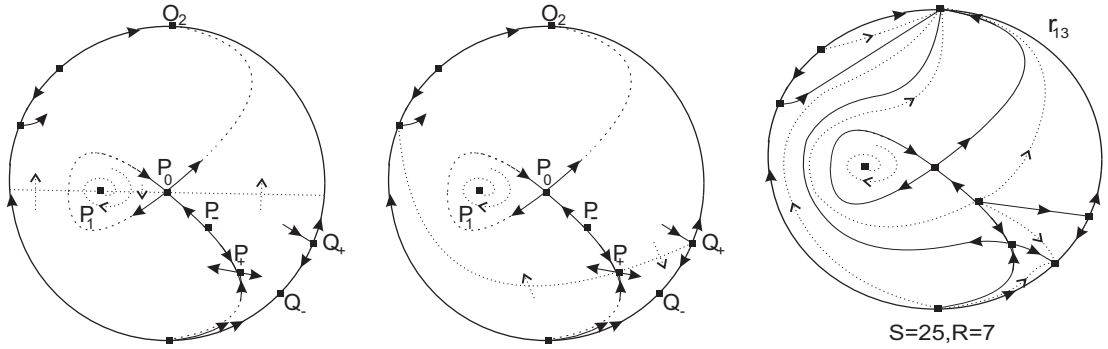


FIGURE 37. The local and the global phase portraits corresponding to the region $r_{13}$.

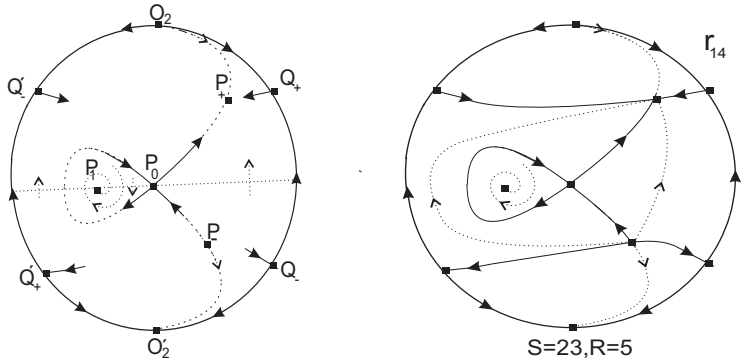


FIGURE 38. The local and the global phase portraits corresponding to the region $r_{14}$.

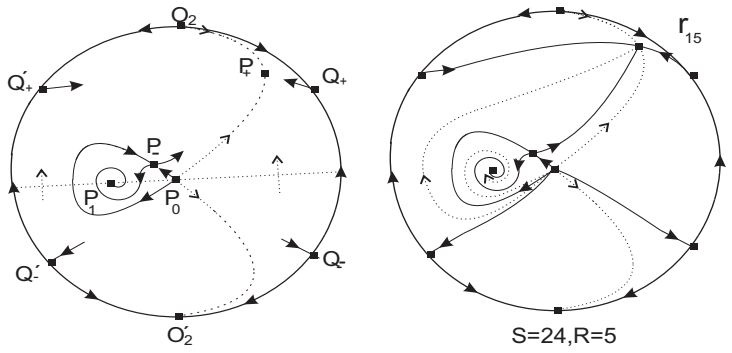


FIGURE 39. The local and the global phase portraits corresponding to the region $r_{15}$.

(ii.2) The point $P_1$ belongs to this straight line and so the straight line is invariant by the vector field (9). This happen when the parameters $a$ and $b$ satisfy equation $j_1 = 0$, see relation (10). Then the unstable separatrix of the point $Q'_-$ can only have as $\omega --$limit the point $P_1$, see Figure 41(d). Then the global phase portrait is given in Figure 41(e).

(ii.3) The point $P_1$ is upper this straight line. Then in the finite region the unstable separatrix $\tilde{\gamma}$ of the point $Q'_-$ must be below this straight line (see Figure 41(f)), otherwise $\tilde{\gamma}$ should have as $\omega --$limit one of the points $P_+$ or $P_1$, see Figure 41(g). If $P_+$ is the $\omega --$limit of $\tilde{\gamma}$ then the unstable separatrices of $P_1$ must go to $P_+$ but then the stable separatrix of $P_1$ has no $\alpha --$limit. So the correct direction of the vector field on the mentioned straight line is the one of Figure 41(f). Now $\tilde{\gamma}$ cannot have as $\omega --$limit the point $Q'_+$. So the only possible $\omega --$limit of $\tilde{\gamma}$ is the point $P_-$. Finally we obtain the global phase portrait, see Figure 41(h).

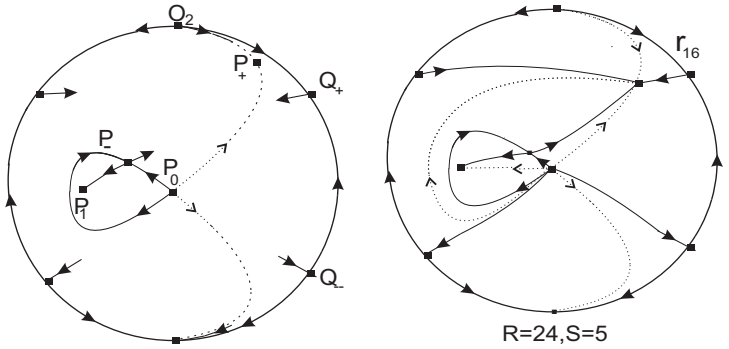


FIGURE 40. The local and the global phase portraits corresponding to the region $r_{16}$.

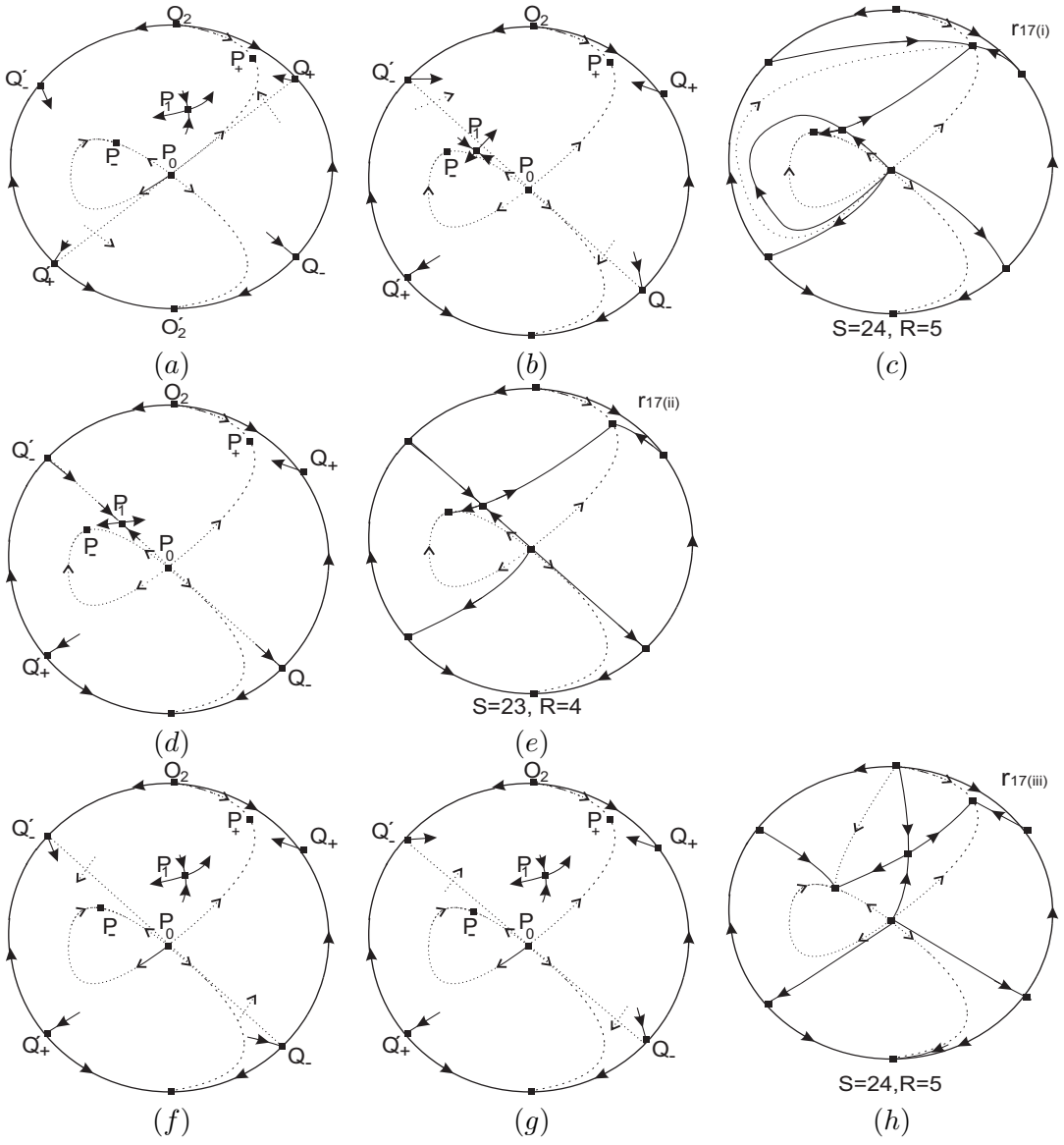


FIGURE 41. The local and the global phase portraits corresponding to the region $r_{17}$.

Next we describe the phase portrait of system (9) corresponding to the region $r_{18}$, see Figure 42.

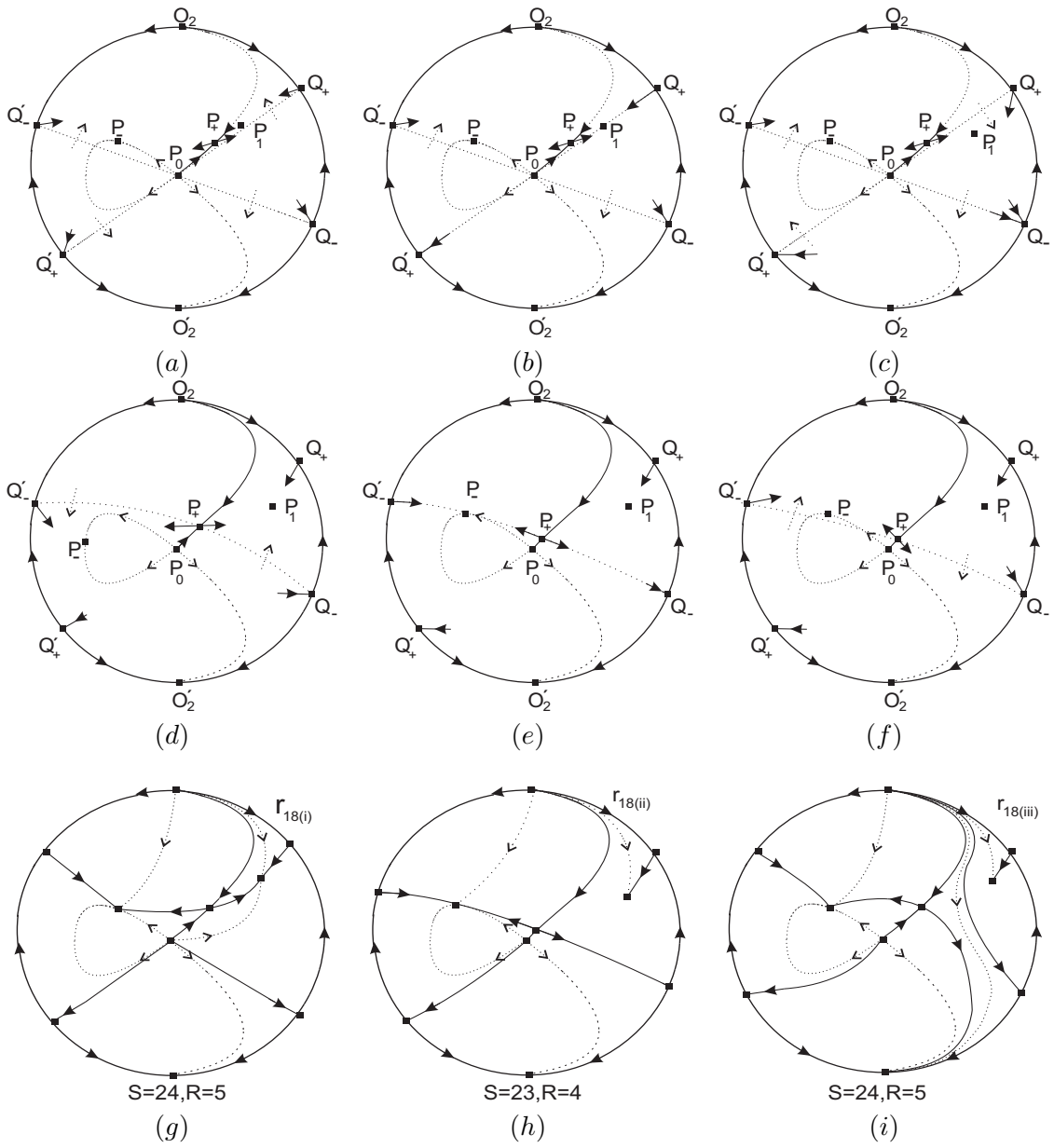


FIGURE 42. The local and the global phase portraits corresponding to the region $r_{18}$.

(i) Consider the straight line passing through the points $Q_-, P_0$ and $Q'_-$. Note that the points $P_1$, $P_-$ and $P_+$ in the region $r_{18}$ are always upper this straight line, see Figure 42(a). The direction of the closed loop of the curve $f_2 = 0$ determines the direction of the vector field over this straight line, see Lemma 13. The unstable separatrix of the point $Q'_-$ is upper this straight line and only can have as $\omega --$ limit the point $P_-$. Additionally the stable separatrix of the point $Q_-$ is upper this straight line.

(ii) Now we prove that there is no connection between the separatrices of the saddles $Q_+$ and $Q_-$. If there is a conexion then in its interior should contain a singular point which must be a focus or a center, and this is a contradiction because $P_1$ is a node, see Theorems 15, 17 and Remark 16.

(iii) Consider the straight line passing through the points $Q_+, P_0$ and $Q'_+$. Note that the points $P_-$ and $P_+$ are always upper this straight line. We consider the following cases for the point $P_1$: (iii.1) The point $P_1$ is upper this straight line, see Figure 42(a). Then, the unstable separatrix $\gamma$ of $Q_+$ must be upper this straight line, otherwise either should

have $O_2'$ as $\omega--$limit, but then the stable separatrix of the point $Q_-$ could not have an $\alpha--$limit, a contradiction; or $\gamma$ connects with the stable separatrix of $Q_-$, but as in (ii) this is a contradiction. This determines the direction of the vector field over this last straight line. Then $\gamma$ can only have as $\omega--$limit the point $P_1$. (iii.2) The point $P_1$ belongs to this straight line, see Figure 42(b). Since this straight line is now invariant, the unstable separatix of $Q_+$ belongs to this line and can only have as $\omega--$limit the point $P_1$. (iii.3) The point $P_1$ is below this straight line, see Figure 42(c). Then the unstable separatrix $\gamma$ of the point $Q_+$ can only be below this straight line. This determines the direction of the vector field over this straight line. Then again the $\omega--$limit of $\gamma$ is the point $P_1$.

(iv) We consider the straight line passing through the points $Q_-, P_+$ and $Q'_-$. We note that on the points of the curve $h = 0$ (see relation (10)) the point $P_-$ belongs to the straight line and system (9) has this straight line invariant. Now we distinguish three cases:

(iv.1) The point $P_-$ is below this straight line. Then the unstable separatrices of the point $P_+$ have as $\omega--$ limit the points $P_1$ and $P_-$, see Figure 42(d).

(iv.2) The point $P_-$ belongs to this straight line. Then the unstable separatrices of the point $P_+$ have as $\omega--$ limit the points $Q_-$ and $P_-$, see Figure 42(e).

(iv.3) The point $P_-$ is upper this straight line. Then the unstable separatrices of the point $P_+$ have as $\omega--$ limit the points $O_2'$ and $P_-$, see Figure 42(f).

(v) $P_0$ is the $\alpha--$ limit of the unstable separatrice of the point $Q'_+$, see Figure 42(a).

(vi) Finally, we obtain the three global phase portraits in the region $r_{18}$ see Figures 42(g),(h) and (i).

Now we study the phase portrait of system (9) corresponding to the region $r_{19}$, see Figure 43.

(i) Consider the straight line passing through the points $Q_+, P_0$ and $Q'_+$ see Figure 43. Note that in the region $r_{19}$ the points $P_-$ and $P_+$ are always upper this straight line and the point $P_1$ is always below the straight line. In the finite region, the unstable separatrix $\gamma$ of the point $Q_+$ is below the straight line, otherwise could not have an $\omega--$limit. This determines the direction of the vector field over the straight line. So the $\omega--$limit of $\gamma$ can only be the point $P_1$. The point $O_2'$ cannot be the $\omega$ limit of $\gamma$ because in this case a stable separatrix of $Q_-$ would be without an $\alpha--$limit. Additionally there is no connection between the separatrices of $Q_+$ and $Q_-$, see Lemma 20.

(ii) Consider the straight line passing through the points $Q_-, P_0$ and $Q'_-$, see Figure 43(c). Note that the point $P_-$ is upper the straight line. Then the direction of the closed loop of the invariant curve $f_2 = 0$ determines the direction of the vector field over this straight line. The unstable separatrix of $Q'_-$ must be over the straight line and can only have as $\omega--$limit the point $P_-$.

(iii) Consider the straight line passing through the points $Q_+, P_+$ and $Q'_+$. For the values of $a$ and $b$ that satisfy equation $h = 0$ (see relation (10)) system (9) has this straight line invariant. Hence we distinguish three cases:

(iii.1) The point $P_-$ is below the straight line. Then the unstable separatrices of the point $P_+$ have as $\omega--$ limit the points $P_1$ and $P_-$.

(iii.2) The point $P_-$ is on the straight line. Then the unstable separatrices of the point $P_+$ have as $\omega--$ limit the points $Q_-$ and $P_-$. (iii.3) The point $P_-$ is upper the straight line. Then the unstable separatrices of the point $P_+$ can only have as $\omega--$ limit the points $O_2'$ and $P_-$.

(iv) Finally we obtain the three global phase portraits in the region $r_{19}$ see Figures 43(a),(b) and (c).

Next we describe the phase portrait of system (9) corresponding to the region $r_{20}$, see Figure 44.

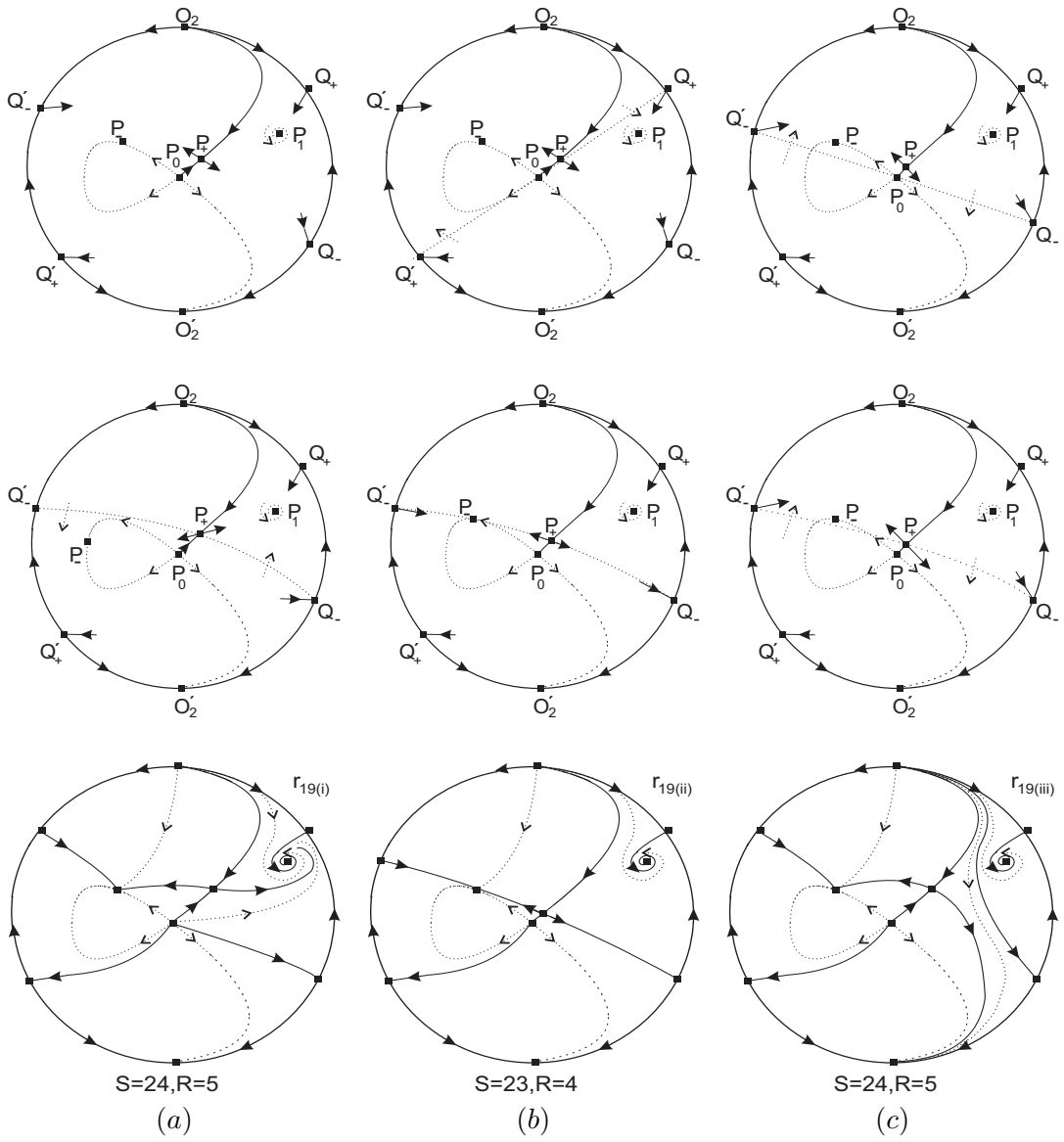


FIGURE 43. The local and the global phase portraits corresponding to the region $r_{19}$.

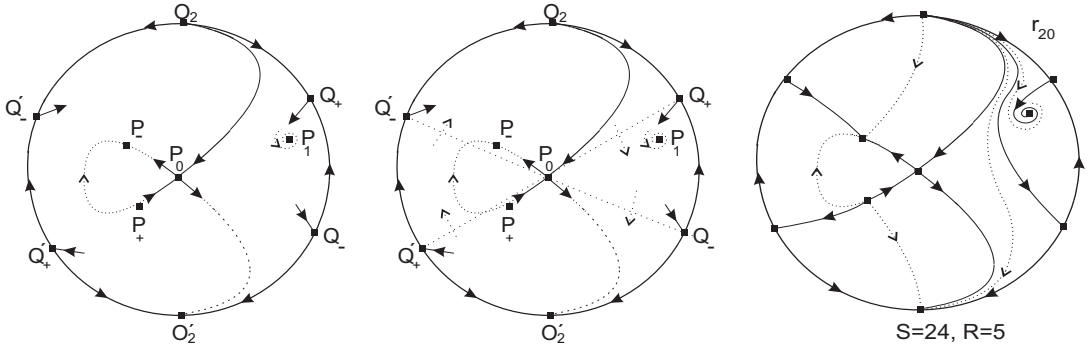


FIGURE 44. The local and the global phase portraits corresponding to the region $r_{20}$.

(i) Consider the straight line passing through the points $Q_-, P_0$ and $Q'_-$. Note that in the region $r_{20}$ the point $P_-$ is always upper the straight line. The direction of the closed loop of the invariant curve $f_2 = 0$ determines the direction of the vector field on this

straight line. The unstable separatrix of $Q'_-$ is upper the straight line and can only have as $\omega--$ limit the point $P_-$. The stable separatrix of the point $Q_-$ is upper this straight line.

(ii) Consider the straight line passing through the points $Q_+, P_0$ and $Q'_+$. Note that in the region $r_{20}$ the points $P_+$ and $P_1$ are always below this straight line. The direction of the closed loop of the invariant curve $f_2 = 0$ determines the direction of the vector field on this straight line. The stable separatrix of the point $Q'_+$ is below the straight line and can only have as $\alpha--$limit the point $P_+$.

(iii) By Lemma 20 we have that there is no connection between the separatrices of $Q_+$ and $Q_-$. Consider the unstable separatrix $\gamma$ of $Q_+$. Then $\gamma$ cannot have $O'_2$ as $\omega--$ limit because then the stable separatrix of $Q_-$ will not have an $\alpha--$limit. Hence the $\omega--$limit of $\gamma$ can only be the point $P_1$.

(iv) Finally we obtain the global phase portrait in the region $r_{20}$, see Figure 44.

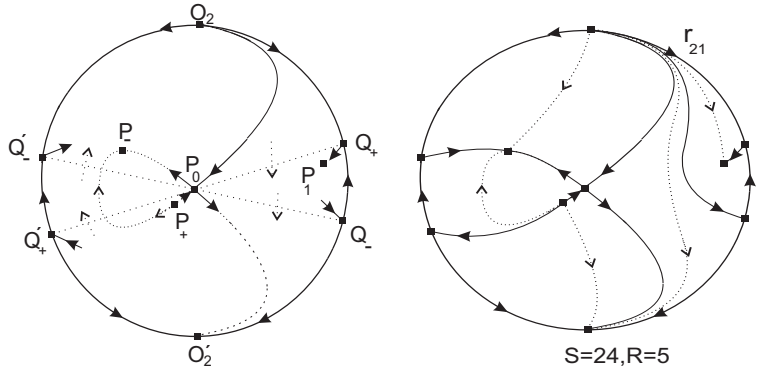


FIGURE 45. The local and the global phase portraits corresponding to the region $r_{21}$.

In what follows we present the phase portrait of system (9) corresponding to the the region $r_{21}$, see Figure 45.

(i) Consider the straight line passing through the points $Q_+$, $P_0$ and $Q'_+$. Then in the region $r_{21}$ the points $P_1$ and $P_+$ are always below this straight line. The stable separatrix of $Q'_+$ can only have as $\alpha--$ limit the point $P_+$.

(ii) Consider also the straight line passing through the points $Q_-, P_0$ and $Q'_-$. Then in the region $r_{21}$ the points $P_-$ and $P_1$ are always upper this straight line. The unstable separatrix $\gamma$ of $Q'_-$ can have as $\omega--$ limit the point $P_-$.

(iii) The unstable separatrix $\tilde{\gamma}$ of $Q_+$ cannot have as $\omega--$ limit the point $Q_-$ because of Theorem 15. If $\tilde{\gamma}$ has as $\omega--$ limit the point $O'_2$ then in the finite region a stable separatrix of $Q_-$ would be without an $\alpha--$ limit. Therefore the only possibility that remains is that $\tilde{\gamma}$ has as $\omega--$ limit the point $P_1$.

(iv) In the finite region the stable separatrix of $Q_-$ must have as $\alpha--$ limit the point $O_2$.

(v) Finally we obtain the global phase portrait in the region $r_{21}$, see Figure 45.

3.2. **Phase portraits on the lines.** The bifurcation curves define 31 lines, see Figure 46. In this section we are going to present the phase portraits of system (9) in each line.

We should provide the details for obtaining the phase portraits on the lines $L_8, L_9, L_{11}, L_{12}$, $L_{24}$ and $L_{25}$. Since the arguments used in the study of the phase portraits corresponding to these lines are the same for studying the remaining lines we only provide their phase portraits in the corresponding figures.

First we explain the phase portrait on the line $L_8$, see Figure 54. By Lemma 20 there is no connection between the separatrices of the points $Q_1$ and $Q_2$. Note that the unstable separatrix of the point $Q_1$ cannot have as $\omega--$ limit the point $O'_2$. In the opposite case using the

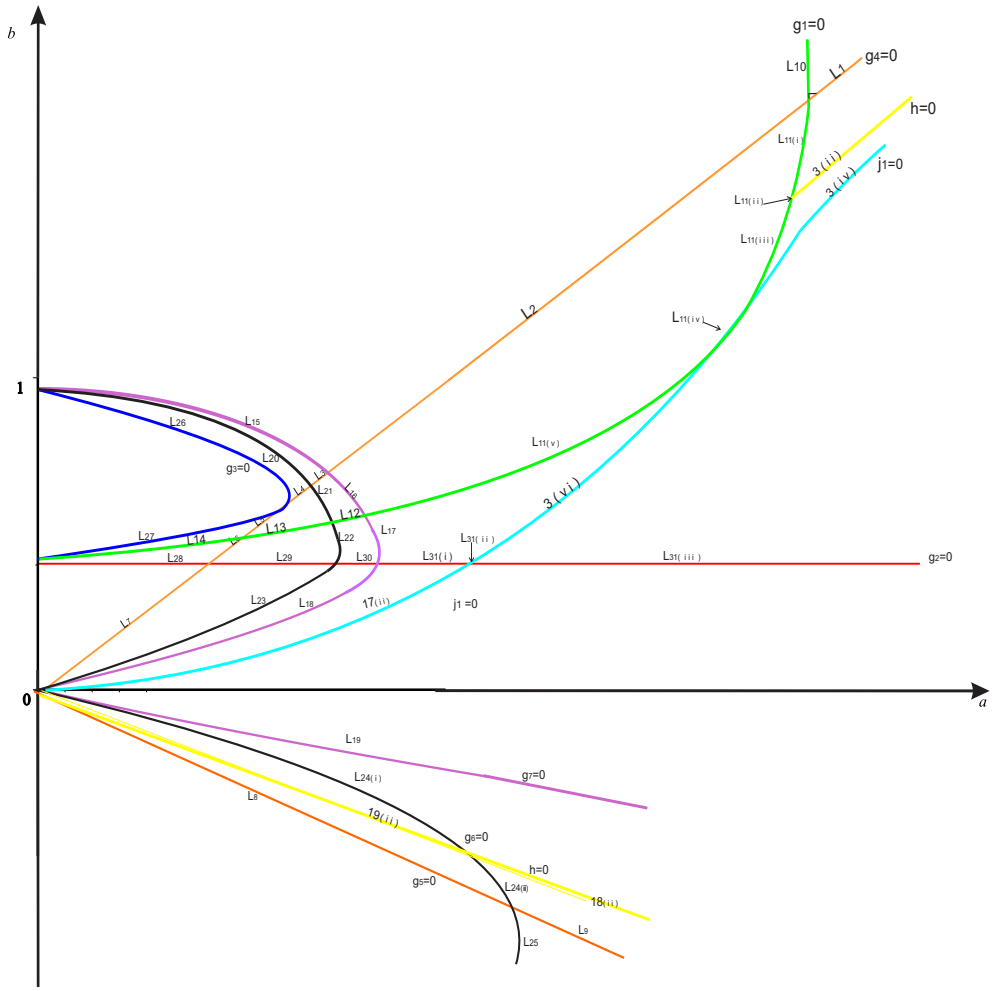


FIGURE 46. $c = 1, a > 0$. The bifurcation curves define 31 lines. It is a qualitative picture.

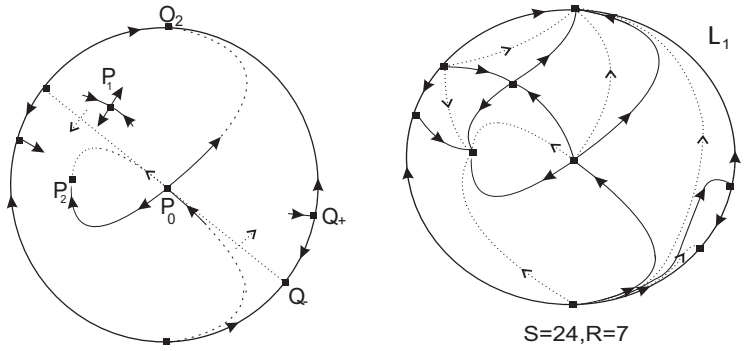


FIGURE 47. The local and the global phase portraits corresponding to the line $L_1$.

continuity we should have a connection between the separatrices of the saddles. Hence, the unstable separatrix of the point $Q_1$ must have as $\omega - -$ limit the point $P_1$. So on the line $L_8$ we obtain a unique global phase portrait, see Figure 54.

For the line $L_9$ note that there is no connection between the separatrices of the saddles $Q_1$ and $Q_2$. If there is a conexion then in its interior should contain a singular point which must be a focus or a center, and this is a contradiction because $P_1$ is a node, see Theorems 15 and

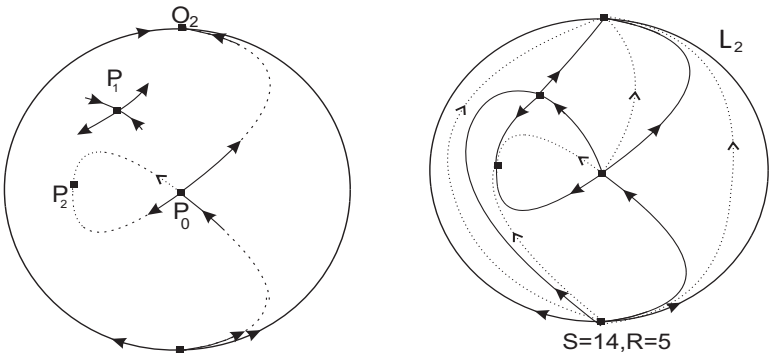


FIGURE 48. The local and the global phase portraits corresponding to the line $L_2$.

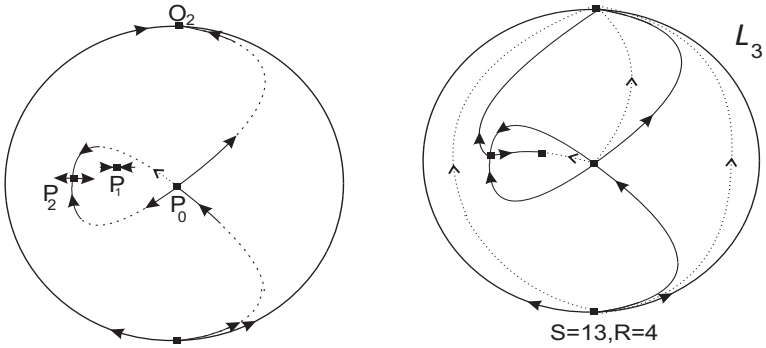


FIGURE 49. The local and the global phase portraits corresponding to the line $L_3$.

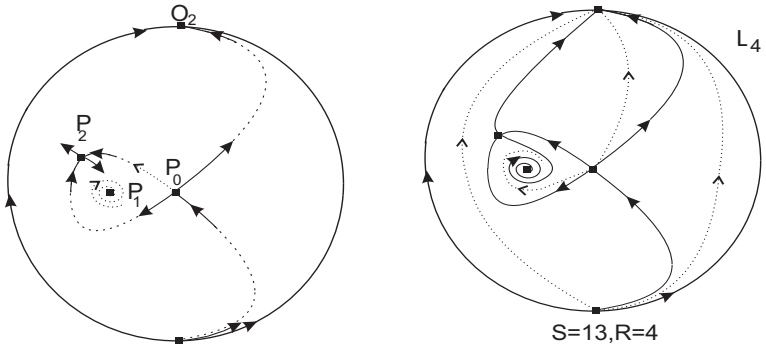


FIGURE 50. The local and the global phase portraits corresponding to the line $L_4$.

17. Now we apply similar arguments as the ones for studying the phase portrait on the line $L_8$ and we obtain the unique global phase portrait on the line $L_9$ given in Figure 55.

Now we will describe the phase portrait on the line $L_{11}$, see Figure 57.

(i) For $a > 4\sqrt{5}$ the point $P_-$ is below the straight line passing through the points Q,$P_+$ and $Q'$, see Figure 57, $L_{11}(i)$.
(ii) The straight line passing through the points $Q, P_+$ and $Q'$ becomes invariant for $a = 4\sqrt{5}$. In this case the point $P_-$ belong to this line, see Figure 57, $L_{11}(ii)$.
(iii) For $4 < a < 4\sqrt{5}$ the point $P_-$ is upper the straight line passing through the points Q,$P_+$ and $Q'$, see Figure 57, $L_{11}(iii)$.
(iv) Consider the straight line passing through the points $P_0, Q$ and $Q'$. For $a > 4$ the point $P_1$ is upper this straight line, see Figure 57, $L_{11}(i), L_{11}(ii), L_{11}(iii)$. For $a = 4$ this straight line becomes invariant. In this case the point $P_1$ belong to this line, see Figure 57, $L_{11}(iv)$. For $a < 4$ the point $P_1$ is below this straight line, see Figure 57, $L_{11}(v)$.

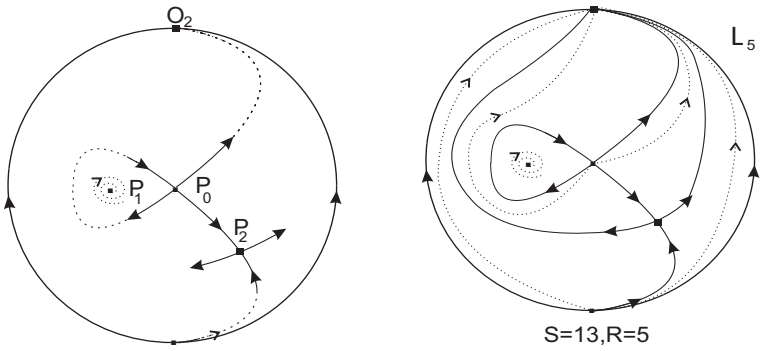


FIGURE 51. The local and the global phase portraits corresponding to the line $L_5$.

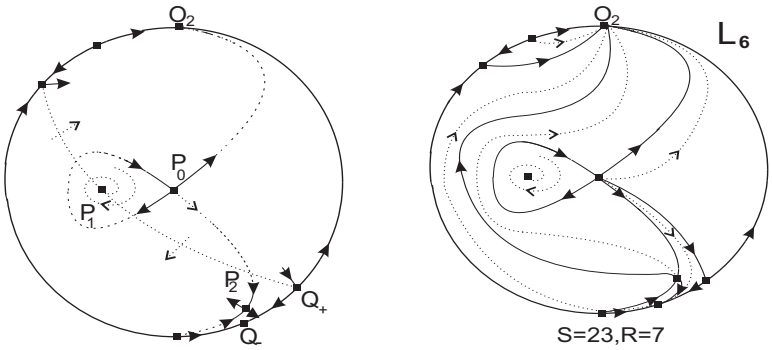


FIGURE 52. The local and the global phase portraits corresponding to the line $L_6$.

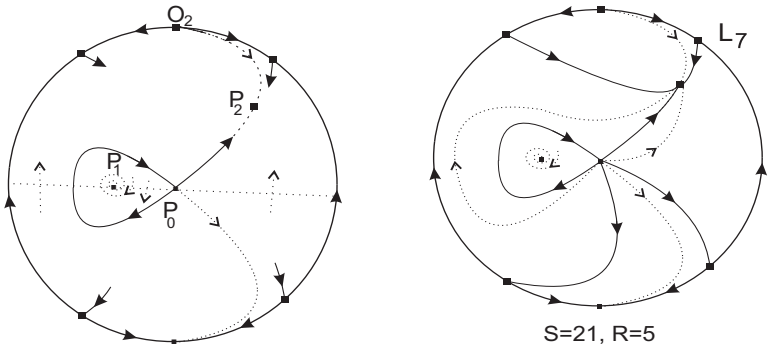


FIGURE 53. The local and the global phase portraits corresponding to the line $L_7$.

For the line $L_{12}$ we consider the straight line passing through the points $Q, P_+$ and $Q'$. Note that the unstable separatrix of the point $Q'$ determines the direction of the vector field on this line. The unique global phase portrait is given in Figure 58.

Now we are going to explain the phase portrait on the line $L_{24}$ see Figure 70. Note that there is no connection between the separatrices of the saddles $Q_1$ and $Q_2$ because the point $P_1$ is a node, see Theorems 15, 17 and Remark 16.

Now consider the straight line passing through the points $Q_2$, $P_+$ and $Q_2'$. There are three possibilities:

(i) The point $P_-$ is bellow the straight line. Then the unstable separatrix of $Q_2'$ must be bellow the straight line, otherwise cannot have an $\omega$–limit. This determines the direction of the vector field on the line and we obtain the global phase portrait $L_{24i}$.

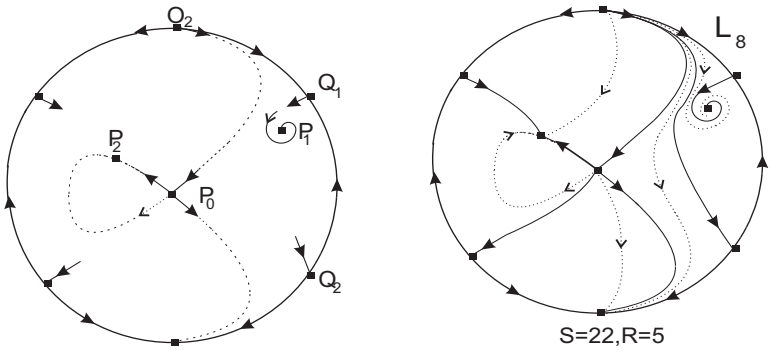


FIGURE 54. The local and the global phase portraits corresponding to the line $L_8$.

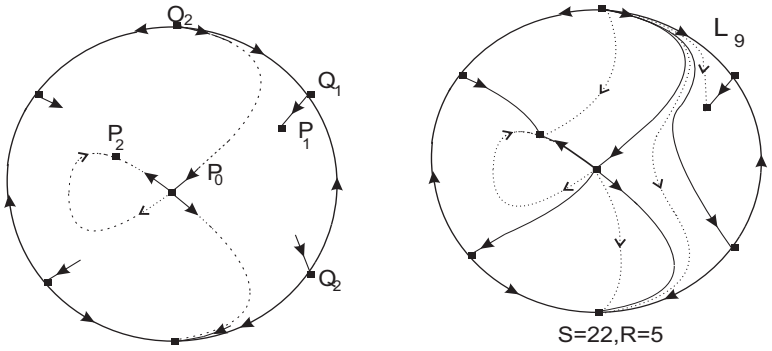


FIGURE 55. The local and the global phase portraits corresponding to the line $L_9$.

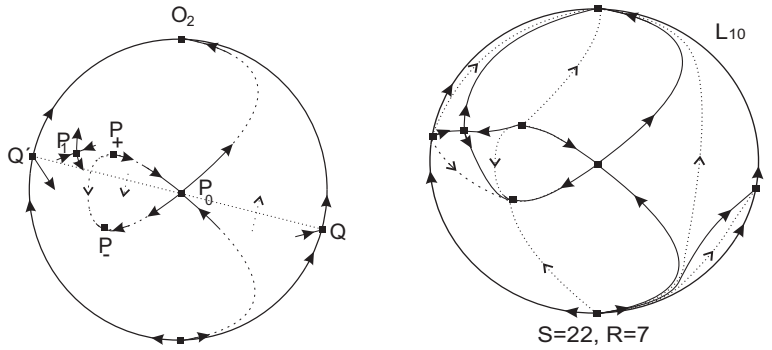


FIGURE 56. The local and the global phase portraits corresponding to the line $L_{10}$.

(ii) The point $P_-$ belongs to the straight line and the line is invariant. Then we obtain the global phase portrait $L_{24ii}$.

(iii) The point $P_-$ is upper the straight line. Then the direction of the loop of the curve $f_2 = 0$ determines the direction of this straight line. Then we obtain the global phase portrait $L_{24iii}$.

Now we are going to explain the phase portrait on the line $L_{25}$, see Figure 71. If there is a connection between the separatrices of the points $Q_1$ and $Q_2$ then they form a heteroclinic loop that must contain the node, a contradiction, see Theorems 15, 17 and also Remark 16. Hence the unstable separatrix of the point $Q_1$ must have as $\omega --$ limit the point $P_1$.

Note that the unstable separatrix of the point $Q_1$ cannot have as $\omega --$ limit the point $O_2'$. In the opposite case using the continuity we should have a connection between the separatrices of the saddles. So on the line $L_{25}$ we obtain a unique global phase portrait, see Figure 71.

3.3. **Phase portraits on the intersection points.** The bifurcation curves intersect into 11 points, see Figure 78. The intersection points are described in what follows, see also Figure 78.

$$
\begin{aligned}
p_1 &= \{g_4 = 0, g_1 = 0\} = \quad (12 + 8\sqrt{2}, \quad 12 + 8\sqrt{2}),\\
p_2 &= \{g_4 = 0, g_7 = 0\} = \quad \left(\frac{8}{9}, \frac{8}{9}\right),\\
p_3 &= \{g_4 = 0, g_6 = 0\} = \quad \left(\frac{-68 + 8\sqrt{78}}{3}, \frac{-68 + 8\sqrt{78}}{3}\right),\\
p_4 &= \{g_4 = 0, g_3 = 0\} = \quad \left(\frac{4}{5}, \frac{4}{5}\right),\\
p_5 &= \{g_4 = 0, g_1 = 0\} = \quad (12 - 8\sqrt{2}, \quad 12 - 8\sqrt{2}),\\
p_6 &= \{g_4 = 0, g_2 = 0\} = \quad \left(\frac{2}{3}, \quad \frac{2}{3}\right),\\
p_7 &= \{g_1 = 0, g_6 = 0\} = \quad \left(\frac{4}{3}\frac{\sqrt{(37 + 9\sqrt{318})^{1/3}(2(37 + 9\sqrt{318})^{2/3} - (37 + 9\sqrt{318})^{1/3} - 58)}}{(37 + 9\sqrt{318})(1/3)},\right.\\
&\qquad \left.\frac{2}{27}\frac{2\left(37 + 9\sqrt{318}\right)^{2/3} - \left(37 + 9\sqrt{318}\right)^{1/3} - 58}{37 + 9\sqrt{318}}^{1/3} + \frac{2}{3}\right),\\
p_8 &= \{g_1 = 0, g_7 = 0\} = \quad \left(2\frac{\sqrt{2}\sqrt{\sqrt[3]{13 + 16\sqrt{2}}\left(\left(13 + 16\sqrt{2}\right)^{2/3} - \sqrt[3]{13 + 16\sqrt{2}} - 7\right)}}{\sqrt[3]{13 + 16\sqrt{2}}},\right.\\
&\qquad \left.1/3\,\frac{\left(13 + 16\sqrt{2}\right)^{2/3} - \sqrt[3]{13 + 16\sqrt{2}} - 7}{\sqrt[3]{13 + 16\sqrt{2}}} + \frac{2}{3}\right),\\
p_9 &= \{g_2, g_7\} = \quad \left(\frac{2}{3}\sqrt{3}, \quad \frac{2}{3}\right),\\
p_{10} &= \{g_2, g_6\} = \quad \left(\frac{4\sqrt{13}}{13}, \quad \frac{2}{3}\right),\\
p_{11} &= \{g_5, g_6\} = \quad \left(\tfrac{68}{3} + \frac{8}{3}\sqrt{78}, \quad -\frac{68}{3} - \frac{8}{3}\sqrt{78}\right).
\end{aligned}
$$

We present the phase portraits in each of these intersection points in Figures 79, 80 and 81.

## 4. Topological classification of the global phase portraits

*Proof of Theorem* 1. In what follows we denote by $S$ the number of separatrices and by $R$ the number of the canonical regions. In order to present the topological classification of all global phase portraits of system (2) we apply Theorem 22 of the Appendix due to Markus, Neumann and Peixoto, see [32, 33, 34] and the notion of separatrix configuration that appears there. We recall that two global phase portrait are not topological equivalent when does not exist a homeomorphism to bring the separatrix configuration of one to the separatrix configuration of the other, see again Theorem 22.

For $a = c = 0$ system (2) becomes system (3) and there is the global phase portrait $C_0$ with $S = 17$ and $R = 4$.

Now for $a = 0$ and $c \neq 0$ system (2) becomes system (4) and we obtain the following phase portraits

| $S$ | $R$ | Phase portraits |
|---|---|---|
| 19 | 6 | $C_2$ |
| 23 | 5 | $C_1, C_3$ |
| 9 | 3 | $C_4$ |
| 12 | 5 | $C_5$ |
| 16 | 5 | $C_6$ |

Note that the phase portrait $C_1$ is not topological equivalent to the phase portrait $C_3$ because their separatrix configurations are not homeomorphic.

Now we consider the case where $a \neq 0$. Because of the symmetry (5) of system (2) we can restrict our study to $a > 0$. First we consider the case where $c = 0$. So we work with system (6) and we obtain

| $S$ | $R$ | Phase portraits |
|---|---|---|
| 16 | 5 | $A_1$ |
| 22 | 5 | $A_2$ |
| 20 | 5 | $A_3$ |
| 21 | 4 | $A_4$ |
| 22 | 5 | $A_5$ |

Note that the phase portrait $A_2$ is not topological equivalent to the phase portrait $A_5$ because their separatrix configurations are not homeomorphic. For the same reason the phase portrait of $A_1$ is not topologically equivalent to the phase portrait $C_6$, or simply $A_1 \neq C_6$.

| $S$ | $R$ | Phase portraits |
|---|---|---|
| 9 | 3 | $p_4 = r_7, C_4$ |
| 10 | 3 | $p_2$ |
| 12 | 5 | $C_5$ |
| 13 | 4 | $p_3 = L_3 = L_4 = L_{26}, L_{15}$ |
| 13 | 5 | $L_5 = L_{27}$ |
| 14 | 5 | $L_2, L_{16}$ |
| 15 | 4 | $r_5 = r_6 = L_{20}$ |
| 15 | 5 | $r_8$ |
| 16 | 5 | $r_9 = r_{10} = L_{21}, r_1 = C_6, r_4, A_1$ |
| 16 | 6 | $p_6$ |
| 17 | 4 | $C_0$ |
| 17 | 6 | $p_9$ |
| 18 | 5 | $L_{31i}, L_{31ii}$ |
| 18 | 6 | $L_{28}$ |
| 19 | 6 | $L_{30} = L_{29}, L_{31iii}, C_2, L_7, p_{10}$ |
| 19 | 7 | $p_5$ |
| 20 | 5 | $A_3$ |
| 20 | 7 | $p_1, p_8$ |
| 21 | 4 | $A_4$ |
| 21 | 5 | $L_7$ |
| 21 | 6 | $L_{11iv}, L_{11ii}$ |
| 21 | 7 | $L_{14}$ |
| 22 | 5 | $p_{11} = L_8 = L_9, L_{19}, L_{18}, A_2, A_5$ |
| 22 | 7 | $p_7 = L_{12} = L_{13}, L_{11i}, L_{11iii} = L_{11v}, L_{12}, L_{10}$ |
| 23 | 4 | $r_{18ii} = r_{19ii} = L_{24ii}, r_{17ii}$ |
| 23 | 5 | $C_1, C_3, r_{14}$ |
| 23 | 7 | $L_6$ |
| 24 | 5 | $L_{23} = r_{15} = r_{16}, r_{17iii} = r_{18i} = r_{19i} = L_{24i}, r_{18iii} = r_{19iii}, r_{20} = L_{24iii} = L_{25} = r_{21}, r_{17i}$ |
| 24 | 7 | $L_1, L_{17}$ |
| 25 | 6 | $r_{3ii}, L_{22}$ |
| 25 | 7 | $r_{13}$ |
| 26 | 7 | $r_2, r_{3iii}, r_{3i}, r_{11} = r_{12}$ |

Case $S = 9$ and $R = 3$. Then $p_4 = r_7$ and $p_4 \neq C_4$ because in $C_4$ in the interior of the loop of the curve $f_2 = 0$ we have a center whereas in $p_4$ we have a focus.

Case $S = 13$ and $R = 4$. We have $p_3 = L_3 = L_4 = L_{26}$, $L_{15} \neq L_{26}$.

Case $S = 13$ and $R = 5$. We have $L_{27} = L_5$.

Case $S = 14$ and $R = 5$. $L_2 \neq L_{16}$.

Case $S = 16$ and $R = 5$. We obtain $r_9 = r_{10} = L_{21}$,$C_6 = r_1$, $r_9 \neq r_1$ $r_9 \neq r_4, r_9 \neq A_1$ $r_4 \neq r_1$, $A_1 \neq r_1$, $A_1 \neq r_4$.

Case $S = 18$ and $R = 5$ There are two phase potraits $L_{31i} \neq L_{31ii}$.

Case $S = 19$ and $R = 5$. We have $p_{10} \neq C_1$.

Case $S = 19$ and $R = 6$ We have $L_{29} = L_{30}$, $L_{29} \neq L_{31iii}$, $L_{29} \neq C_2$, $L_{29} \neq C_2$, $L_{29} \neq L_7$, $L_{29} \neq p_{10}$, $L_{31iii} \neq C_2$, $L_{31iii} \neq L_7$, $L_{31iii} \neq p_{10}$, $C_2 \neq L_7$, $C_2 \neq p_{10}$, $L_7 \neq p_{10}$.

Case $S = 20$ and $R = 7$ The two phase portraits are $p_1 \neq p_8$.

Case $S = 21$ and $R = 6$. We have two different phase portraits $L_{11iv} \neq L_{11ii}$.

Case $S = 22$ and $R = 5$. We have $L_8 = L_9 = p_{11}, L_8 \neq L_{19}, L_8 \neq L_{18}$, $L_8 \neq A_2, L_8 \neq A_5$, $L_{19} \neq L_{18}, L_{19} \neq A_2, L_{19} \neq A_5$, $A_2 \neq L_{18}, A_5 \neq L_{18}, A_5 \neq A_2$.

Case $R = 22$ and $S = 7$. We have $L_{12} = L_{13} = p_7$, $L_{11iii} = L_{11v}$, $L_{11i} \neq L_{11iii}$, $L_{11i} \neq L_{12}$, $L_{11i} \neq L_{10}$, $L_{11iii} \neq L_{10}$, $L_{11iii} \neq L_{12}$, $L_{12} \neq L_{10}$.

Case $S = 23$ and $R = 4$. We have $r_{18ii} = r_{19ii} = L_{24ii}, r_{18ii} \neq r_{17ii}$.

Case $S = 23$ and $R = 5$. We have $C_1 \neq C_3, C_1 \neq r_{14}, C_3 \neq r_{14}$.

Case $R = 24$ and $S = 5$. We have $L_{23} = r_{15} = r_{16}$, $r_{17iii} = r_{18i} = r_{19i} = L_{24i}$, $r_{18iii} = r_{19iii}$, $r_{20} = L_{24iii} = L_{25} = r_{21}$, $r_{15} \neq r_{18i}$, $r_{15} \neq r_{18iii}$, $r_{15} \neq r_{20}$, $r_{15} \neq r_{17i}$ $r_{18i} \neq r_{18iii}, r_{18i} \neq r_{20}, r_{18i} \neq r_{17i}$, $r_{18iii} \neq r_{20}, r_{18iii} \neq r_{17i}$, $r_{17i} \neq r_{20}$.

Case $R = 24$ and $S = 7$. We have $L_1 \neq L_{17}$.

Case $S = 25$ and $R = 6$. We have $r_{3ii} \neq L_{22}$.

Case $S = 26$ and $R = 7$ We have $r_{11} = r_{12}$, $r_2 \neq r_{3i}, r_2 \neq r_{3iii}, r_2 \neq r_{12}, r_{3i} \neq r_{3iii}, r_{3i} \neq r_{12}, r_{3iii} \neq r_{12}$.

In summary, we can compute 65 different topological phase portraits in the Poincaré disc for the quadratic systems (2). This completes the proof of the theorem. □

## 5. Appendix

This appendix has two subsections.

5.1. **Poincaré compactification.** We consider the polynomial differential system (1) of degree $m$ and its corresponding vector field $\mathcal{X}$. In order to plot the global phase portrait of system (1) we need to control the orbits that come or escape at infinity. For doing this control we consider the *Poincaré compactification* of system (1). For more details on this compactification see Chapter 5 of [20].

Let $\mathbb{R}^2$ be the plane in $\mathbb{R}^3$ defined by $(y_1, y_2, y_3) = (x_1, x_2, 1)$. We define the *Poincaré sphere* $\mathbb{S}^2 = \{y = (y_1, y_2, y_3) \in \mathbb{R}^3 : y_1^2 + y_2^2 + y_3^2 = 1\}$ and we denote by $T_{(0,0,1)}\mathbb{S}^2$ the tangent space to $\mathbb{S}^2$ at the point $(0, 0, 1)$ (see [35]). We consider the central projection $f : T_{(0,0,1)} : \mathbb{R}^2 \to \mathbb{S}^2$. Note that $f$ defines two copies of $\mathcal{X}$, one in the northern hemisphere $\{y \in \mathbb{S}^2 : y_3 > 0\}$ and the other in the southern hemisphere. Let $\hat{\mathcal{X}} = Df \circ \mathcal{X}$ and note that $\hat{\mathcal{X}}$ is defined on $\mathbb{S}^2$ except on its equator $\mathbb{S}^1$. Then the points at infinity of $\mathbb{R}^2$ are in bijective correspondence with $\mathbb{S}^1 = \{y \in \mathbb{S}^2 : y_3 = 0\}$, ( the equator of $\mathbb{S}^2$). Hence $\mathbb{S}^1$ is identified to be the infinity of $\mathbb{R}^2$. Then the *Poincaré compactified vector field* $p(\mathcal{X})$ of $\mathcal{X}$ will be analytic vector field induced on $\mathbb{S}^2$ as follows. If we multiply $\hat{\mathcal{X}}$ by the factor $y_3^m$, the vector field $y_3^m \hat{\mathcal{X}}$ defined in the whole $\mathbb{S}^2$.

Note that on $\mathbb{S}^2 \setminus \mathbb{S}^1$ there are two symmetric copies of $\mathcal{X}$. Hence the behavior of $p(\mathcal{X})$ around $\mathbb{S}^1$ gives the behavior of $\mathcal{X}$ near the infinity. The *Poincaré disc* $\mathbb{D}$ is the projection of the closed northern hemisphere of $\mathbb{S}^2$ on $y_3 = 0$ under $(y_1, y_2, y_3) \longmapsto (y_1, y_2)$. Moreover, $\mathbb{S}^1$ is invariant under the flow of $p(\mathcal{X})$.

Two polynomial vector fields $\mathcal{X}$ and $\mathcal{Y}$ on $\mathbb{R}^2$ are *topologically equivalent* if there exists a homeomorphism on $\mathbb{S}^2$ preserving the infinity $\mathbb{S}^1$ carrying orbits of the flow induced by $p(\mathcal{X})$ into orbits of the flow induced by $p(\mathcal{Y})$. Note that the homeomorphism should preserve or reverse simultaneously the sense of all orbits of the two compactified vector fields $p(\mathcal{X})$ and $p(\mathcal{Y})$.

Since $\mathbb{S}^2$ is a differentiable manifold we can consider the six local charts $U_i = \{y \in \mathbb{S}^2 : y_i > 0\}$, and $V_i = \{y \in \mathbb{S}^2 : y_i < 0\}$ for $i = 1, 2, 3$ with the diffeomorphisms $F_i : V_i \longrightarrow \mathbb{R}^2$ and $G_i : V_i \longrightarrow \mathbb{R}^2$, which are the inverses of the central projections from the planes tangent at the points $(1, 0, 0), (-1, 0, 0), (0, 1, 0), (0, -1, 0), (0, 0, 1)$ and $(0, 0, -1)$, respectively. Let $z = (z_1, z_2)$ be the value of $F_i(y)$ or $G_i(y)$ for any $i = 1, 2, 3$. Then the expressions of the compactified vector field ,$p(\mathcal{X})$ of $\mathcal{X}$ are

$$\begin{aligned}
z_2^m \Delta(z)\left(Q\Big(\frac{1}{z_2}, \frac{z_1}{z_2}\Big) - z_1 P\Big(\frac{1}{z_2}, \frac{z_1}{z_2}\Big), -z_2 P\Big(\frac{1}{z_2}, \frac{z_1}{z_2}\Big)\right) \qquad &\text{in} \qquad U_1, \\
z_2^m \Delta(z)\left(P\Big(\frac{z_1}{z_2}, \frac{1}{z_2}\Big) - z_1 Q\Big(\frac{z_1}{z_2}, \frac{1}{z_2}\Big), -z_2 Q\Big(\frac{z_1}{z_2}, \frac{1}{z_2}\Big)\right) \qquad &\text{in} \qquad U_2, \\
\Delta(z)\big(P(z_1, z_2), Q(z_1, z_2)\big) \qquad &\text{in} \qquad U_3,
\end{aligned}$$

where $\Delta(z) = (z_1^2 + z_2^2 + 1)^{-\frac{1}{2(m-1)}}$. The expressions of the vector field $p(\mathcal{X})$ in the local chart $V_i$ is the same as in the chart $U_i$ multiplying by the factor $(-1)^{m-1}$. In these coordinates $z_2 = 0$ denotes the points of $\mathbb{S}^1$. We omit the factor $\Delta(z)$ by rescaling the vector field $p(\mathcal{X})$, and so we obtain a polynomial vector field in each local chart. The infinity $\mathbb{S}^1$ is invariant with $p(\mathcal{X})$.

5.2. **Separatrix configuration.** Let $p(\mathcal{X})$ be the Poincaré compactification in $\mathbb{S}^2$ of a polynomial vector field $\mathcal{X}$ in $\mathbb{R}^2$.

We consider the definition of parallel flows given by Markus [32] and Neumann in [33]. Let $\phi$ be a $\mathcal{C}^\omega$ local flow on the two dimensional manifold $\mathbb{R}^2$ or $\mathbb{R}^2 \setminus \{0\}$. The flow $(M, \phi)$ is $\mathcal{C}^k$ *parallel* if it is $\mathcal{C}^\omega$-equivalent to one of the following ones:

*strip:* $(\mathbb{R}^2, \phi)$ with the flow $\phi$ defined by $\dot{x} = 1, \dot{y} = 0$;
*annular:* $(\mathbb{R}^2 \setminus \{0\}, \phi)$ with the flow $\phi$ defined (in polar coordinates) by $\dot{r} = 0, \dot{\theta} = 1$;
*spiral:* $(\mathbb{R}^2 \setminus \{0\}, \phi)$ with the flow $\phi$ defined by $\dot{r} = r, \dot{\theta} = 1$.

The *separatrices* of the vector field $p(\mathcal{X})$ in the Poincaré disc $\mathbb{D}$ are

(i) all the orbits of $p(\mathcal{X})$ which are in the boundary $\mathbb{S}^1$ of the Poincaré disc (recall that $\mathbb{S}^1$ is the infinity of $\mathbb{R}^2$);
(ii) all the finite singular points of $p(\mathcal{X})$;
(iii) all the limit cycles of $p(\mathcal{X})$; and
(iv) all the separatrices of the hyperbolic sectors of the finite and infinite singular points of $p(\mathcal{X})$.

We denote by $\Sigma$ the union of all separatrices of the flow $(\mathbb{D}, \phi)$ defined by the compactified vector field $p(\mathcal{X})$ in the Poincaré disc $\mathbb{D}$. Then $\Sigma$ is a closed invariant subset of $\mathbb{D}$. Every connected component of $\mathbb{D} \setminus \Sigma$, with the restricted flow, is called a *canonical region* of $\phi$.

For a proof of the following result see [27] and [33].

**Theorem 21.** *Let $\phi$ be a $\mathcal{C}^\omega$ flow in the Poincaré disc with finitely many separatrices, and let $\Sigma$ be the union of all its separatrices. Then the flow restricted to every canonical region is $\mathcal{C}^\omega$ parallel.*

The *separatrix configuration* $\Sigma_c$ of a flow $(D, \phi)$ is the union of all the separatrices $\Sigma$ of the flow together with an orbit belonging to each canonical region. The separatrix configuration $\Sigma_c$ of the flow $(D, \phi)$ is said to be *topologically equivalent* to the separatrix configuration $\tilde{\Sigma}_c$ of the flow $(D, \tilde{\phi})$ if there exists a homeomorphism from $\Sigma_c$ to $\Sigma_c$ which transforms orbits of $\Sigma_c$ into orbits of $\tilde{\Sigma}_c$, and orbits of $\Sigma$ into orbits of $\tilde{\Sigma}$.

**Theorem 22.** *Let $(D, \phi)$ and $(D, \tilde{\phi})$ be two compactified Poincaré flows with finitely many separatrices coming from two polynomial vector fields* (1)*. Then they are topologically equivalent if and only if their separatrix configurations are topologically quivalent.*

For a proof of Theorem 22 see [32, 33, 34].

In sort, in order to classify the phase portraits in the Poincaré disc of a planar polynomial differential system having finitely many separatrices, it is enough to describe their separatrix configuration.

## Acknowledgments

J. Llibre is partially supported by the Agència de Gestió d'Ajuts Universitaris i de Recerca grant 2017SGR1617, and the H2020 European Research Council grant MSCA-RISE-2017-777911. J. Llibre and C. Pantazi are also supported by the Ministerio de Ciencia, Innovación y Universidades, Agencia Estatal de Investigación grant MTM2016-77278-P (FEDER). C. Pantazi is additionally partially supported by the Catalan Grant 2017SGR1049 and the Spanish MINECO-FEDER Grant PGC2018-098676-B-I00/AEI/FEDER/UE.

## References

[1] J.C. Artés, R.E. Kooij and J. Llibre, *Structurally stable quadratic vector fields*, Mem. Amer. Math. Soc. **134** (1998), 108 pp.

[2] J.C. Artés and J. Llibre, *Hamiltonian quadratic systems*, J. Diff. Eqns. **107** (1994), 80–95.

[3] J.C. Artés and J. Llibre, *Phase portraits for quadratic systems having a focus and one antisaddle*, Rocky Mount.J. Math. **24** (1994), 875–889.

[4] J.C. Artés, J. Llibre, D. Schlomiuk and N. Vulpe, *Geometric configurations of singularities of planar polynomial differential systems*, to appear in Birkhäuser, 2020.

[5] J.C. Artés, J. Llibre and N. Vulpe, *Quadratic systems with a rational first integral of degree two: a complete classification in the coefficient space* $\mathbb{R}^{12}$, Rend. Circ. Mat. di Palermo **56** (2007), 417–444.

[6] J.C. Artés, J. Llibre and N. Vulpe, *Quadratic systems with a rational first integral of degree three: a complete classification in the coefficient space* $\mathbb{R}^{12}$, Rend. Circ. Mat. di Palermo **59** (2010), 419–449.

[7] J.C. Artés, J. Llibre and N. Vulpe, *Quadratic systems with a polynomial first integral: A complete classification in the coefficient space* $\mathbb{R}^{12}$, J. Diff. Eqns. **246** (2009), 3535–3558.

[8] J.C. Artés, A.C. Rezende and R.D.S. Oliveira, *Global phase portraits of quadratic polynomial differential systems with a semi–elemental triple node*, Internat. J. Bifur. Chaos Appl. Sci. Engrg. **23** (2013), no. 8, 1350140, 21 pp.

[9] A. N. Berlinskiĭ, *On the behavior of the integral curves of a differential equation*, (Russian). Izv. Vyssš. Učebn. Zaved. Matematika, (1960), **15**, 3–18.

[10] A.N. Berlinskiĭ, *Qualitative study of the differential equation* $\dot{x} = x + b_0x^2 + b_1xy + b_2y^2, \dot{y} = y + a_0x^2 + a_1xy + a_2y^2$ J. Diff. Eqns, (1966), **2**, 174–178.

[11] R. Bix, *Conics and cubics. A concrete introduction to algebraic curves*, Second Edition, Undergraduate Texts in Math., Springer, 2006

[12] L. Cairó and J. Llibre, *Phase portraits of planar semi–homogeneous vector fields*, Nonlinear Analisis, Th. Meth. & App. (1997) **29**, 783–811.

[13] F. Chen, C. Li, J. Llibre and Z. Zhang, *A uniform proof on the weak Hilbert's 16th problem for* $n = 2$, J. Diff. Eqns. **221** (2006), 309–342.

[14] W.A. Coppel, *A survey of quadratic systems*, J. Diff. Eqns. **2** (1966), 293–304.

[15] S.-N. Chow, C. Li and Y. Yi, *The cyclicity of period annulus of degenerate quadratic Hamiltonian system with elliptic segment loop*, Erg. Th. & Dyn. Syst. **22** (2002), 1233–1261.
[16] B. Coll, A. Gasull and J. Llibre, *Some theorems on the existence, uniqueness and nonexistence of limit cycles for quadratic systems*, J. Diff. Eqns. **67** (1987), 372–399.
[17] B. Coll, C. Li and R. Prohence, *Quadratic perturbations of a class of quadratic reversible systems with two centers,* Disc. & Contin. Dyn. Sys. **24** (2009), 699–729.
[18] R.J. Dickson and L.M. Perko, *Bounded quadratic systems in the plane*, J. Diff Eqns. **6** (1970), 251–273.
[19] F. Dumortier and C. Li, *Quadratic Lienard equations with quadratic damping*, J. Diff. Eqns. **139** (1997), 41–59.
[20] F. Dumortier, J. Llibre and J. C. Artés, *Qualitative theory of planar polynomial systems*, Springer, 2006.
[21] A. Gasull, S. Li-Ren and J. Llibre, *Chordal quadratic systems*, Rocky Mount. J. Math. **16** (1986), 751–782.
[22] A. Gasull and J. Llibre, *On the nonsingular quadratic differential equations in the plane*, Proc. Amer. Math. Soc. **104** (1988), 793–794.
[23] L. Gavrilov, *The infinitesimal 16th Hilbert problem in the quadratic case*, Invent. Math. **143** (2001), 449–497.
[24] L. Gavrilov and I. D. Iliev, *Second order analysis in polynomially perturbed reversible quadratic Hamiltonian systems*, Erg. Th. & Dyn. Syst. **20** (2000), 1671–1686.
[25] D.D. Hua, L. Cairo, M.R. Feix, K.S. Govinder and P.G.L. Leach, *Connection between the existence of first integrals and the Painlevé property in two-dimensional Lotka-Volterra and quadratic systems*, Proc. Roy. Soc. London **452** (1996), 859–880.
[26] M. Han and C. Yang, *On the cyclicity of a 2-polycycle for quadratic systems*, Chaos, Solitons Fract. **23** (2005), 1787–1794.
[27] W. Li, J. Llibre, M. Nicolau and X. Zhang, *On the differentiability of first integrals of two dimensional flows*, Proc. Amer. Math. Soc. **130** (2002), 2079–2088.
[28] J. Llibre, J.S. Pérez del Río and J.A. Rodríguez, *Phase portraits of a new class of integrable quadratic vector fields,* Dyn. Cont. Disc. Impulsive Syst. **7** (2000), 595–616.
[29] C. Li and J. Llibre, *A unified study on the cyclicity of period annulus of the reversible quadratic Hamiltonian systems*, J. Dyn. and Diff. Eqns. **16** (2004), 271–295.
[30] C. Li and Z. Zhang, *Remarks on 16th weak Hilbert problem for n=2*, Nonlinearity **15**, (2002), 1975–1992.
[31] V.A. Lunkevich and K.S. Sibirskii, *Integrals of a general quadratic differential system in cases of a center*, Diff. Eqns. **18** (1982), 563–568.
[32] L. Markus, *Global structure of ordinary differential equations in the plane*, Trans. Amer. Math Soc. **76** (1954), 127–148.
[33] D.A. Neumann, *Classification of continuous flows on 2–manifolds*, Proc. Amer. Math. Soc. **48** (1975), 73–81.
[34] M.M. Peixoto, *Dynamical Systems. Proccedings of a Symposium held at the University of Bahia*, 389–420, Acad. Press, New York, 1973.
[35] H. Poincaré, *Sur l'intégration des équations différentielles du premier ordre et du premier degré I*, Rend. Circ. Mat. di Palermo **5** (1891), 161–191.
[36] H. Poincaré, *Sur les courbes définies par une équation différentielle*, Oevres compltes, Vol.1, 1928.
[37] J.W. Reyn, *A bibliography of the qualitative theory of quadratic systems of differential equations in the plane*, Third edition. Delft University of Technology, Report 94–02, 1994.
[38] I.G. Roset, *Nonlocal bifurcation of limit cycles and quadratic differential equations in the plane* (Russian), Dissertation Kand. Phys. Mat. Samarkand University, 1991.
[39] R. Roussarie and D. Schlomiuk, *On the geometric structure of the class of planar quadratic differential systems*, Qual. Th. of Dyn. Syst. **3** (2002), 93–121.
[40] D. Schlomiuk and N. Vulpe, *Geometry of quadratic differential systems in the neighborhood of infinity*, J. Diff. Eqns. **215** (2005), 357–400.
[41] A. Schlomiuk and N. Vulpe, *Integrals and phase portraits of planar quadratic differential systems with invariant lines of at least five total multiplicity*, Rocky Mountain J. Math. **38** (2008), 1887–2104.
[42] N.I. Vulpe, *Affine-invariant conditions for the topological discrimination of quadratic systems with a center*, J. Diff. Eqns. **19** (1983), 273–280.
[43] Ye, Yan Qian; Cai, Sui Lin; Chen, Lan Sun; Huang, Ke Cheng; Luo, Ding Jun; Ma, Zhi En; Wang, Er Nian; Wang, Ming Shu and Yang, Xin., *A Theory of limit cycles*, Translated from the Chinese by Chi Y. Lo. Second edition. Translations of Mathematical Monographs. **66**. Amer. Math. Soc., Providence, RI, 1986.
[44] P. Zhang, *On the distribution and number of limit cycles for quadratic systems with two foci*, Qual. Theory Dyn. Syst. **3** (2002), 437–463.
[45] H. Żołądek, *The cyclicity of triangles and lines in quadratic systems*, J. Diff. Eqns. **122** (1995), 137–159.

[1] Departament de Matemàtiques, Universitat Autònoma de Barcelona, Edifici C, 08193 Bellaterra, Barcelona, Catalonia, Spain

*Email address*: jllibre@mat.uab.cat

[2] Departament de Matemàtiques, Universitat Politècnica de Catalunya, (EPSEB), Av. Doctor Marañón, 44–50, 08028 Barcelona, Spain

*Email address*: chara.pantazi@upc.edu

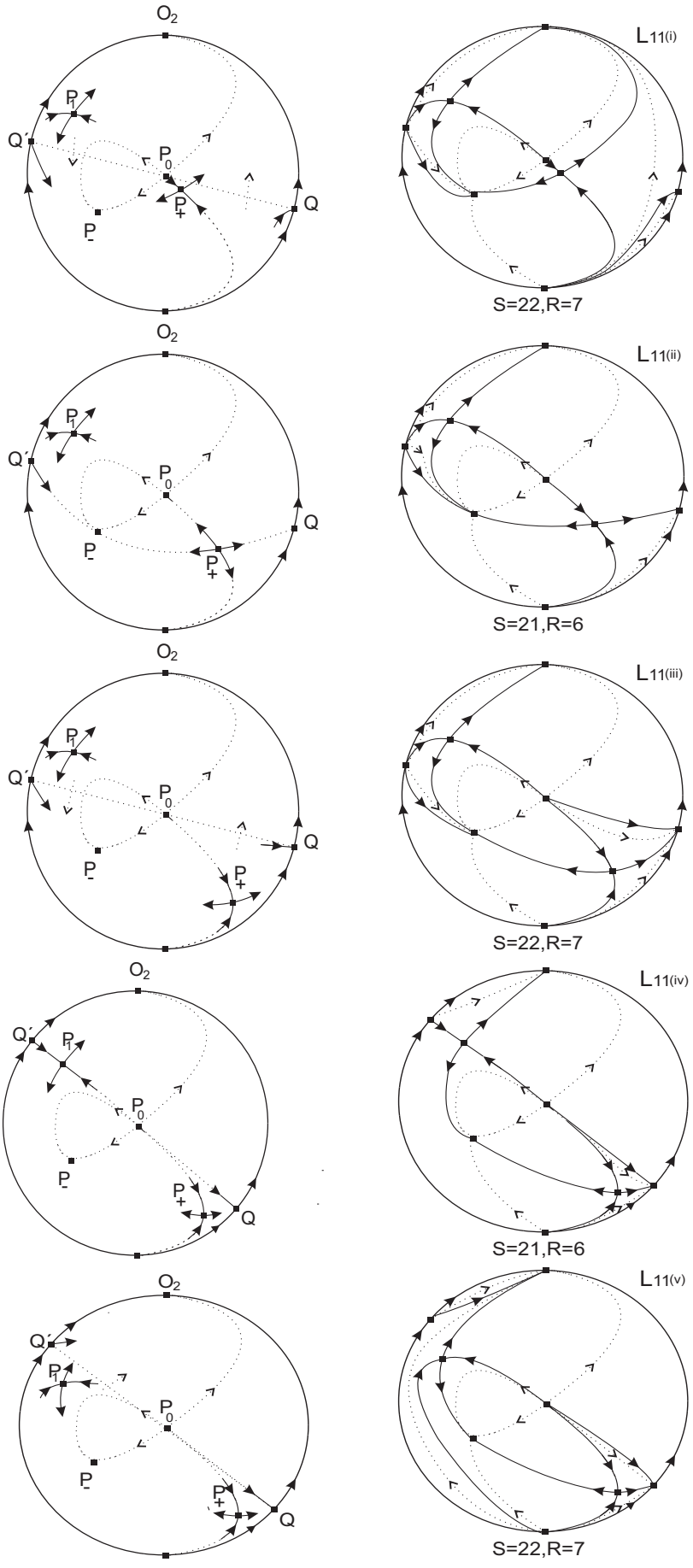




FIGURE 57. The local and the global phase portraits corresponding to the line $L_{11}$.

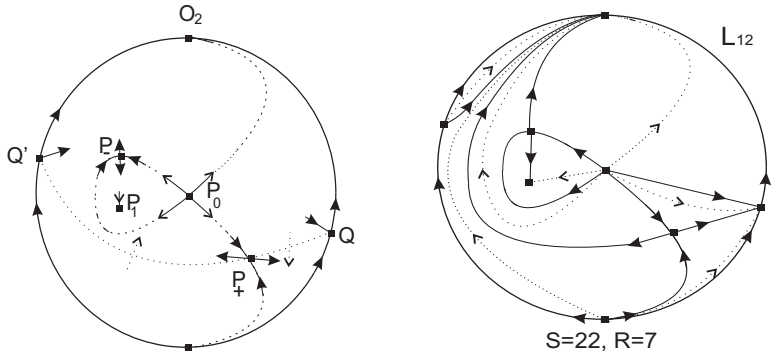


FIGURE 58. The local and the global phase portraits corresponding to the line $L_{12}$.

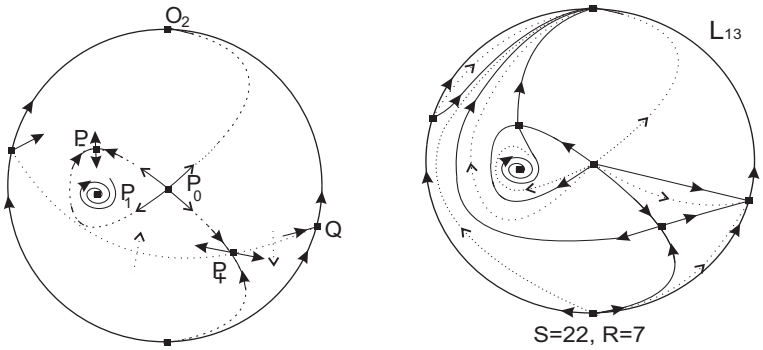


FIGURE 59. The local and the global phase portraits corresponding to the line $L_{13}$.

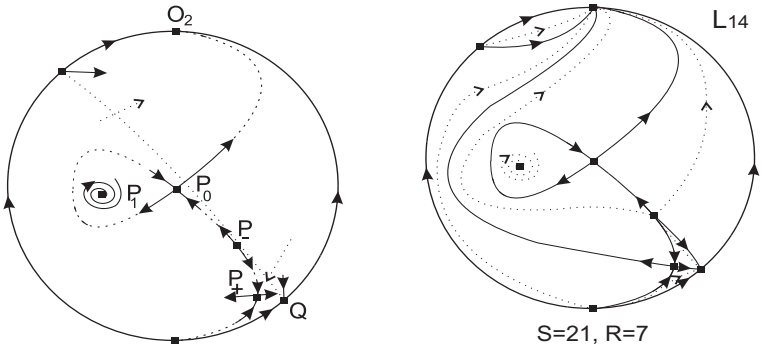


FIGURE 60. The local and the global phase portraits corresponding to the line $L_{14}$.

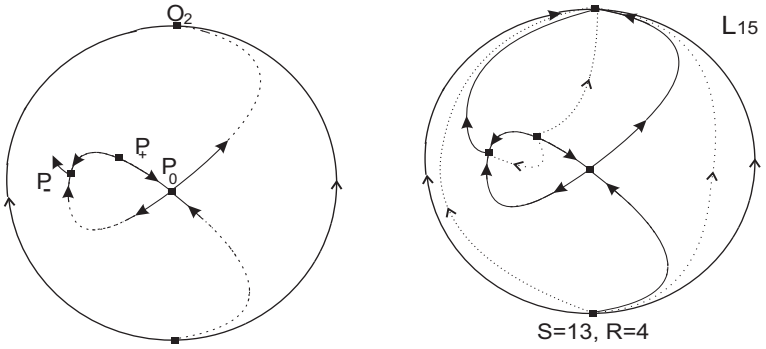


FIGURE 61. The local and the global phase portraits corresponding to the line $L_{15}$.

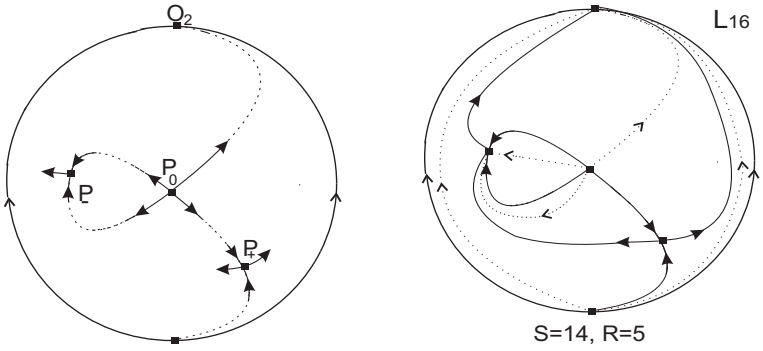


FIGURE 62. The local and the global phase portraits corresponding to the line $L_{16}$.

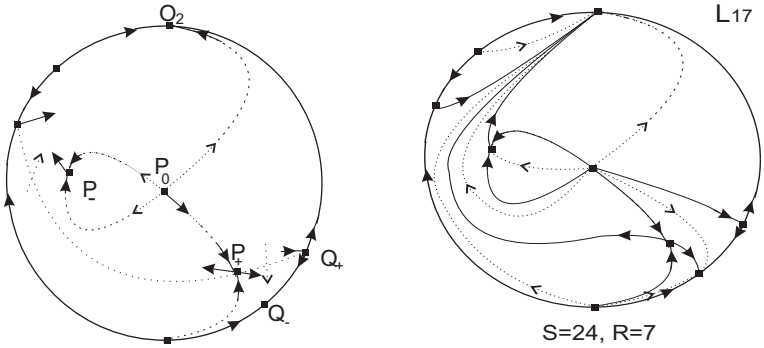


FIGURE 63. The local and the global phase portraits corresponding to the line $L_{17}$.

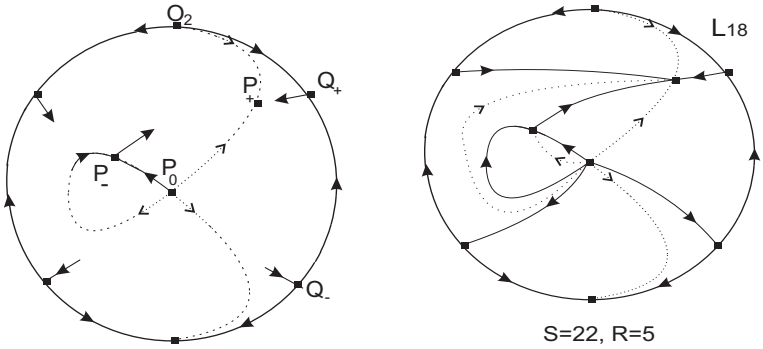


FIGURE 64. The local and the global phase portraits corresponding to the line $L_{18}$.

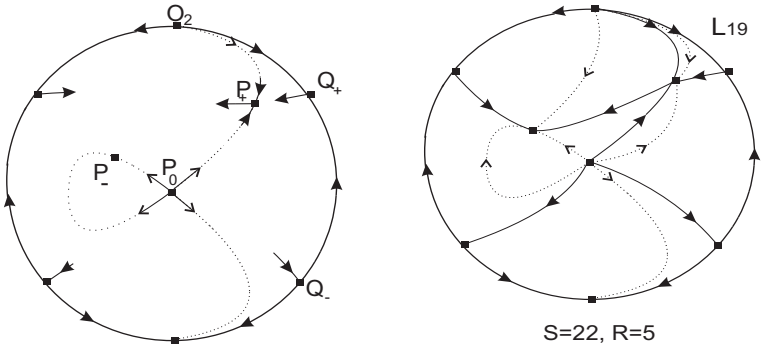


FIGURE 65. The local and the global phase portraits corresponding to the line $L_{19}$.

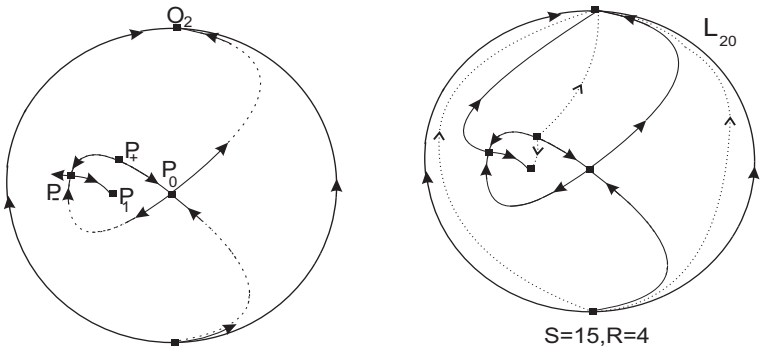


FIGURE 66. The local and the global phase portraits on the line $L_{20}$.

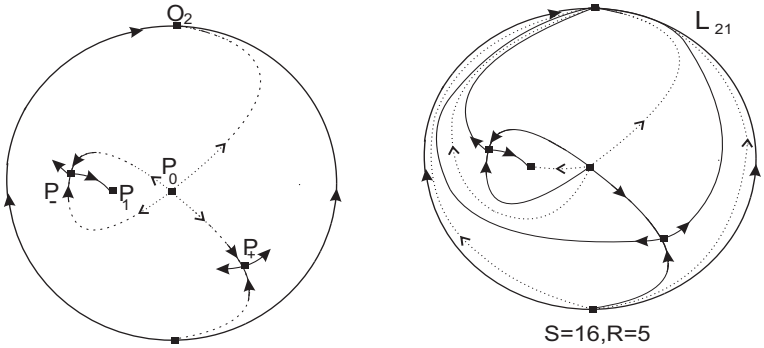


FIGURE 67. The local and the global phase portraits on the line $L_{21}$.

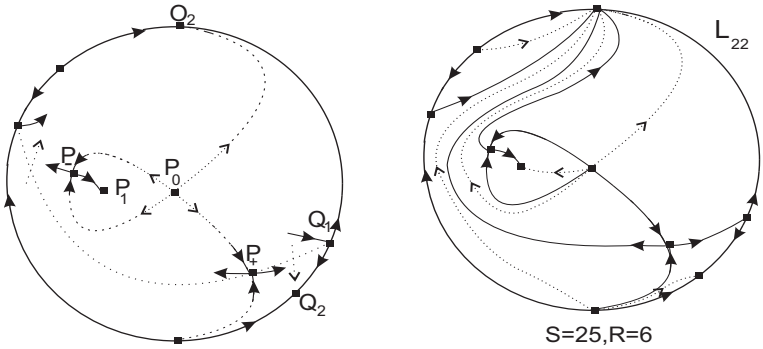


FIGURE 68. The local and the global phase portraits on the line $L_{22}$.

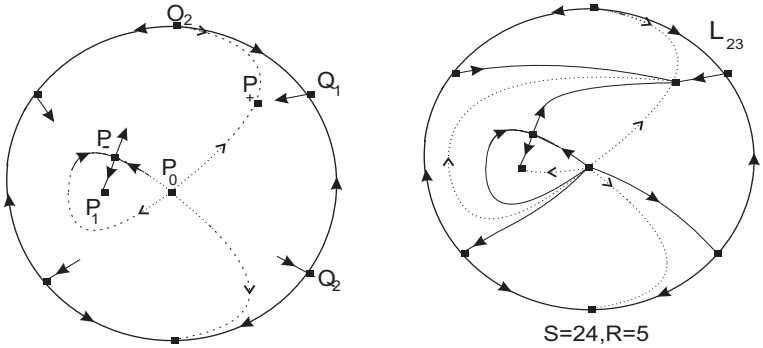


FIGURE 69. The local and the global phase portraits on the line $L_{23}$.

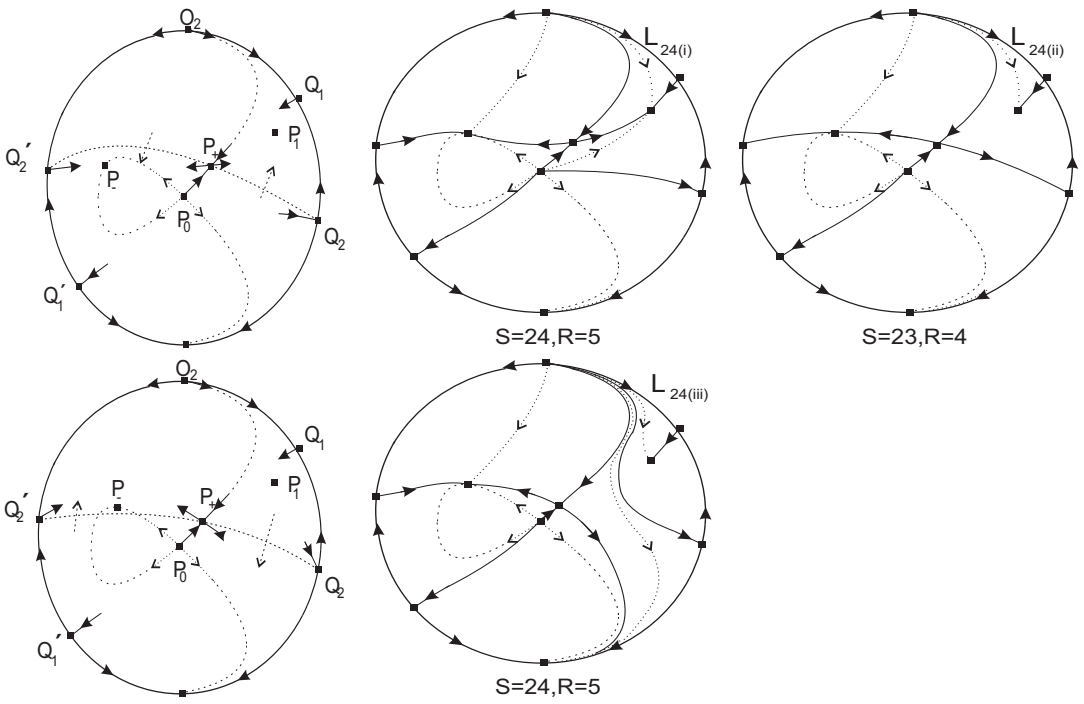


FIGURE 70. The local and the global phase portraits on the line $L_{24}$.

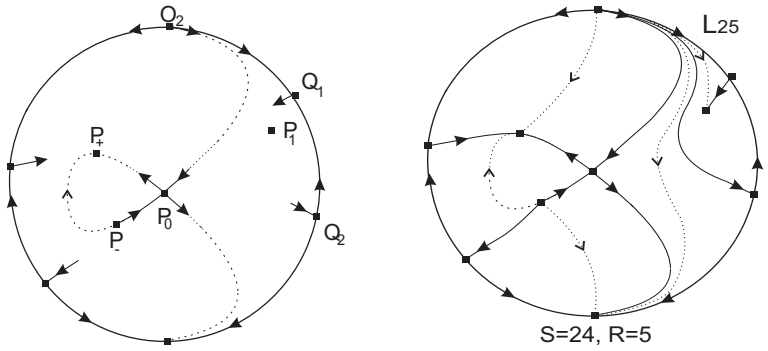


FIGURE 71. The local and the global phase portraits on the line $L_{25}$.

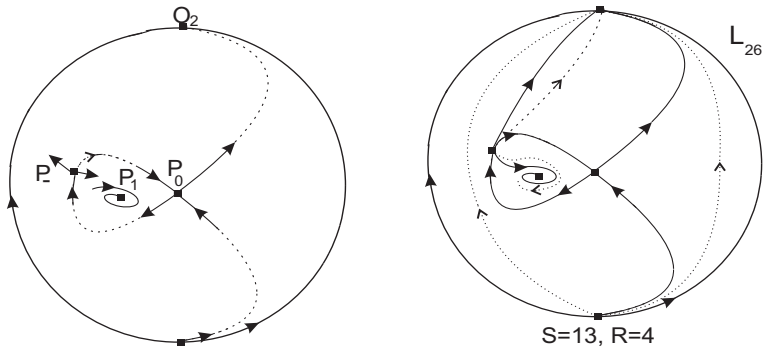


FIGURE 72. The local and the global phase portraits on the line $L_{26}$.

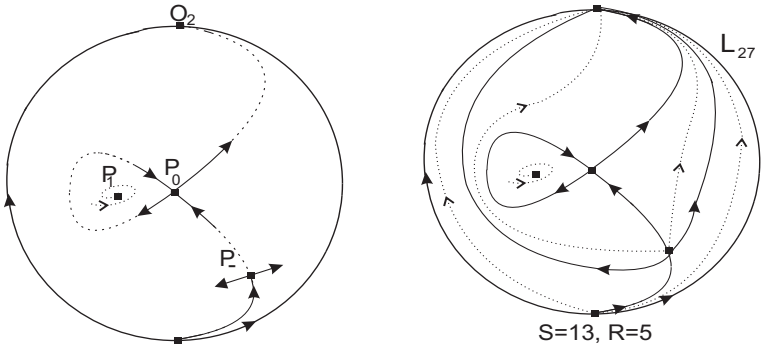


FIGURE 73. The local and the global phase portraits on the line $L_{27}$.

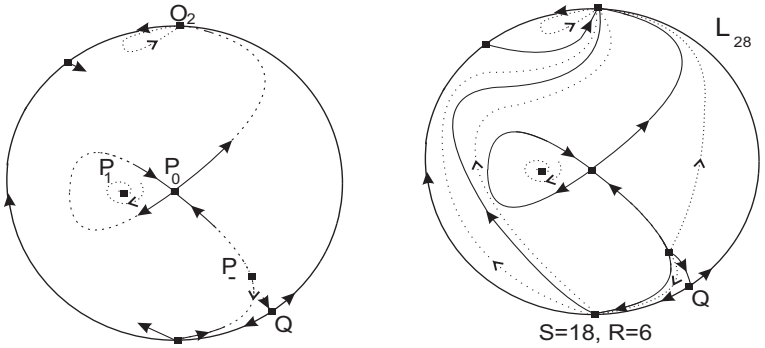


FIGURE 74. The local and the global phase portraits on the line $L_{28}$.

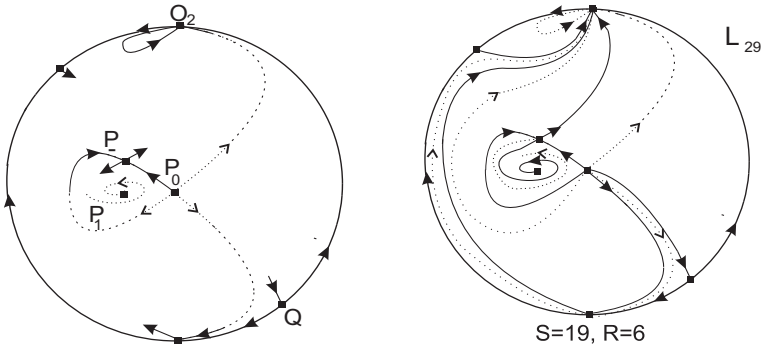


FIGURE 75. The local and the global phase portraits on the line $L_{29}$.

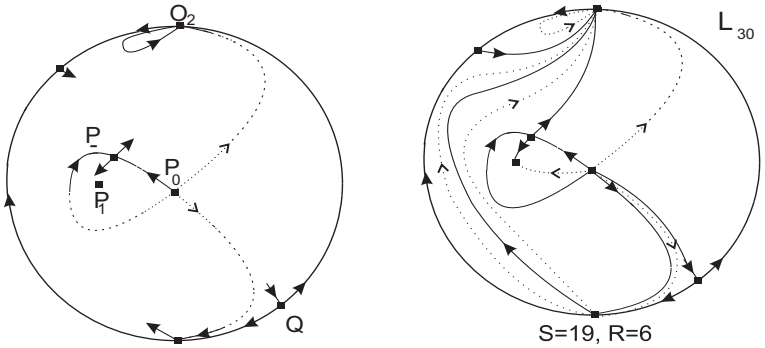


FIGURE 76. The local and the global phase portraits on the line $L_{30}$.

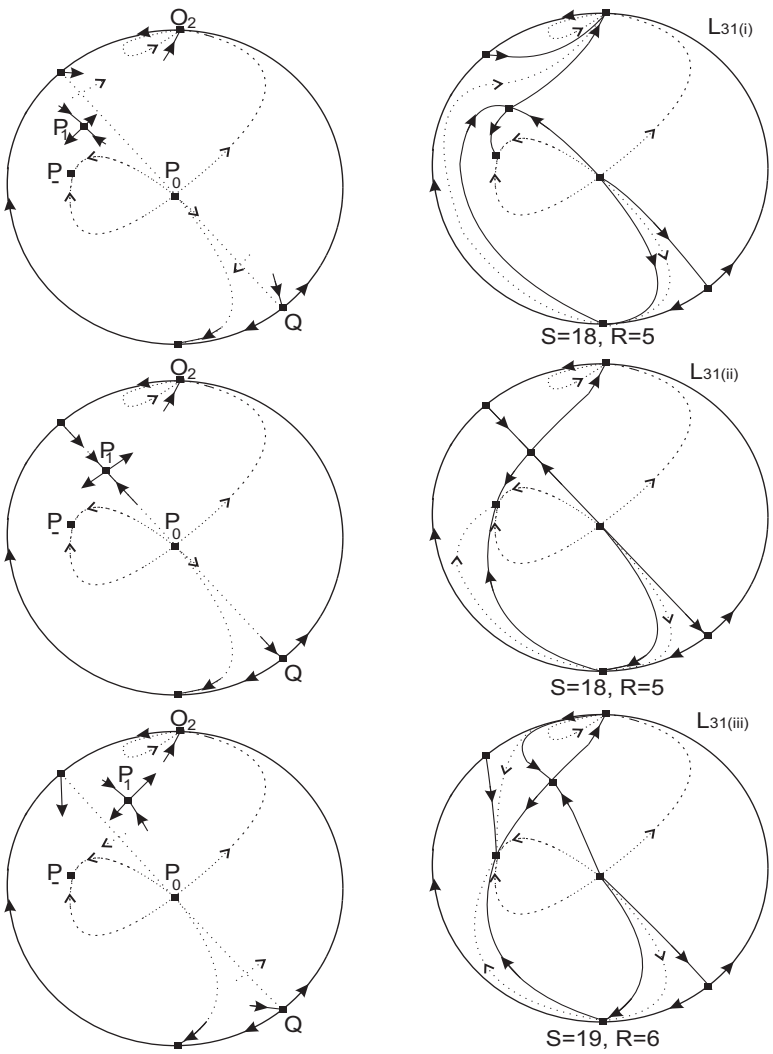


FIGURE 77. The local and the global phase portraits on the line $L_{31}$.

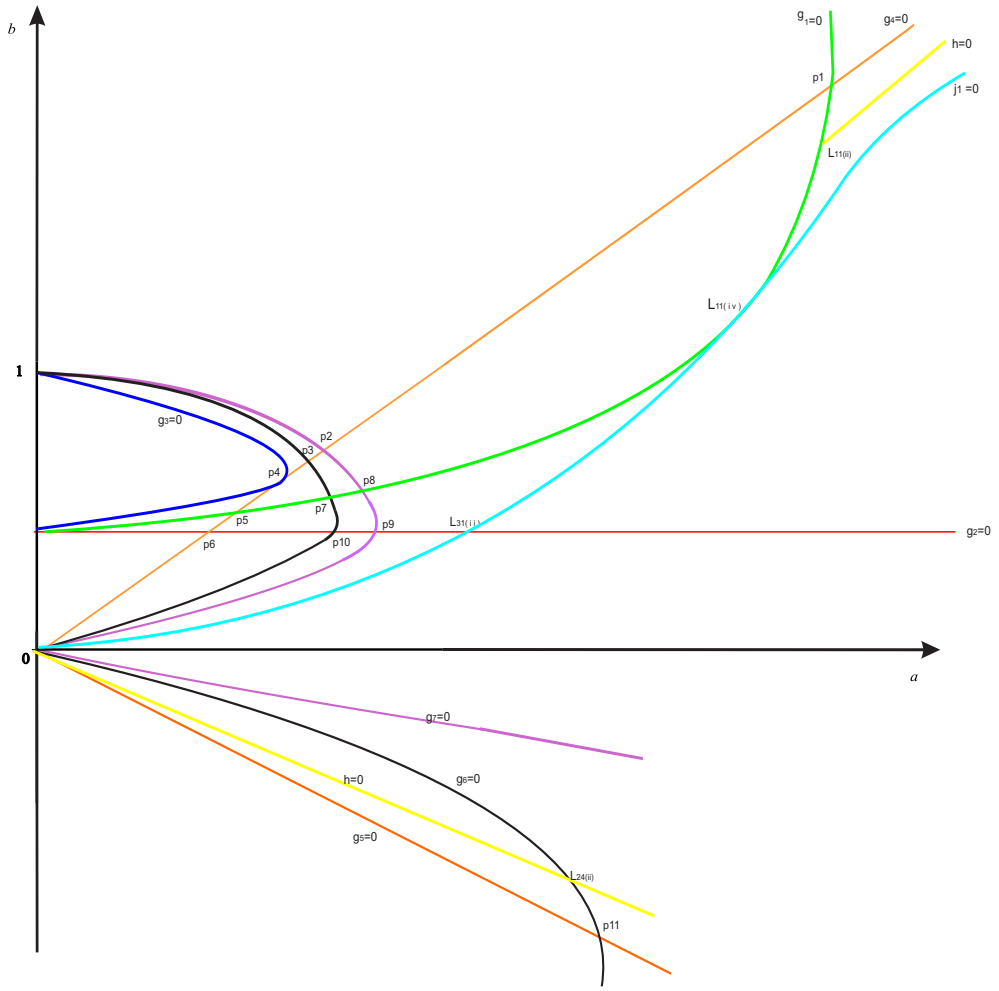


FIGURE 78. $c = 1, a > 0$. The bifurcation curves intersect into 11+4 points. It is a qualitative picture.

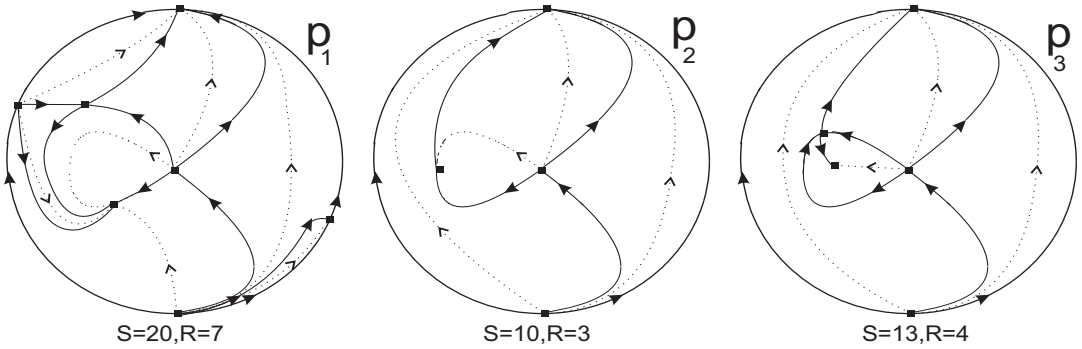


FIGURE 79. The phase portraits in the points $p_1$, $p_2$ and $p_3$.

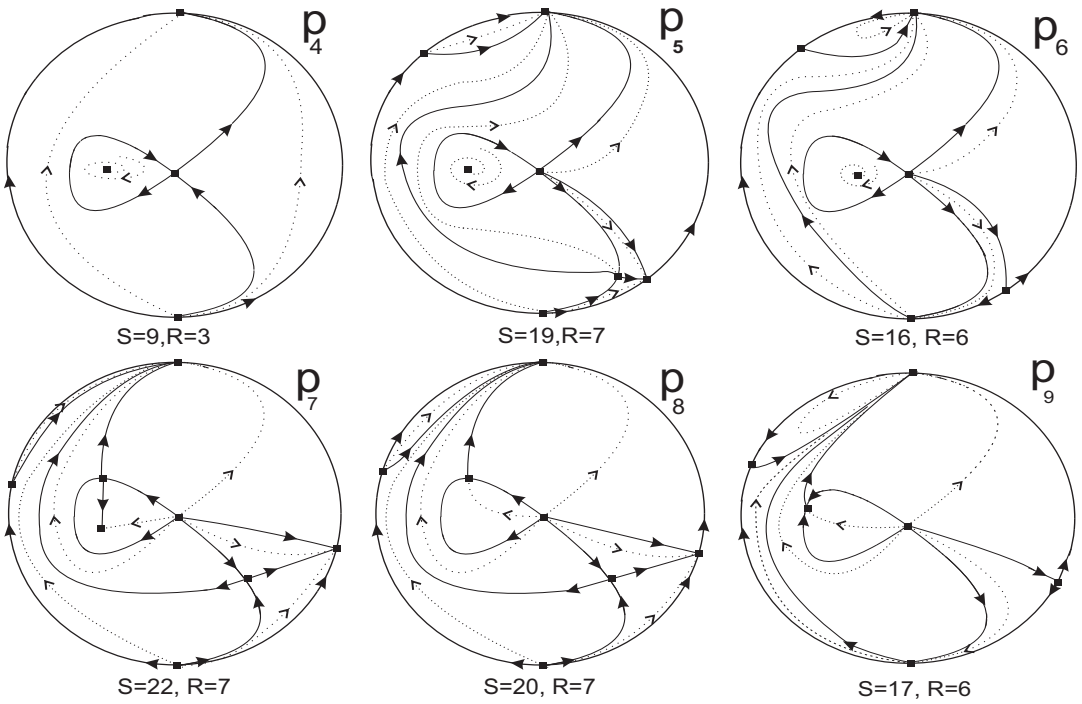


FIGURE 80. The phase portraits in the points $p_k$ for $k = 4, ..., 9$.

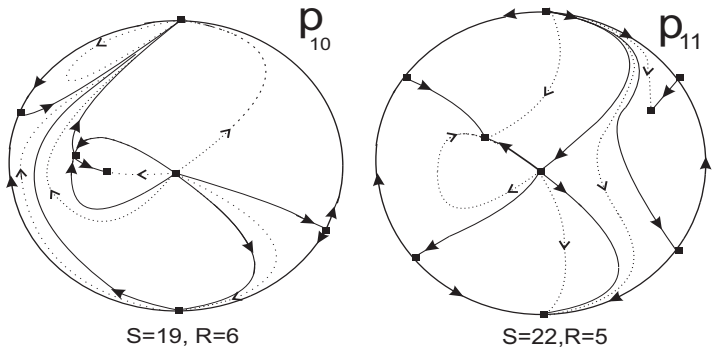


FIGURE 81. The phase portraits in the points $p_10$ and $p_{11}$.